INFORMATION TO USERS

The most advanced technology has been used to photograph and reproduce this manuscript from the microfilm master. UMI films the original text directly from the copy submitted. Thus, some dissertation copies are in typewriter face, while others may be from a computer printer.

In the unlikely event that the author did not send UMI a complete manuscript and there are missing pages, these will be noted. Also, if unauthorized copyrighted material had to be removed, a note will indicate the deletion.

Oversize materials (e.g., maps, drawings, charts) are reproduced by sectioning the original, beginning at the upper left-hand corner and continuing from left to right in equal sections with small overlaps. Each oversize page is available as one exposure on a standard 35 mm slide or as a 17″ × 23″ black and white photographic print for an additional charge.

Photographs included in the original manuscript have been reproduced xerographically in this copy. 35 mm slides or 6″ × 9″ black and white photographic prints are available for any photographs or illustrations appearing in this copy for an additional charge. Contact UMI directly to order.

Accessing the World's Information since 1938

300 North Zeeb Road, Ann Arbor, MI 48106-1346 USA

Order Number 8821059

Quasiparticle method in relativistic mean-field theories of nuclear structure

Ai, Hsiao-bai, Ph.D.

City University of New York, 1988

U·M·I
300 N. Zeeb Rd.
Ann Arbor, MI 48106

QUASIPARTICLE METHOD IN RELATIVISTIC MEAN-FIELD THEORIES OF NUCLEAR STRUCTURE

by

HSIAO-BAI AI

A dissertation submitted to the Graduate Faculty in Physics in partial fulfillment of the requirements for the degree of Doctor of Philosophy, The City University of New York

1988

This manuscript has been read and accepted for the Graduate Faculty in Physics in satisfaction of the dissertation requirement for the degree of Doctor of Philosophy.

March 30, 1988
Date

Carl Shakin
Chair of Examining Committee

March 30, 1988
Date

Executive Officer

C.M. Shakin
L.S. Celenza
V. Franco
P. Lesser
A.Z. Mekjian
Supervisory Committee

The City University of New York

Abstract

QUASIPARTICLE METHOD IN RELATIVISTIC MEAN-FIELD THEORIES OF NUCLEAR STRUCTURE

by

Hsiao-bai Ai

Adviser: Distinguished Professor Carl Shakin

In recent years, in order to understand the success of Dirac phenomenology, relativistic Brueckner-Hartree-Fock (RBHF) theory has been developed. This theory is a relativistic many-body theory of nuclear structure. Based upon the RBHF theory, which is characterized as having no free parameters other than those introduced in fitting free-space nucleon-nucleon scattering data, we construct an effective interaction. This interaction, when treated in a relativistic Hartree-Fock approximation, reproduces, rather accurately, the nucleon self-energy in nuclear matter, Migdal parameters obtained via relativistic Brueckner-Hartree-Fock calculations, and the saturation curves calculated with the full

relativistic Brueckner-Hartree-Fock theory. This effective interaction is constructed by adding a number of pseudoparticles to the "mesons" used to construct one-boson-exchange (OBE) models of the nuclear force. The pseudoparticles have relatively large masses and either real or imaginary coupling constants. (For example, exchange of a pseudo-sigma with an imaginary coupling constant has the effect of reducing the scalar attraction arising from sigma exchange, while exchange of a pseudo-omega with an imaginary coupling constant has the effect of reducing the repulsion arising from omega exchange. The terms beyond the Born term in the case of pion exchange are well simulated by pseudo-sigma exchange with a real coupling constant.) The effective interaction constructed here may be used for calculations of the properties of finite nuclei in a relativistic Hartree-Fock approximation.

Acknowledgements

To Professor Carl M. Shakin, my thesis advisor, I wish to express my deepest gratitude for his valuable guidance and constant encouragement throughout this thesis work.

I would also like to express my sincere gratitude to Professor Louis S. Celenza of Brooklyn College of CUNY for the help given to me during the course of this work.

I would like to express my special thanks to Professor and Mrs. Shakin for their providing "MATH-TEXT" software and allowing me to use their laser printer.

I wish to acknowledge with gratitude the Department of Physics of Brooklyn College and the Research Foundation of CUNY for the financial support during the course of this work, and the Brooklyn College Computer Center for allowing me to use their facilities.

CONTENTS

List of Tables

List of Figures

Chapter 1

General Survey

1.1 Introduction

One of the principal goals of theoretical nuclear physics is to understand nuclear structure in terms of the free nucleon-nucleon interaction. It is generally believed that the following steps:

(a) Determination of the free-space nucleon-nucleon potential,

(b) Calculation of the binding energy and saturation density of infinite nuclear matter,

(c) Calculation of the binding energy, energy levels, density distribution, and so forth, for finite nuclei,

are suitable procedures in a systematic application of a microscopic many-body theory in the study of nuclear structure.

In this work we will use the Dirac equation to describe nucleon motion. No one has yet provided a theoretical basis for using the Dirac equation to describe the motion of large composite objects such as the nucleon. In the past, the nucleons were assumed to interact via potentials. Such models have their limitations, since one does not explain the origin of the potentials. After 1935, in an attempt to understand the nature of nucleon interactions, one saw the formulation of the meson theory. The meson theory is formulated as

a quantum field theory. Such a formulation is especially suitable for perturbative methods. However, since perturbative methods are not particularly successful in strong interaction physics, researchers have used effective interactions and phenomenological approaches, in the context of Schroedinger theory.

The reaction matrix formalism of nuclear many-body theory (in short: Brueckner theory) has been widely used since 1958.[1-2] This theory achieved some quantitative success in explaining the ground state properties of nuclear matter and closed-shell nuclei. The principal difficulty appeared in the attempt to reproduce the empirical values of the binding energy and the saturation density (simultaneously) within conventional Brueckner theory, in lowest order calculations.

In the 1970's one started to use the Dirac equation with some effective potentials to solve some long standing puzzles in the theory of nuclear structure.[3-5,9-11] The modern description of nuclear matter as a relativistic system has led to a good understanding of various nuclear properties.[6-8,12-16] Further, the use of the relativistic impulse approximation has been quite successful in describing nucleon-nucleus scattering.[29-31] A natural extension of the relativistic analysis lies in the study of the structure of finite nuclei.[13-16] While it is possible to describe finite nuclei using either a mean-field (Dirac-Hartree) approach[15] or a Dirac-Hartree-Fock analysis[16], such calculations involve the introduction of a number of free-parameters. The phenomenological theories, such as the

Relativistic Brueckner-Hartree-Fock theory [6,7](in short: RBHF theory) or the relativistic impulse approximation[29-31], are parameter free. We would like to describe the properties of finite nuclei using the parameter-free (phenomenological) approach. To that end one might contemplate the calculation of relativistic Brueckner reaction matrices for a finite system. However, that is a very difficult program and we do not attempt such calculations.

It is often the case that one can obtain an effective interaction to avoid the difficult calculations required in a study of finite nuclei. Historically, in order to account for nuclear saturation, effective interactions are usually taken to be either density or momentum dependent, or both. Recently, a very simple effective interaction was proposed based upon the relativistic mean-field model of Walecka[8](QHD-I). This model made use of relativistic meson theory (a Dirac-Hartree approach) in which the interaction was mediated by two types of mesons (a neutral scalar meson and a neutral vector meson) to describe the properties of nuclear matter.

These initial attempts, which reproduced the nuclear properties at saturation density only, rarely included a study of other properties of nuclear matter, for instance, the effective interaction between nuclear quasiparticles. We are here interested in obtaining an effective interaction which may be used in a (Dirac) Hartree-Fock approximation for the study of finite nuclei. This interaction should be "realistic" in the sense that the matrix elements of the effective interaction should reproduce the matrix elements calculated with the

reaction matrices obtained in RBHF studies of nuclear matter.[6,7] We require, in particular, that the self-energy of a particle in nuclear matter be reproduced correctly. Futher, we also require that certain matrix elements of the quasiparticle interaction (Migdal parameters), nuclear matter binding energy, and the saturation density be given correctly. As we will see, it is fairly easy to reproduce the corrections required to go from the Hartree-Fock results for the nucleon self-energy to the results of the relativistic reaction matrix calculations. In addition, the effective interaction determined from our study of the nucleon self-energy also reproduces, quite well, the Migdal parameters and saturation curves of nuclear matter obtained from reaction matrix calculations.[6,7] It is also interesting to note that if one adjusts the strength of the pseudoparticle couplings, so that the saturation curves of various boson-exchange potentials yield the generally accepted values for the binding energy and saturation density of nuclear matter, one obtains quite reasonable values for the incompressibility parameter. (These values are quite similar to those obtained earlier using the full RBHF analysis.)

In Chapter 1 we present an introduction and a general survey of the One -Boson-Exchange model and the relativistic mean-field theory of nuclear structure. In Chapter 2 we review some definitions of the nucleon self-energy introduced in an earlier work[6,7] and some of the central equations of the BRHF theory. In Chapter 3 we describe our model for the effective interaction. In Chapter 4 we present the results of our calculations of the nucleon self-energy and the results for the Migdal parameters. In Chapter 5 we present the results of

our calculations of saturation curves using our pseudoparticle method. In Chapter 6 we present a fully - self-consistent pseudoparticle approximation and the results of our calculations. Finally, we present some conclusions and suggestions for applications of this pseudoparticle method in Chapter 7.

1.2 Conventions

In this work we use the conventions specified in the textbooks: Relativistic Quantum Mechanics by J.D. Bjorken and S.D. Drell[17] and Relativistic Nuclear Physics: Theory of Structure and Scattering by L.S. Celenza and C.M. Shakin.[7]

The metric tensor is

$$g_{\mu\nu} = g^{\mu\nu} = \begin{pmatrix} 1 & 0 & 0 & 0 \\ 0 & -1 & 0 & 0 \\ 0 & 0 & -1 & 0 \\ 0 & 0 & 0 & -1 \end{pmatrix} .$$

Contravariant coordinate:

$$x^{\mu} \equiv (x^0, x^1, x^2, x^3) \equiv (x^0, \vec{x}) \quad ,$$

Covariant coordinate:

$$x_\mu \equiv (x_0, x_1, x_2, x_3) \equiv (x_0, -\vec{x}) = g_{\mu\nu} x^\nu .$$

For any two four-vectors, p and q, we denote the scalar product by

$$p \bullet q = p_\mu q^\mu = p^0 \bullet q^0 - \vec{p} \bullet \vec{q} ,$$

$$p^2 = p^\mu p_\mu = p_0^2 - \vec{p}^2 .$$

We may expand spinor field operators as

$$\psi(x) = \sum_s \int d\vec{p} \, \frac{1}{(2\pi)^{3/2}} \sqrt{\frac{m}{E(\vec{p})}} \left\{ u(\vec{p},s) e^{-ip\bullet x} \, a_{\vec{p},s} + v(\vec{p},s) e^{ip\bullet x} \, b^+_{\vec{p},s} \right\} ,$$

where

$$u(\vec{p},s) = \sqrt{\frac{E(\vec{p})+m}{2m}} \begin{pmatrix} \chi_s \\ \frac{\vec{\sigma}\bullet\vec{p}}{E(\vec{p})+m} \chi_s \end{pmatrix} ,$$

$$v(\vec{p},s) = \sqrt{\frac{E(\vec{p})+m}{2m}} \begin{pmatrix} \frac{\vec{\sigma}\bullet\vec{p}}{E(\vec{p})+m} \chi_{-s} \\ \chi_{-s} \end{pmatrix} .$$

Here $u(\vec{p},s)$ and $v(\vec{p},s)$ denote positive-energy and negative-energy spinor solutions of the Dirac equation, respectively; m and $\vec{p}$ are the

mass and momentum of the fermion, and χ_s is a Pauli spinor. The $u(\vec{p},s)$ and $v(\vec{p},s)$ satisfy the Dirac equation:

$$[\ \gamma^0 E(\vec{p}) - \vec{\gamma}\cdot\vec{p} - m\ ]u(\vec{p},s) = 0 \quad ,$$

$$[\ \gamma^0 E(\vec{p}) - \vec{\gamma}\cdot\vec{p} + m\ ]v(\vec{p},s) = 0 \quad .$$

The adjoint spinors

$$\bar{u}(\vec{p},s) = u^+(\vec{p},s)\ \gamma^0 \quad ,$$

$$\bar{v}(\vec{p},s) = v^+(\vec{p},s)\ \gamma^0 \quad ,$$

satisfy

$$\bar{u}(\vec{p},s)\ (\ \not{p} - m\ ) = 0 \quad ,$$

$$\bar{v}(\vec{p},s)\ (\ \not{p} + m\ ) = 0 \quad ,$$

where

$$\gamma^0 = \begin{pmatrix} I & 0 \\ 0 & I \end{pmatrix} \quad ,$$

and

$$\vec{\gamma} = \begin{pmatrix} 0 & \vec{\sigma} \\ -\vec{\sigma} & 0 \end{pmatrix} \quad .$$

Here I is 2x2 unit matrix and the $\vec{\sigma}$ are the 2x2 Pauli spin matrices

$$\vec{\sigma} = (\sigma_1,\ \sigma_2,\ \sigma_3) \quad ,$$

$$\sigma_1 = \begin{pmatrix} 0 & 1 \\ 1 & 0 \end{pmatrix} ,\ \sigma_2 = \begin{pmatrix} 0 & -i \\ i & 0 \end{pmatrix} ,\ \sigma_3 = \begin{pmatrix} 1 & 0 \\ 0 & -1 \end{pmatrix} .$$

Frequently appearing combinations are

$$\sigma^{\mu\nu} = \frac{i}{2} [\ \gamma^{\mu}\ ,\ \gamma^{\nu}\ ] \quad ,$$

and

$$\gamma^5 \ = \ i\ \gamma^0\gamma^1\gamma^2\gamma^3 = \gamma_5 \quad .$$

In this representation, the components of $\sigma^{\mu\nu}$ are

$$\sigma^{ij} = \begin{pmatrix} \sigma^k & 0 \\ 0 & \sigma^k \end{pmatrix} \quad ,$$

with i,j,k = 1,2,3 in cyclic order and

$$\sigma^{0i} = i \begin{pmatrix} 0 & \sigma^i \\ \sigma^i & 0 \end{pmatrix} \quad , \qquad \gamma^5 = \gamma_5 = \begin{pmatrix} 0 & I \\ I & 0 \end{pmatrix} \quad .$$

The inner product of a γ matrix with an ordinary four-vector is often denoted by

$$\gamma_\mu A^\mu \equiv \not{A} = \gamma^0 A^0 - \vec{\gamma}\cdot\vec{A} \quad ,$$

$$p^\mu \gamma_\mu \equiv \not{p} = E^0\gamma^0 - \vec{\gamma}\cdot\vec{p} \quad ,$$

$$p_\mu \gamma^\mu \equiv i\not{\partial} = i\gamma^\mu \frac{\partial}{\partial x^\mu} \quad ,$$

$$(\ \Box = \partial_0^2 - \partial_1^2 - \partial_2^2 - \partial_3^2 \ ) .$$

1.3 One-Boson-Exchange (OBE) Model

The formulation of the π meson theory of nuclear forces took place about 50 years ago. This model developed into the One-Boson-Exchange Potential (OBEP) model in the early 1960's. In this model, a derivation of the nucleon-nucleon potential can be obtained by using a quantum field theory of mesons. The potential acting between a pair of nucleons due to the exchange of a meson has a range of the order of the meson Compton wavelength, which is inversely proportional to the meson mass. Various potentials (attractive or repulsive), spin-orbit potentials, tensor potentials, etc., have been derived by considering the exchange of different types of meson fields.

In recent years, the OBEP model has been quite successful in explaining two-body data.[2,26-28] It was realized that multi-meson systems often have strongly correlated resonance states which behave as a single boson. Besides the exchange of one π-meson, which determines the long-range part of the two-nucleon potential, some of these multi-meson resonances were introduced to describe medium-range and short-range behaviour of the two-nucleon potential. For instance: (1) the ρ-meson may be thought of as a two-pion resonance, (2) ω-meson is a three-pion resonance, (3) the ϕ-meson, which has the same quantum numbers as the ω, is a resonance in the $K\bar{K}$ system; (4) the σ-meson is regarded as a convenient parameterization of the effect of the two-pion system in the S-state

(J=0); (5) the η-meson has the quantum numbers of the π-meson, except that it has isospin T=0. Information concerning masses, coupling constants, and other quantum numbers of these mesons are listed in Table 1.1 - Table 1.3 for different OBE potentials.

In the OBEP model, the masses and coupling constants are determined by a detailed fit to the two-nucleon data. Because most of the resonance states have a finite width there is some uncertainty in the specification of the mass.[22] The main difference among various meson-theoretic two-nucleon potentials lies in the treatment of the two-pion system and in the details of the mesonic coupling and the cut-off factors.

According to the OBE model, the two-nucleon potential can be described as a superposition of Born terms obtained from the (single) exchange of various mesons. Thus, in momentum space, OBE potentials have the following structure

$$V_{OBE}(\vec{q}', \vec{q}) \cong \sum_{\alpha} \frac{g_\alpha^2 F_\alpha^2(t)}{t - m_\alpha^2} \quad ,$$

where m_α denotes the mass of the exchanged meson, g_α denotes the meson-nucleon coupling constant and $\vec{q}$ ($\vec{q}'$) is the initial (final)-state relative three-momentum of the two interacting nucleons; t is the momentum transfer

$$t = (E_q, - E_q)^2 - (\vec{q}' - \vec{q})^2 \quad ,$$

$$E_p^2 = \vec{p}^2 + m_N^2 \quad ,$$

where m_N the nucleon mass. Cut-off-factors, F_α, are introduced to avoid divergences and to improve the asymptotic behaviour.

For the HEA potential,[18] and for a scalar meson,

$$F_\alpha^2(t) = \left(\frac{\lambda^2 - m_\alpha^2}{\lambda^2 - t} \right)^2, \quad \alpha = \pi,\ \eta,\ \sigma,\ \delta \ ,$$

while, for a vector meson

$$F_\alpha^2(t) = \left(\frac{\lambda^2 - m_\alpha^2}{\lambda^2 - t} \right)^2 \left(\frac{\lambda_v^2 - m_\alpha^2}{\lambda_v^2 - t} \right) , \quad \alpha = \rho,\ \omega,\ \phi \ ,$$

where λ = 1950 MeV, λ_v = 1250 MeV.

For the HM2 potential [19] we use an Eikonal form factor (See Appendix A)

$$F_\alpha^2\ (t) = F_\alpha^2(\ t,\ u \mid q_0^2\ ) \ , \quad \alpha = \sigma,\ \omega,\ \pi,\ \rho,\ \delta,\ \eta \ .$$

For the BMR2 potential:[20]

$$F_\sigma^2\ (\vec{q}) = \left(\frac{\lambda_1^2 - m_\sigma^2}{\lambda_1^2 + \vec{q}^2} \right)^2 ,$$

$$F_i^2\ (\vec{q}) = \left(\frac{\lambda_2^2 - m_i^2}{\lambda_2^2 + \vec{q}^2} \right)^2 , \quad i = \pi,\ \rho \ ,$$

$$F_j^2\ (\vec{q}) = \left(\frac{\lambda_3^2 - m_j^2}{\lambda_3^2 + \vec{q}^2} \right)^2 , \quad j = \omega,\ \delta,\ \eta \ ,$$

where λ_1 = 1 GeV, λ_2 = 1.3 GeV, λ_3 = 1.5 GeV.

In spite of the obvious success of the OBEP model in correlating a great amount of data, one can argue that any attempt to couple boson fields to particles as large as the nucleon would destroy the success of the OBE model of the nuclear force. Therefore, the OBEP model may not be "correct". Recently C.M. Shakin , L.S. Celenza and V.M. Bannur[32],[33] have shown that a large number of mesons may be described as nontopological solitons. They argue however, that the important "meson-fields" used in nuclear structure physics and in the OBEP model of the nuclear force, which have the same quantum numbers as the σ, π, ρ, and ω mesons, should not be identified with physical mesons. The quanta of the fields in the OBE model can be considered as never going on mass-shell. (These meson-fields can be defined to be "non-propagating modes".) The "exchange of mesons" between a pair of interacting nucleons is related to fluctuations of the quark self-energy in the model of Bannur, Celenza and Shakin.

1.4 Mean-Field Theory and the Elementary σ-ω Model

Walecka and Serot's QHD-1 (i.e. the σ-ω model) is a very simple field theoretic model. It is formulated in terms of a massive neutral scalar-meson field, $\sigma(x)$, coupled to the scalar density $\overline{\Psi}_N(x)\Psi_N(x)$,

and a massive neutral vector-meson field $\omega_\mu(x)$ coupled to the baryon current $\overline{\psi}_N(x)\gamma^\mu\psi_N(x)$. In the static limit this theory gives rise to a effective nucleon-nucleon potential of the form

$$V_{static} = \frac{g_\omega^2}{4\pi}\,\frac{e^{-m_\omega r}}{r} - \frac{g_\sigma^2}{4\pi}\,\frac{e^{-m_\sigma r}}{r} \quad .$$

The relativistic model of nuclear matter may be represented by the following Lagrangian density

$$\mathfrak{L} = L_N^0 + L_\sigma^0 + L_\omega^0 + L_\sigma^I + L_\omega^I \quad ,$$

where

$$L_N^0 = \overline{\psi}_N(x)\left(i\gamma^\mu\partial_\mu - m_N \right)\psi_N(x) \quad ,$$

$$L_\sigma^0 = \frac{1}{2}\left[\partial_\mu \sigma(x)\, \partial^\mu \sigma(x) - m_\sigma^2\, \sigma^2(x) \right] ,$$

$$L_\omega^0 = -\frac{1}{4} F_{\mu\nu}^\omega(x)\, F_\omega^{\mu\nu}(x) + \frac{1}{2} m_\omega^2\, \omega^\mu(x)\omega_\mu(x) \quad ,$$

$$L_\sigma^I = - g_\sigma \overline{\psi}_N(x)\sigma(x)\psi_N(x) \quad ,$$

$$L_\omega^I = \quad g_\omega \overline{\psi}_N(x)\gamma^\mu\omega_\mu(x)\psi_N(x) \quad ,$$

$$F_{\mu\nu}^\omega(x) = \partial_\mu\omega_\nu(x) - \partial_\nu\omega_\mu(x) \quad .$$

The equations of motion are therefore

$$(\partial_\nu F_\omega^{\mu\nu}(x) + m_\omega^2) \omega_\mu(x) = g_\omega \bar{\psi}_N(x) \gamma^\mu \psi_N(x) \quad , \tag{1.1}$$

$$(\Box + m_\sigma^2) \sigma(x) = - g_\sigma \bar{\psi}_N(x) \psi_N(x) \quad , \tag{1.2}$$

$$(i\gamma^\mu \partial_\mu - m_N) \psi_N(x) = g_\sigma \sigma(x) \psi_N(x) - g_\omega \gamma^\mu \omega_\mu(x) \psi_N(x) \quad . \tag{1.3}$$

The vector-meson field equation, Eq.(1.1), is a inhomogeneous Proca equation with the conserved nucleon current, $\bar{\psi}_N(x) \gamma^\mu \psi_N(x)$, as the source. Equation (1.2) is a Klein-Gordon equation with the baryon scalar density as source. Equation (1.3) is the Dirac equation for the nucleon field.

In general, the solutions for the meson fields obtained from the equations of motion are

$$\sigma(x) = - g_\sigma \int d^3x' \; D_\sigma(x-x') \bar{\psi}_N(x') \psi_N(x') \quad , \tag{1.4}$$

$$\omega^\mu(x) = g_\omega \int d^3x' \; D_\omega(x-x') \bar{\psi}_N(x') \gamma^\mu \psi_N(x') \quad , \tag{1.5}$$

where D_σ and D_ω are the retarded Green's functions of the Klein-Gordon equation,

$$(\Box + m_\alpha^2) D_\alpha(x-x') = \delta (x-x') , \quad (\alpha = \sigma, \omega)$$

$$D_\alpha(x-x') = 0 \qquad \text{for } x_0 - x'_0 < 0 , \tag{1.6}$$

The coupling constants g_σ and g_ω are large, implying the need for a strong-coupling theory. We have thus not made much progress by simple writing down a set of field equations such as those above. However, consider a uniform system of baryons in a volume V. To a good approximation we may replace the meson field by a classical field and the sources by their ground state expectation values. This is the mean-field approach to the nuclear matter problem. We have

$$\sigma(x) \longrightarrow \sigma = < \psi_g \mid \sigma(x) \mid \psi_g > , \tag{1.7}$$

and

$$\omega_\mu(x) \longrightarrow \omega_\mu = < \psi_g \mid \omega_\mu(x) \mid \psi_g > , \tag{1.8}$$

where ψ_g is the ground state wave function. In this approximation the equation of motion for the nucleon field is simplified and may be readily solved. For example, in the nuclear matter problem, the ground state is expected to be uniform and isotropic, and hence the ground state expectation value of the spatial part of the vector field

$\omega(x)$ should vanish by rotational invariance, $\vec{\omega}(x) = 0$; σ_0 and ω_0 will be constants, independent of space and time, for uniform nuclear matter.

The vector-meson field, Eq.(1.1), in this case reduces to

$$\omega_0 = \frac{g_\omega}{m_\omega^2} < \psi_g \mid \bar{\psi}_N(x)\gamma^0\psi_N(x) \mid \psi_g > \qquad (1.9)$$

$$= \frac{g_\omega}{m_\omega^2} \rho_B \quad ,$$

and the scalar-meson field, Eq.(1.2), becomes

$$\sigma_0 = -\frac{g_\sigma}{m_\sigma^2} < \psi_g \mid \bar{\psi}_N(x)\psi_N(x) \mid \psi_g > \qquad (1.10)$$

$$= -\frac{g_\sigma}{m_\sigma^2} \rho_s \quad .$$

Since the baryon current is conserved, the baryon number and the baryon density ρ_B for a uniform system is a constant of the motion. The expectation value of $\Psi^+_N(x)\Psi_N(x)$ in a uniform ground state is given by the nucleon number density, $n_B(x)$. The integral $\int d^3x \Psi^+_N(x)\Psi_N(x)$ is the number operator, which yields the total number of nucleons in the system, when acting on ψ_g.

Now the Dirac equation (1.3) is linearized with the substitution of Eq.(1.9) and Eq.(1.10):

$$(i\gamma^{\mu}\partial_{\mu} - M_N - g_{\sigma}\sigma_0 + g_{\omega}\omega_0\gamma^0)\psi_N(x) = 0 \quad , \tag{1.11}$$

and it may be solved exactly; all the eigenstates and eigenvalues are known. The values of ρ_B and ρ_s are ultimately given in terms of g_σ, g_ω, m_σ and m_ω. In Chapter 6, we shall present an application of this simple model.

One may consider the OBE model as only providing a parameterization of the free nucleon-nucleon interaction. However, in the RBHF theory, we take the OBE model seriously and have calculated matrix elements of the reaction matrix which do not enter in the study of nucleon-nucleon scattering. One may conjecture that the Lagrangian of the OBE model is a useful effective Lagrangian containing fields with the quantum numbers of the σ, ω, π, ρ, δ, etc. mesons. (The Lagrangian serves only as a reminder of the structure of the coupling of the boson fields to the nucleon, since there is no possibility of solving the strong-coupling dynamics associated with such a Lagrangian.) For a sufficiently large system we may use a relativistic mean-field approximation and include the effects of short-range correlations by the method to be described in this work.

Table 1.1

HM2 Potential

meson	Isospin T	Spin Parity J^{π}	Mass (MeV)	Coupling Constant $(g^2/4\pi)$	f/g	propagator	Vertex form Factor
σ	0	0^+	520.0	5.6596	0.0	$\Delta_1(p)$	$F_\sigma^2(t)$
ω	0	1^-	782.8	10.0	0.0	$\Delta_2(p)$	$F_\omega^2(t)$
π	1	0^-	138.0	14.2	0.0	$\Delta_1(p)$	$F_\pi^2(t)$
ρ	1	1^-	711.0	0.5	6.2	$\Delta_2(p)$	$F_\rho^2(t)$
δ	1	0^+	960.0	0.8175	0.0	$\Delta_1(p)$	$F_\delta^2(t)$
η	0	0^-	548.5	2.0	0.0	$\Delta_1(p)$	$F_\eta^2(t)$

The propagator for scalar meson is $\Delta_1(p)$

$$\Delta_1(P) = (t - m_i^2)^{-1} \qquad (i = \sigma, \pi, \delta, \eta).$$

For vector meson the propagator is $\Delta_2(p)$,

$$\Delta_2(p) = - g_{\mu\nu}(t - m_j^2)^{-1} \quad (j = \omega, \rho, \phi),$$

and

$$F_\alpha^2(t) = E_\alpha^2(t,u|q_0^2) \quad (\alpha = \sigma, \omega, \pi, \rho, \delta, \eta).$$

See Appendix A.

Table 1.2

HEA Potential

meson	Isospin T	Spin Parity J^{π}	Mass (MeV)	Coupling Constant $(g^2/4\pi)$	f/g	propagator	Vertex form Factor
σ	0	0^+	500.0	4.63	0.0	$\Delta_1(p)$	$F_i^2(t)$
ω	0	1^-	782.8	14.00	0.0	$\Delta_2(p)$	$F_j^2(t)$
π	1	0^-	138.5	13.00	0.0	$\Delta_1(p)$	$F_i^2(t)$
ρ	1	1^-	763.0	1.50	3.5	$\Delta_2(p)$	$F_j^2(t)$
δ	1	0^+	960.0	4.74	0.0	$\Delta_1(p)$	$F_i^2(t)$
η	0	0^-	548.5	6.00	0.0	$\Delta_1(p)$	$F_i^2(t)$
ϕ	0	1^-	1020.	7.00	0.0	$\Delta_2(p)$	$F_j^2(t)$

The propagators are the same as Table 1.1 and

$$F_\alpha^2(t) = \left(\frac{\lambda^2 - m_\alpha^2}{\lambda^2 - t} \right)^2, \quad \alpha = \pi,\ \eta,\ \sigma,\ \delta \quad ,$$

$$F_\alpha^2(t) = \left(\frac{\lambda^2 - m_\alpha^2}{\lambda^2 - t} \right)^2 \left(\frac{\lambda_v^2 - m_\alpha^2}{\lambda_v^2 - t} \right) , \quad \alpha = \rho,\ \omega,\ \phi \ ,$$

and λ= 1950 MeV, λ_v= 1250 Mev.

Table 1.3

BMR2 Potential

meson	Isospin T	Spin Parity J^{π}	Mass (MeV)	Coupling Constant $(g^2/4\pi)$	f/g	propagator	Vertex form Factor
σ	0	0^+	550.0	7.8749	0.0	$\Delta_1(p)$	$F_\sigma^2(q)$
ω	0	1^-	782.0	20.0	0.0	$\Delta_2(p)$	$F_j^2(q)$
π	1	0^-	138.0	14.60	0.0	$\Delta_1(p)$	$F_i^2(q)$
ρ	1	1^-	769.0	0.95	6.1	$\Delta_2(p)$	$F_i^2(q)$
δ	1	0^+	983.0	4.9973	0.0	$\Delta_1(p)$	$F_j^2(q)$
η	0	0^-	548.8	3.0	0.0	$\Delta_1(p)$	$F_j^2(q)$

The propagators are the same as Table 1.1 and

$$F_\sigma^2(\vec{q}) = \left(\frac{\lambda_1^2 - m_\sigma^2}{\lambda_1^2 + \vec{q}^2}\right)^2 ,$$

$$F_i^2(\vec{q}) = \left(\frac{\lambda_2^2 - m_i^2}{\lambda_2^2 + \vec{q}^2}\right)^2 , \quad i = \pi, \rho ,$$

$$F_j^2(\vec{q}) = \left(\frac{\lambda_3^2 - m_j^2}{\lambda_3^2 + \vec{q}^2}\right)^2 , \quad j = \omega, \delta, \eta ,$$

with λ_1= 2.0 GeV, λ_2= 1.3GeV, λ_3= 1.5 GeV.

Chapter 2

A Brief Review of RBHF Theory

2.1 The Bethe-Salpeter Equation and the Reaction Matrix

Bethe and Salpeter have shown that the relativistic two-nucleon amplitude M can be represented as the solution of a covariant integral equation[23 24], (in short: BSE) depicted in Fig.2.1

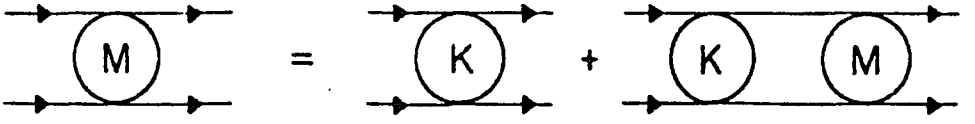

$$M = K + KG_F M \tag{2.1}$$

Fig.2.1

Here -iM is the relativistic two-nucleon scattering amplitude, G_F is a Feynman propagator for the intermediate-state nucleons; the interaction kernel K is the sum of all irreducible two-particle diagrams. (Of course, this must be regarded as an operator equation in the spin and isospin space of the two nucleons.) It is obviously hopeless to try to solve the BSE exactly, since the kernel K cannot be given in a closed form.

Note that the BSE involves a four-dimensional integration over the intermediate nucleon four-momenta. In Ref.24 one finds a discussion of procedures which may be used to reduce the four-dimensional BSE to a tractable three-dimensional covariant equation.

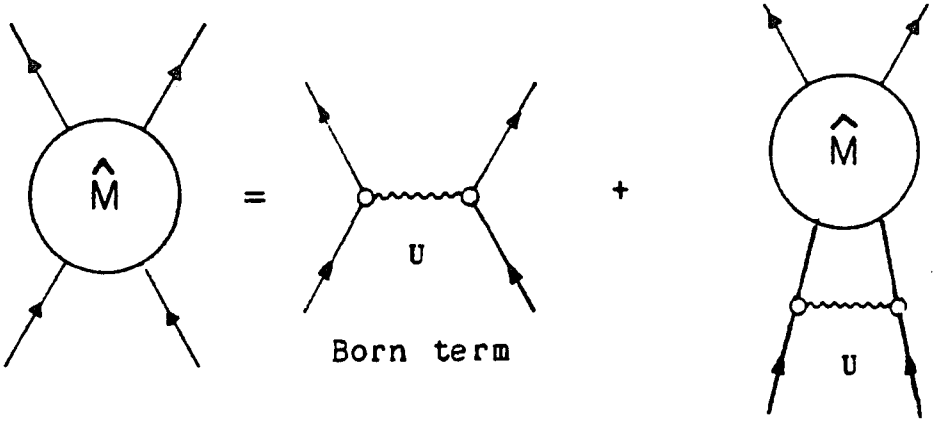

Fig.2.2

The technique involves replacing Eq.(2.1) by two equations,

$$M = U + UgM \ , \tag{2.2}$$

$$U = K + K(G_F - g)U. \tag{2.3}$$

Here g is propagator that has the same right-hand cut as G_F, and g contains a delta function, which reduces the four-dimensional equation to a three-dimensional equation. In the physical energy region G_F and g have similiar cut structure and that leads to the possibility that $(G_F - g)$ is "small".

There are many possible choices for g and for each choice one can determine a relativistic quasi-potential U. Various quasi-potentials have been determined by fitting the two-nucleon scattering data using the OBE model of nuclear forces. (See Section 1.3.) The discussion in Ref.7 uses the approximation discussed in Ref.24, where Eq.(2.2) is replaced by

$$\hat{M}^{++++} = U^{++++} + U^{++++}\hat{g}^{++}\hat{M}^{++++} \quad . \tag{2.4}$$

Here the "+" signs denote matrix elements taken between only positive-energy spinor states of the Dirac equation without interaction, u(p,s), where

$$\langle \vec{p}s_1, \vec{q}s_2 | \hat{M}^{++++} | \vec{p}'s'_1, \vec{q}'s'_2 \rangle = \langle \bar{u}(\vec{p}, s_1)\bar{u}(\vec{q}, s_2) | \hat{M} | u(\vec{p}', s'_1)u(\vec{q}'s'_2) \rangle \tag{2.5}$$

etc. In the study of nuclear matter Eq.(2.4) was generalized to the form

$$\hat{M} = U + U\hat{g}^{++}\hat{M} \quad . \tag{2.6}$$

The propagator $\hat{g}^{++}$ is taken to include dispersive effects and Pauli-principle restrictions. Various forms for $\hat{g}^{++}$ are discussed in Ref.24. We have neglected the effect of the medium in modifying the kernel

U. The solution $\hat{M}$ of Eq.(2.6) is the effective interaction in the medium. ($\hat{M}$ is usually called the reaction matrix.)

We can introduce the matrix elements,

$$\langle \vec{p}, s_1, \vec{q} s_2 | \hat{M} | \vec{p}'s'_1, \vec{q}'s'_2 \rangle = \langle \bar{f}(\vec{p}, s_1) \bar{f}(\vec{q}, s_2) | \hat{M} | f(\vec{p}'s'_1) f(\vec{q}'s'_2) \rangle \tag{2.7}$$

and a corresponding relation for the quasi-potential U. Here $f(\vec{p}, s)$ is the solution of Eq.(2.8) of the next subsection. One may consider the reaction matrix $\hat{M}$ in Eq.(2.6) as the appropriate generalization, for the RBHF theory, of the nonrelativistic Brueckner reaction matrix.

We note that, in principle, $\hat{M}$ can be calculated in the " ladder approximation ". However, the coupling constants are very large and a systematic solution of a strongly-coupled field theory is not available. The one-boson-exchange model provides a scheme for constructing a relativistic quasipotential and scattering amplitude. The kernel of the BSE is approximated by the Born term (see Fig.2.2) in most applications.

2.2 The Relativistic Nucleon Wave Function in Nuclear Matter

The relativistic nucleon wave function in nuclear matter is a product of a Dirac spinor and isospinor and a plane wave

$$\Psi^{rel}_{s,\tau}(\vec{p}) = \sqrt{\frac{m_N}{E_N(\vec{p})}}\, f(\vec{p},s)\frac{e^{i\vec{p}\cdot\vec{x}}}{(2\pi)^{3/2}}\,\chi_\tau \ .$$

The spinor $f(\vec{p},s)$ satisfies the Dirac equation

$$[\gamma\cdot p - m_N - \Sigma(\{f(\vec{p},s)\},p)]f(\vec{p},s)=0 \ . \qquad (2.8)$$

Here $\Sigma(p)$ is the self-energy which depends on the spinor $f(\vec{p},s)$ and the density of the system.

L. Celenza and C. Shakin have stressed that the nucleon mass is different in a nuclear environment than in vacuum[7]. The equation governing the modification of the mass from the vacuum mass is

$$\widetilde{m}(p^2)=m_N + \tfrac{1}{4}\mathrm{Tr}\,\Sigma(p^2,\widetilde{m}(p^2),k_F) \ , \qquad (2.9)$$

where $\Sigma(p)$ is again the self-energy of the nucleon due to the presence of nuclear matter. If we determine the relation between the energy and the momentum, $p^0 = \widetilde{E}(\vec{p})$, we can write Eq.(2.9) as

$$\widetilde{m}(\vec{p})=m_N + \tfrac{1}{4}\mathrm{Tr}\,\Sigma(\vec{p},\widetilde{m}(\vec{p}),k_F) \ . \qquad (2.10)$$

For example, if $\Sigma(p) = A(p) + \gamma^0 B(p)$ we would have, for $p^0 \geq 0$,

$$p^0=\tilde{E}(\vec{p})=B(p)+[\vec{p}^2+\{m_N+A(p)\}^2]^{\frac{1}{2}} \ , \tag{2.11}$$

as the dispersion relation relating the quasi-particle energy and momentum in the nuclear matter. Further we see that

$$\tilde{m}(\vec{p}) = m_N + A(p) \ . \tag{2.12}$$

The models to be discussed here are characterized as having large negative values for A(p), of the order of -400 MeV, and large positive values for B(p) of about 300 MeV.[7]

For the above form of $\Sigma(p)$ we obtain,

$$f(\vec{p},s) = \sqrt{\frac{E_N(\vec{p})}{m_N}\frac{\tilde{m}}{\tilde{E}(\vec{p})}\left(\frac{\tilde{E}(\vec{p})+\tilde{m}}{2\tilde{m}}\right)}\begin{pmatrix} \chi_s \\ \frac{\vec{\sigma}\cdot\vec{p}}{\tilde{E}(\vec{p})+\tilde{m}}\chi_s \end{pmatrix} \tag{2.13}$$

$$= \sqrt{\frac{E_N(\vec{p})}{2m_N}\frac{\tilde{\epsilon}(\vec{p})}{\tilde{E}(\vec{p})}}\begin{pmatrix} \chi_s \\ \frac{\vec{\sigma}\cdot\vec{p}}{\tilde{\epsilon}(\vec{p})}\chi_s \end{pmatrix} \ ,$$

where $E_N(\vec{p}) = [\vec{p}^2 + m_N^2]^{\frac{1}{2}}$, $\tilde{E}(\vec{p}) = [\vec{p}^2 + \tilde{m}^2(\vec{p})]^{\frac{1}{2}}$, and $\tilde{\epsilon}(\vec{p}) = [\vec{p}^2 + \tilde{m}^2(\vec{p})]^{\frac{1}{2}} + \tilde{m}(\vec{p})$. We have chosen the normalization, (see Appendix B)

$$f^+(\vec{p},s')f(\vec{p},s) = \frac{E_N(\vec{p})}{m_N}\delta_{ss'} \tag{2.14}$$

for the spinors $f(\vec{p},s)$. Therefore,

$$\Phi^{+}_{s}(\vec{p})\Phi_{s}(\vec{p}) = 1 \ . \tag{2.15}$$

Note that if $\widetilde{m} \to m_N$ we have $f(\vec{p},s) \to u(\vec{p},s)$, where

$$u(\vec{p},s) = \sqrt{\frac{E_N(\vec{p})+m_N}{2m_N}} \begin{pmatrix} \chi_s \\ \dfrac{\vec{\sigma}\cdot\vec{p}}{E_N(\vec{p})+m_N}\,\chi_s \end{pmatrix} \tag{2.16}$$

is the standard, positive-energy solution of the free Dirac equation normalized such that $\bar{u}(\vec{p},s)u(\vec{p},s') = \delta_{ss'}$.

2.3 The Energy of Relativistic Nuclear Matter

Using various approximations, one obtains an expression for the energy of relativistic nuclear matter in RBHF theory,

$$E = \sum_s \int \frac{d\vec{p}}{(2\pi)^3} \left(\frac{m_N}{E_N(\vec{p})}\right) \bar{f}(\vec{p},s)(\vec{\gamma}\cdot\vec{p} + m_N) f(\vec{p},s)\theta(k_F - |\vec{p}|)$$

$$+ \frac{1}{2}\sum_{ss'} \int \frac{d\vec{p}}{(2\pi)^3}\frac{d\vec{q}}{(2\pi)^3} \left(\frac{m_N}{E_N(\vec{p})}\right)\left(\frac{m_N}{E_N(\vec{q})}\right) \theta(k_F - |\vec{p}|)\ \theta(k_F - |\vec{q}|)$$

$$\times \langle \bar{f}(\vec{p},s)\bar{f}(\vec{q},s') | \hat{M}(1-P_{12}) | f(\vec{p},s) f(\vec{q},s') \rangle \ , \tag{2.17}$$

or

$$E = \sum_s \int \frac{d\vec{p}}{(2\pi)^3} \left(\frac{m_N}{E_N(\vec{p})}\right) \bar{f}(\vec{p},s)(\vec{\gamma}\cdot\vec{p} + m_N + \tfrac{1}{2}\Sigma(\vec{p}))f(\vec{p},s)\theta(k_F - |\vec{p}|) . \tag{2.18}$$

The self-energy $\Sigma(p)$ is a 4 x 4 Dirac matrix

$$\Sigma(\vec{p}) = \sum_s \int \frac{d\vec{q}}{(2\pi)^3} \left(\frac{m_N}{E_N(\vec{q})}\right) \langle \vec{p}, \bar{f}(\vec{q},s) | \hat{M}(1-p_{12}) | \vec{p}, f(\vec{q},s) \rangle \theta(k_F - |\vec{q}|) . \tag{2.19}$$

Here $\hat{M}$ is a reaction matrix, which satisfies the three-dimensional BSE (2.2), and includes Pauli-Principle restrictions and dispersive effects; P_{12} is an exchange operator. (We suppress reference to isospin for simplicity.)

2.4 Matrix Elements of the Self-Energy

It is useful to introduce various matrix elements of the self-energy

$$\Sigma^{++}_{s',s}(\vec{p}) = \sum_{s'',} \int \frac{d\vec{q}}{(2\pi)^3} \left(\frac{m_N}{E_N(\vec{q})}\right) \theta(k_F - |\vec{q}|) \times \langle \bar{u}(\vec{p},s') \bar{f}(\vec{q},s'') | \hat{M}(1-p_{12}) | u(\vec{p},s) f(\vec{q},s'') \rangle , \tag{2.20}$$

$$\Sigma^{-+}_{s',s}(\vec{p}) = \langle s' | \vec{\sigma}\cdot\vec{p} | s \rangle \sum_{s''} \int \frac{d\vec{q}}{(2\pi)^3} \left(\frac{m_N}{E_N(\vec{q})}\right) \theta(k_F - |\vec{q}|)$$

$$\times \langle \bar{w}(\vec{p},\tfrac{1}{2}) \bar{f}(\vec{q},s'') | \hat{M}(1-p_{12}) | u(\vec{p},\tfrac{1}{2}) f(\vec{q},s'') \rangle \ , \tag{2.21}$$

$$\Sigma^{--}_{s',s}(\vec{p}) = \sum_{s''} \int \frac{d\vec{q}}{(2\pi)^3} \left(\frac{m_N}{E_N(\vec{q})}\right) \theta(k_F - |\vec{q}|)$$

$$\times \langle \bar{w}(\vec{p},s') \bar{f}(\vec{q},s'') | \hat{M}(1-p_{12}) | w(\vec{p},s) f(\vec{q},s'') \rangle \ . \tag{2.22}$$

In these equations the spinor $w(\vec{p},s) = v(-\vec{p},-s)$. Also $u(\vec{p},s)$ and $v(\vec{p},s)$ are the free Dirac spinors. (See Section 1.2.) If these matrix elements are defined in terms of a density matrix characterized by the free spinors, $u(\vec{p},s)$, we have

$$\Sigma^{++}_{0}(\vec{p}) = \sum_{s''} \int \frac{d\vec{q}}{(2\pi)^3} \left(\frac{m_N}{E_N(\vec{q})}\right) \theta(k_F - |\vec{q}|),$$

$$\times \langle \bar{u}(\vec{p},s) \bar{u}(\vec{q},s') | \hat{M}(1-p_{12}) | u(\vec{p},s) u(\vec{q},s') \rangle \ , \tag{2.23}$$

$$\Sigma^{+-}_{ss'}(\vec{p}) = \langle s' | \vec{\sigma}\cdot\hat{p} | s \rangle \Sigma^{+-}_{0}(\vec{p})$$

$$= \sum_{s''} \int \frac{d\vec{q}}{(2\pi)^3} \left(\frac{m_N}{E_N(\vec{q})}\right) \theta(k_F - |\vec{q}|), \tag{2.24}$$

$$\times \langle \bar{u}(\vec{p},s') \bar{u}(\vec{q},s'') | \hat{M}(1-p_{12}) | w(\vec{p},s) u(\vec{q},s'') \rangle \ ,$$

and

$$\Sigma^{--}_{0}(\vec{p}) = \sum_{s''} \int \frac{d\vec{q}}{(2\pi)^3} \left(\frac{m_N}{E_N(\vec{q})}\right) \theta(k_F - |\vec{q}|) \tag{2.25}$$

$$\times \langle \bar{w}(\vec{p},s) \bar{u}(\vec{q},s') | \hat{M}(1-p_{12}) | w(\vec{p},s) u(\vec{q},s') \rangle \ ,$$

etc. Note that $\Sigma^{++}(\vec{p})$ and $\Sigma^{--}(\vec{p})$, are independent of the spin index s.

Various figures and tables appearing in Ref.7 give the values obtained for $\Sigma_0{}^{++}(\vec{p})$, $\Sigma_0{}^{+-}(\vec{p})$ and $\Sigma_0{}^{--}(\vec{p})$ for different values of the Fermi momentum, k_F, and for two different interactions, HEA and HM2. The Hartree-Fock results for $\Sigma_0{}^{++}(\vec{p})$, $\Sigma_0{}^{+-}(\vec{p})$ and $\Sigma_0{}^{--}(\vec{p})$, obtained by replacing $\hat{M}$ by U in the above equations, can also found in Ref.7.

2.5 Calculation of the Self-Energy

L.Celenza and C.Shakin have presented a general formalism for the study of the scattering of a relativistic nucleon from a spin-zero target.[7,24] In the center-of-mass of the nucleon-nucleus system, the form of the relativistic optical potential for the case of an off-mass-shell nucleon is

$$\begin{aligned}
&\langle \vec{k}' | \Sigma(\vec{p}) | \vec{k} \rangle \\
&= A + \gamma^0 B + \frac{\vec{\gamma}\cdot(\vec{k}+\vec{k}')}{2m_N} C + \frac{iD}{m_N} \vec{\gamma}\cdot(\vec{k}'-\vec{k}) - \frac{E}{2m_N} \gamma^0 \vec{\gamma}\cdot(\vec{k}'-\vec{k}) \\
&- \frac{iF}{2m_N} [\, \gamma^0 \vec{\gamma}\cdot(\vec{k}'+\vec{k})] + \frac{iG}{m_N{}^2} \vec{\Sigma}\cdot(\vec{k}' \times \vec{k}) - \frac{iH}{m_N{}^2} \gamma^0 \vec{\Sigma}\cdot(\vec{k}' \times \vec{k}) \,,
\end{aligned} \tag{2.26}$$

where A, B, C, D, E, F, G and H are eight scalar invariants that should be determined. In the case of nuclear matter, where $\vec{k} = \vec{k}'$, the number of functions required to specify the self-energy is three if the Hamiltonian is invariant under the time reversal operation. Thus, in the case of nuclear matter, where N = Z, we have

$$\Sigma_{\alpha_T',\alpha_T}(p) = \delta_{\alpha_T',\alpha_T}\left[\, A(p) + \gamma^0 B(p) + \frac{\vec{\gamma}\cdot\vec{p}}{m_N} C(p) \,\right], \qquad (2.27)$$

where α_T, α'_T are isospin indices. Using the formulas listed in Appendix 9 (Ref.7), we can calculate the self-energy $\Sigma(p)$ for the exchange of σ, ω, ρ and π mesons. For the case of the exchange of δ, η and ϕ meson one can calculate the self-energy $\Sigma(p)$ using following formulas:

δ -meson

$$\Sigma^{\delta}_{\substack{\alpha',\alpha \\ \alpha'_T\alpha}}(p) = 3\delta_{\alpha'_T\alpha_T}\int \frac{d\vec{q}}{(2\pi)^3}\left(\frac{m_N}{E_N(\vec{q})}\right)\left(\frac{g_\delta^2}{m_\delta^2}\right)\left(\frac{F^2(p-q)}{1-\frac{(p-q)^2}{m_\delta^2}}\right)\left(\frac{\not{q}+m_N}{2m_N}\right)_{\alpha'\alpha}.$$

$$A_\delta(p) = \frac{3}{2}\int \frac{d\vec{q}}{(2\pi)^3}\left(\frac{m_N}{E_N(\vec{q})}\right)\left(\frac{g_\delta^2}{m_\delta^2}\right)\left(\frac{F^2(p-q)}{1-\frac{(p-q)^2}{m_\delta^2}}\right),$$

$$B_\delta(p) = \frac{3}{2}\int \frac{d\vec{q}}{(2\pi)^3}\left(\frac{m_N}{E_N(\vec{q})}\right)\left(\frac{g_\delta^2}{m_\delta^2}\right)\left(\frac{F^2(p-q)}{1-\frac{(p-q)^2}{m_\delta^2}}\right),$$

$$C_\delta(p) = -\frac{3}{2}\int \frac{d\vec{q}}{(2\pi)^3}\left(\frac{m_N}{E_N(\vec{q})}\right)\left(\frac{g_\delta^2}{m_\delta^2}\right)\left(\frac{\vec{q}\cdot\vec{p}}{\vec{p}^2}\right)\left(\frac{F^2(p-q)}{1-\frac{(p-q)^2}{m_\delta^2}}\right) .$$

η -meson

$$\Sigma^{\eta(pv)}_{\substack{\alpha',\alpha \\ \alpha_T'\alpha_T}}(p) = (-1)\int \frac{d\vec{q}}{(2\pi)^3}\left(\frac{m_N}{E_N(\vec{q})}\right)\left(\frac{g_\eta^2}{m_\eta^2}\right)\left(\frac{F^2(p-q)}{1-\frac{(p-q)^2}{m_\eta^2}}\right)\delta_{\alpha_T'\alpha_T}$$

$$\times \frac{1}{8m_\eta^2}\left(2m_N^2 - 2(p\cdot q)\left(1+\frac{\not{q}}{m_N}\right) + 2\not{p}m_N\right) .$$

$$A_\eta^{(pv)}(p) = \int \frac{d\vec{q}}{(2\pi)^3}\left(\frac{m_N}{E_N(\vec{q})}\right)\left(\frac{g_\eta^2}{m_\eta^2}\right)\left(\frac{F^2(p-q)}{1-\frac{(p-q)^2}{m_\eta^2}}\right)\frac{1}{8m_N^2}(2p\cdot q-2m_N^2) ,$$

$$B_\eta^{(pv)}(p) = \int \frac{d\vec{q}}{(2\pi)^3}\left(\frac{m_N}{E_N(\vec{q})}\right)\left(\frac{g_\eta^2}{m_\eta^2}\right)\left(\frac{F^2(p-q)}{1-\frac{(p-q)^2}{m_\eta^2}}\right)\frac{1}{8m_N^3}2p^0\left((p\cdot q)-m_N^2\right),$$

$$C_\eta^{(pv)}(p) = -\int \frac{d\vec{q}}{(2\pi)^3}\left(\frac{m_N}{E_N(\vec{q})}\right)\left(\frac{g_\eta^2}{m_\eta^2}\right)\left(\frac{F^2(p-q)}{1-\frac{(p-q)^2}{m_\eta^2}}\right)\frac{1}{8m_N^2}2\left((p\cdot q)-m_N^2\right) .$$

ϕ -meson

$$\Sigma^{\phi}_{\substack{\alpha',\alpha \\ \alpha_T'\alpha}}(p) = \delta_{\alpha_T'\alpha_T}\int \frac{d\vec{q}}{(2\pi)^3}\left(\frac{m_N}{E_N(\vec{q})}\right)\left(\frac{g_\phi^2}{m_\phi^2}\right)\left\{(\gamma_\mu)_{\alpha',\alpha}F^2(o)T_r\left(\gamma^\mu\left(\frac{\not{q}+m_N}{2m_N}\right)\right)T_r\mathbb{I}^{iso}\right.$$

$$\left. - \left(\frac{F^2(p-q)}{1-\frac{(p-q)^2}{m_\phi^2}}\right)\left(\gamma_\mu\left(\frac{\not{q}+m_N}{2m_N}\right)\gamma^\mu\right)_{\alpha',\alpha}\right\} .$$

$$A_\phi(p) = 4\int \frac{d\vec{q}}{(2\pi)^3}\left(\frac{m_N}{E_N(\vec{q})}\right)\left(\frac{g_\phi^2}{m_\phi^2}\right)\left(-\frac{F^2(p-q)}{2\left(1-\frac{(p-q)^2}{m_\phi^2}\right)}\right) ,$$

$$B_\phi(p) = 4\int \frac{d\vec{q}}{(2\pi)^3}\left(\frac{m_N}{E_N(\vec{q})}\right)\left(\frac{g_\phi^2}{m_\phi^2}\right)\left(F^2(o)+\frac{F^2(p-q)}{4\left(1-\frac{(p-q)^2}{m_\phi^2}\right)}\right) ,$$

$$C_\phi(p) = 4\int \frac{d\vec{q}}{(2\pi)^3}\left(\frac{m_N}{E_N(\vec{q})}\right)\left(\frac{g_\phi^2}{m_\phi^2}\right)\left(\frac{\vec{q}\cdot\vec{p}}{\vec{p}^2}\right)\left(-\frac{F^2(p-q)}{4\left(1-\frac{(p-q)^2}{m_\phi^2}\right)}\right) .$$

Chapter 3

The Pseudoparticle Model

3.1 Motivation

In Fig.3.1[7] we can see the role of correlations in the calculation of $\Sigma_0^{++}(\vec{p})$. We can ask if the Hartree-Fock results for $\Sigma_0^{++}(\vec{p})$ for the potential HEA can be "shifted" to the curves which include the effects of correlations. The required shifts can be obtained by adding a short-range interaction (see Fig.3.2), that is, an interaction which arises from the exchange of a few massive pseudoparticles.

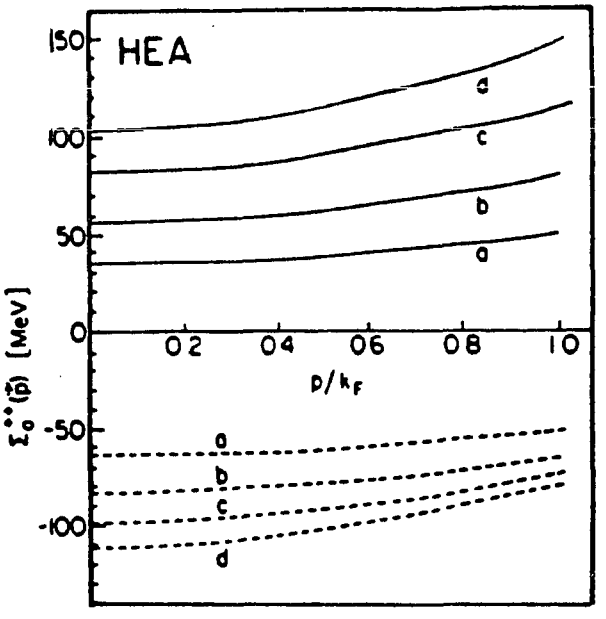

The solid lines: Hartree-Fock approximation($\hat{M}$ = U); the dashed curves include correlation effects. (a)k_F=1.2 fm^{-1}, (b)k_F=1.36 fm^{-1}, (c)k_F=1.5 fm^{-1}, (d)k_F=1.6 fm^{-1}.

Fig.3.1

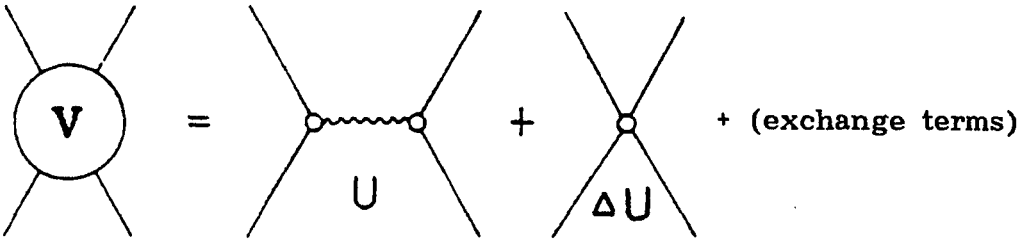

Fig.3.2

Our first goal is to find a $V_{eff} = U + \Delta U$, which when inserted into Eqs.(2.19) - (2.22), will reproduce the results obtained with the reaction matrix $\hat{M}$. It turns out that this can be done by adding a few massive pseudoparticles with appropriate (real or imaginary) coupling constants. In order to understand our model, let us look at the contribution of sigma exchange to certain matrix elements of the potential U:

$$\langle \vec{p}_1' s_1', \vec{p}_2' s_2' | U^{++++}(1 - p_{12}) | \vec{p}_1 s_1, \vec{p}_2 s_2 \rangle$$

$$= g_0^2 \left(\frac{[\bar{u}(\vec{p}_1' s_1') u(\vec{p}_1 s_1)][\bar{u}(\vec{p}_2' s_2') u(\vec{p}_2 s_2)]}{q^2 - m_\sigma^2 + i\eta} \right.$$

$$\left. - \frac{[\bar{u}(\vec{p}_2' s_2') u(\vec{p}_1 s_1)][\bar{u}(\vec{p}_1' s_1') u(\vec{p}_2 s_2)]}{(p_1 - p_2')^2 - m_\sigma^2 + i\eta} \right) .$$

Here we have again suppressed reference to isospin and to the vertex cut-off (or form factors) used in the one-boson-exchange model. These features are included in our calculations, however.

We now defined the contribution of pseudo-sigma exchange as follows,

$$\begin{aligned}
&\langle \vec{n}'s'\ \vec{n}'s' |\ \Delta U^{++++}(1-P_{NN})|\vec{n}\,s\ \vec{n}\,s\rangle \\
&\langle \vec{p}_1's_1', \vec{p}_2's_2' |\ \Delta U_\sigma^{++++}(1-P_{12})|\vec{p}_1s_1, \vec{p}_2s_2\rangle \\
&= -\delta g_\sigma^2 \left(\frac{[\bar{u}(\vec{p}_1's_1')u(\vec{p}_1s_1)][\bar{u}(\vec{p}_2's_2')u(\vec{p}_2s_2)]}{q^2 - M_\sigma^2 + i\eta} \right. \\
&\qquad \left. - \frac{[\bar{u}(\vec{p}_2's_2')u(\vec{p}_1s_1)][\bar{u}(\vec{p}_1's_1')u(\vec{p}_2s_2)]}{(p_1 - p_2')^2 - M_\sigma^2 + i\eta} \right),
\end{aligned}$$

where the minus sign to the right of the equals sign can be thought of as arising from the use of an imaginary coupling constant for the pseudoparticle of mass M_σ. The extension of these definitions to the exchange of omega "mesons" and pseudo-omega "mesons" is straightforward.

Again, with reference to the OBE potential, we put

$$V_{eff} = V^{(1)}_{eff} + V^{(2)}_{eff} \quad , \tag{3.1}$$

where

$$V^{(1)}_{eff} = U = \sum_i U_i \quad . \tag{3.2}$$

Here the U_i represent the Born terms of OBE model (including the exchange terms) and

$$V^{(2)}_{\text{eff}} = \Delta U = \sum_j \Delta U_j \ , \tag{3.3}$$

represents the Born terms arising from the exchange of pseudoparticles. We shall use this approximation in our calculations.

Using the results of Appendix 9 (Ref.7) and the formulas in Section 2.5, we calculate the following quantities in the Hartree-Fock approximation:

$$A(p) = \sum_i A_i(p) + \sum_j \Delta A_j(p) \ , \tag{3.4}$$

$$B(p) = \sum_i B_i(p) + \sum_j \Delta B_j(p) \ , \tag{3.5}$$

$$C(p) = \sum_i C_i(p) + \sum_j \Delta C_j(p) \ . \tag{3.6}$$

We then calculate the matrix elements of the self-energy

$$\Sigma^{++}_{ss'}(\vec{p}) = \delta_{ss'}\left[A(p) + \frac{E_N(\vec{p})}{m_N} B(p) + \frac{\vec{p}^2}{m_N^2} C(p) \right], \tag{3.7}$$

$$\Sigma^{-+}_{ss'}(\vec{p}) = \langle s | \vec{\sigma}\cdot\hat{\vec{p}} | s' \rangle \frac{|\vec{p}|}{m_N} \left[C(p) - A(p) \right], \tag{3.8}$$

and

$$\Sigma^{--}_{ss'}(\vec{p}) = \delta_{ss'}\left[-A(p) + \frac{E_N(\vec{p})}{m_N} B(p) - \frac{\vec{p}^2}{m_N^2} C(p) \right] . \tag{3.9}$$

As an example, let us look at the contributions of omega and pseudo-omega exchange:

$$A_\omega(p) = 4 \int \frac{d\vec{q}}{(2\pi)^3} \left(\frac{m_N}{E_N(\vec{q})}\right) \left(\frac{g_\omega^2}{m_\omega^2}\right) \left(- \frac{F^2(p-q)}{2\left(1 - \frac{(p-q)^2}{m_\omega^2}\right)} \right) \ , \tag{3.10}$$

$$\Delta A_\omega(p) = -4 \int \frac{d\vec{q}}{(2\pi)^3} \left(\frac{m_N}{E_N(\vec{q})}\right) \left(\frac{\delta g_\omega^2}{M_\omega^2}\right) \left(- \frac{F^2(p-q)}{2\left(1 - \frac{(p-q)^2}{M_\omega^2}\right)} \right) . \quad (3.11)$$

We see that we are using the potential, ΔU, to replace the higher-order terms in the ladder diagrams (see Fig.3.3) of the theory with correlations.

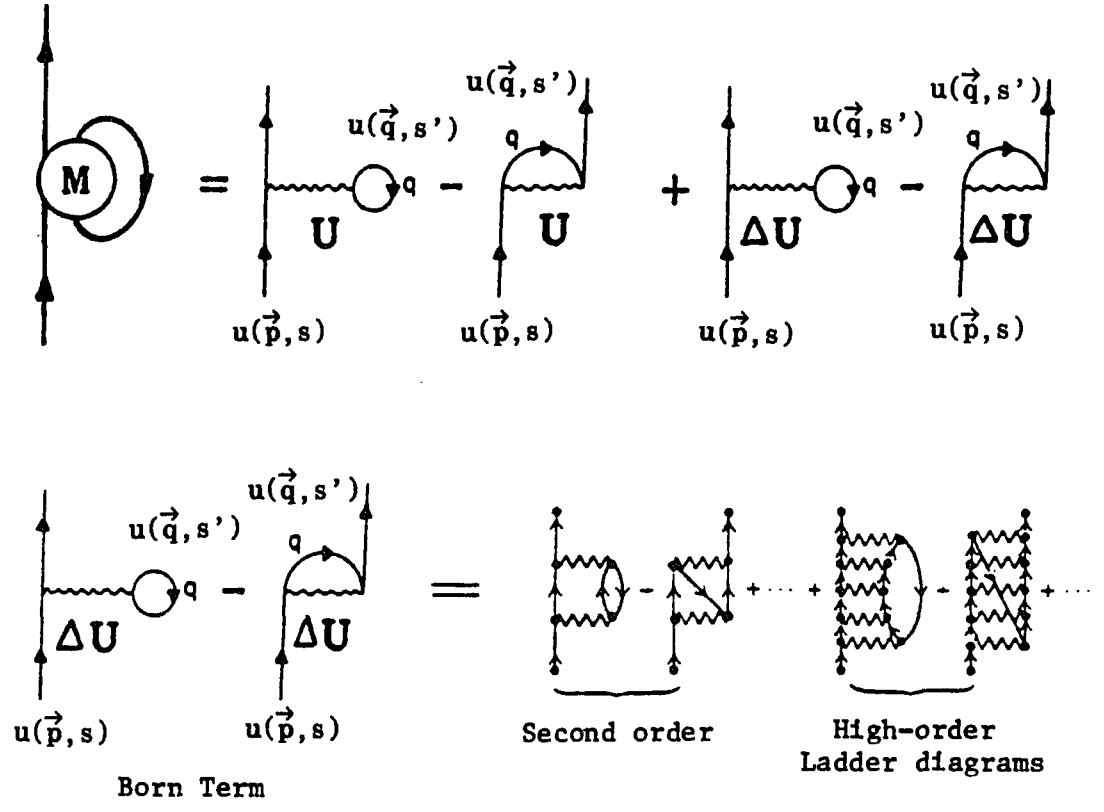

Fig.3.3

With reference to the potential HEA, it turns out that we only need introduce three pseudoparticles to reproduce various matrix

elements of the reaction matrix. These are pseudo-sigma, pseudo-omega and pseudo-delta fields. One might think that a pseudo-pion would be required, but, as may be seen from the figures in Ref.7, the exchange of pions, beyond the Born term, gives rise to effects that can be readily simulated by sigma exchange. Therefore, in first approximation, the role of pseudoparticle exchange is to reduce the repulsion of the omega-exchange Born term, reduce the attraction of the sigma-exchange Born term, and to simulate the sigma-like attraction obtained from higher-order terms in the exchange of pions. As we will see, the simulation of correlation effects in pion exchange will lead to the use of a negative value for δg^2_σ in Eq.(3.2). This corresponds to the use of a real coupling constant for the pseudo-sigma field. We put

$$V^{(1)}_{eff} = U$$
$$= U_\sigma + U_\omega + U_\rho + U_\pi + U_\delta + U_\eta + U_\phi \tag{3.12}$$

and

$$V^{(2)}_{eff} = \Delta U$$
$$= \Delta U_\sigma + \Delta U_\omega + \Delta U_\delta \ . \tag{3.13}$$

Therefore, there are six parameters (at each density): (δg^2_σ), (δg^2_ω), (δg^2_δ) , M_σ , M_ω and M_δ. We fix the values of the mass

parameters to be M_σ=1.0 GeV, M_ω=1.0 GeV and M_δ=1.25 GeV, leaving only three parameters to be determined. We remark that the choice of fairly large masses for the pseudoparticles follows from the observation that the role of correlations in the calculation of Σ^{++}, for example, is to shift the magnitude of Σ^{++} without changing the momentum dependence.[7] Such a shift can be obtained from a short-range interaction, that is, an interaction which aries from the exchange of a massive particle. It is obvious that this choice is not unique. Further discussion of this matter can be found in Section 3.4.

3.2 The Determination of the Coupling Constants of the Pseudoparticles

Our discussion is facilitated by making use of the figures appearing in Ref.7, which gave the contributions of the various mesons in the calculation of the self-energy. First, we study the potential HEA. We reproduce some of the relevant figures in this work.(See Figs.1-8.) As a specific example, let us consider the repusion in Σ^{++} obtained from ω and ϕ exchange (as shown in Fig.2) for the potential HEA. The solid line is the Hartree-Fock result and the dashed line includes the effects of correlations. We want to choose the coupling constants of the pseudoparticles so that, instead of the results shown by the solid line, we get the results shown by

the dashed lines. We can accomplish this by adding a pseudo-omega to the model to adjust the contribution of the ω field, so that one obtains values corresponding to the dashed lines rather than the solid lines. The contributions of particle plus pseudoparticle exchange are denoted by the black dots. It can be seen that, with the appropriate choice of coupling constant for the pseudoparticle, the black dots can be made to fall on the dashed curve. This can also be done for the ϕ field.

At this point we have adjusted the ω and ϕ contributions by adding pseudo-omega particles to the model. With the coupling constants fixed from the study of Σ^{++}, we can then calculate the contributions of the pseudoparticles to Σ^{+-}. With reference to Fig.5, we note that the solid lines denote the Hartree-Fock results for σ, ω and ϕ exchange. If we then add the contributions of pseudo-omega exchange (with the coupling constants fixed as discussed above), we obtain the black dots. Note that the black dots fall on the curves which describe the effects of correlations (dashed lines).

Therefore, we see that once we fix the pseudoparticle coupling constants from the study of Σ^{++}, no further parameter modifications are needed to adjust the contributions to Σ^{+-}. (Again, the use of a single pseudo-omega particle will adjust the summed contribution of the ω and ϕ fields to Σ^{+-}.) In a similar fashion we can adjust the contributions of σ, ω , π and δ exchange to Σ^{++} by adding the appropriate pseudoparticles. Again, the coupling constants can be determined by studying the role of correlations in the calculation of

Σ^{++}. It is then found that the situation in the case of Σ^{+-} is satisfactory(see Figs.5 and 6).

We should note that the σ and ω fields behave quite differently in the calculation of Σ^{+-}. For example, in the Hartree approximation, the contribution of the ω field is zero, while the contribution from σ exchange is large. (The contributions of the ω field to Σ^{+-} shown in the figures comes from the exchange terms of the Hartree-Fock approximation.) Therefore, while one might fix the (total) value of Σ^{++} by adding only one type of pseudoparticle, that procedure would lead to a poor fit to Σ^{+-}. On the other hand, the procedure we chose works quite well.

In summary, we can say that the coupling constants of the pseudoparticles may be adjusted to fit the contributions of the various mesons to Σ^{++} which were obtained in the reaction matrix calculations. It is then found that the corresponding results for Σ^{+-} are satisfactory, without the need for further modification of the coupling constants.

For other potentials we use the same method to determine the coupling constants of the pseudoparticles. The results for the potential HM2 can be found in Figs.9-16.

3.3 The Density Dependence of the Coupling Constants

We have carried out our calculations at a number of different densities. It is useful to parameterize the density dependence of the various δg^2_i. Let i denote either pseudo-sigma, pseudo-omega, or pseudo-delta mesons. We consider values of $\rho/\rho_{NM} \leq 1.25$.

For the potential HEA:

$$\delta g_i^2(k_F)=\delta g_i^2(k_F^{NM})\{1+a_1[1-(\frac{\rho}{\rho_{NM}})^{2/3}]+a_2[1-(\frac{\rho}{\rho_{NM}})^{4/3}]+a_3[1-(\frac{\rho}{\rho_{NM}})^2]\} \quad . \tag{3.14}$$

$$(\text{ for values of } \rho/\rho_{NM} \leq 1.25)$$

Here $k_F^{NM} = 1.36\ fm^{-1}$ and ρ_{NM} is the density of nuclear matter. The results presented in the following discussion are for the values

$$\begin{aligned} &\delta g^2_\sigma=-2.81,\ M_\sigma=1.0\ GeV,\ a_1=0.357, \\ &\delta g^2_\omega=14.2,\ M_\omega=1.0\ GeV,\ a_2=-0.0735, \\ &\delta g^2_\delta=5.54,\ M_\delta=1.25\ GeV,\ a_3=0.00297. \end{aligned} \tag{3.15}$$

In Table 3.1 we present the values of $\delta g_i^2(k_F)$ obtained from Eq.(3.14) and from the parameters listed above.

For the potential HM2:

$$\delta g_i^2(k_F)=\delta g_i^2(k_F^{NM})\{1+b_1[1-(\frac{\rho}{\rho_{NM}})^{2/3}]+b_2[1-(\frac{\rho}{\rho_{NM}})^{4/3}]+b_3[1-(\frac{\rho}{\rho_{NM}})^2]\} \quad . \tag{3.16}$$

$$(\text{ for values of } \rho/\rho_{NM} \leq 1.25)$$

Again $k_F^{NM} = 1.36$ fm^{-1} and ρ_{NM} is the density of nuclear matter. The results presented in the following are for the values

$$\delta g^2{}_\sigma = -1.15, \; M_\sigma = 1.0 \text{ GeV},$$

$$\delta g^2{}_\omega = 6.52, \; M_\omega = 1.0 \text{ GeV}, \tag{3.17}$$

$$b_1 = 3.6753, \; b_2 = -2.7150, \; b_3 = 0.6724.$$

In Table 3.2 we present the values of $\delta g_i{}^2(k_F)$ obtained from Eq.(3.16) and from the parameters listed above.

Note that $\delta g^2{}_\sigma$ is a negative number. With our conventions that means that the total pseudo-sigma exchange gives an attractive contribution. The reason for this will be made clear in the next chapter. Further, $\delta g^2{}_\omega$ and $\delta g^2{}_\delta$ are positive numbers, leading to attractive contributions from the exchange of these pseudoparticles. Therefore we see that all the pseudoparticle exchanges lead to attractive contributions to the mean field, Σ^{++}.

Table 3.1

The coupling constants δg^2_σ, δg^2_ω and δg^2_δ are given as a function of density(see text) for the potential HEA.

	$\frac{1}{4\pi}\delta g^2_\sigma(\rho)$	$\frac{1}{4\pi}\delta g^2_\omega(\rho)$	$\frac{1}{4\pi}\delta g^2_\delta(\rho)$
$(1/4)\rho_{NM}$	-3.25	16.42	6.40
$(1/2)\rho_{NM}$	-3.06	15.48	6.04
$(3/4)\rho_{NM}$	-2.92	14.77	5.76
ρ_{NM}	-2.81	14.20	5.54
$(5/4)\rho_{NM}$	-2.72	13.73	5.35

Table 3.2

The coupling constants δg^2_σ, and δg^2_ω are given as a function of density(see text) for the potential HM2.

	$(1/4\pi)\delta g^2_\sigma(\rho)$	$(1/4\pi)\delta g^2_\omega(\rho)$
$(1/4)\rho_{NM}$	-1.79	10.17
$(1/2)\rho_{NM}$	-1.41	8.00
$(3/4)\rho_{NM}$	-1.23	6.98
ρ_{NM}	-1.15	6.52
$(5/4)\rho_{NM}$	-1.12	6.34

3.4 Alternative Parameter Choices

(1) If we make another choice of mass parameters for the pseudoparticles , we find other values for (δg^2_i). For instance, for the potential HEA, we fix the values of the mass parameters to be $M_\sigma = M_\omega = M_\delta = 1.5$ GeV. We found that either

$$\delta g^2_\sigma = 5.0 \quad , \quad a_1 = 1.7036 \ ,$$

$$\delta g^2_\omega = 20.2 \ , \quad a_2 = -1.5968 \ , \tag{3.18}$$

$$\delta g^2_\delta = -6.54, \quad a_3 = 0.5369 \ ,$$

or

$$\delta g^2_\sigma = 1.81 \ , \quad a_1 = 1.7764 \ ,$$

$$\delta g^2_\omega = 26.8 \ , \quad a_2 = -1.6624 \ , \tag{3.19}$$

$$\delta g^2_\delta = -4.49, \quad a_3 = 0.5563 \ ,$$

are satisfactory choices. (See Fig.17.)

(2) For the potential HEA, we fix the values of the mass parameters to be $M_\sigma = M_\omega = 1$ GeV, $M_\delta = 1.25$ GeV. We have also found other sets of δg_i^2 and a_i (see Table 3.3).

For the calculations of the matrix elements of the self-energy, however, the use of these alternate sets yield results which differ only slightly from those given in Section 3.3. (See Figs.18-20.) However, if we consider other properties of nuclear matter, the range of choice for the coupling constants of the pseudoparticles is limited. (See Section 4.2.3.)

Table 3.3

The coupling constants $\delta g^2{}_\sigma$, $\delta g^2{}_\omega$ and $\delta g^2{}_\delta$ and constants a_1, a_2, a_3 in Eq.(3.14) are given for different approximations used in the calculation of matrix elements corresponding to the potential HEA.

	$\frac{1}{4\pi}\delta g^2_\sigma$	$\frac{1}{4\pi}\delta g^2_\omega$	$\frac{1}{4\pi}\delta g^2_\delta$	a_1	a_2	a_3
Approx.1	-2.81	14.2	5.54	0.357	-0.0735	0.00297
Approx.2	-2.81	13.6	5.89	4.0544	-3.7106	1.1604
Approx.3	-2.60	19.0	2.43	5.7242	-5.2140	1.6043
Approx.4	-5.00	11.6	3.44	4.3563	-3.9830	1.2410
Approx.5	-6.20	10.0	2.45	4.4119	-4.0338	1.2562
Approx.6	-1.81	16.2	5.81	4.4842	-4.0977	1.2746
Approx.7	-3.50	16.6	2.54	5.3599	-4.8866	1.5077
Approx.8	-4.30	13.2	3.54	4.5871	-4.1908	1.3024

Chapter 4

The Nucleon Self-Energy and the Migdal Parameters

4.1 The Nucleon Self-Energy

4.1.1 The Contributions from Pseudoparticle Exchange

In Fig.1 we present the results obtained for $\Sigma_0^{++}(\vec{p})$, for various densities, for the potential HEA. The solid lines are the Hartree-Fock results and the dashed lines include the effects of correlation[7]. The small dots in the lower part of the figure are based upon the use of V_{eff}[see Eqs.(3.1)-(3.16)].

It is useful at this point to consider the contribution of each meson to the calculation of $\Sigma_0^{++}(\vec{p})$. In Figs.2 and 3 we show the contributions of ω, ϕ, π, σ, and δ mesons. (The contribution of the η meson is small and is not shown here.) In Figs. 2 and 3 the solid lines are the Hartree-Fock contributions at nuclear matter densities. Therefore, adding these various contributions will yield the solid curve labeled by b in Fig.1. The dashed lines in Figs.2 and 3 are the contributions arising from the exchange of each meson between correlated wave functions.[7] The various solid circles in Figs.2 and 3 are obtained as follows. The attractive contribution from pseudo-omega exchange, with coupling $\delta g^2_\omega/(4\pi)=14.20$(see Table 3.1), is divided into two parts, one part $[(\delta g^2_\omega)_1=12.30]$ ascribed to correct the result of ω exchange and another part $[(\delta g^2_\omega/4\pi)_2=1.90]$ ascribed

to correct the result of ϕ exchange - see Table 4.1. With this choice we obtain the results shown in Fig.2. (Of course, it is only the summed result of both these corrections, that is relevant to the construction of Fig.1.)

Table 4.1

Coupling constants and meson masses for the pseudoparticles for the potential HEA for $k_F = k_F^{NM} = 1.36$ fm^{-1}. (A factor of m^2/M^2 is included so that the strengths of the potentials arising from particle and pseudoparticle exchange at zero momentum transfer can be compared.)

pseudoparticle	Mass (GeV)	$\frac{\delta g^2}{4\pi}$	$\left(\frac{\delta g^2}{4\pi}\right)_1$	$\left(\frac{\delta g^2}{4\pi}\right)_2$	$\left(\frac{\delta g^2}{4\pi}\right)\left(\frac{m^2}{M^2}\right)$
pseudo-sigma	1.00	-2.81	3.78	-6.59	-0.70
pseudo-omega	1.00	14.20	12.30	1.90	8.70
pseudo-delta	1.25	5.54			3.27

Now consider the results shown in Fig.3. The solid circles for the δ exchange contribution reproduce the results of δ exchange in the presence of correlations(dashed line). Now consider pseudo-sigma exchange. From Table 3.1 we see that $(\delta g^2_\sigma/4\pi)$=-2.81 at

nuclear matter densities. The negative sign here means that the total result for pseudo-sigma exchange is attractive. This can be understood from Table 4.1 and Fig.3. As can be seen from Fig.3, pseudo-sigma exchange is required to provide attraction to give the correct result for correlated pion exchange(dashed line) and repulsion to yield the correct result for correlated sigma exchange(dashed line.) This is accomplished by separating $(\delta g^2_\sigma/4\pi)= -2.81$ into two terms: $[(\delta g^2_\sigma/4\pi)_1]= 3.78$ and $[(\delta g^2_\sigma/4\pi)_2]= -6.59$ as in Table 4.1. (Formally we can consider a negative value for $\delta g^2/(4\pi)$ as arising from the exchange of the pseudoparticle with a real rather than a complex coupling constant. We can avoid confusion with respect to our choice of signs by referring to Figs.2 and 3. There one can see whether pseudoparticle exchange yields a repulsive or attractive contribution.)

In Fig.4 we exhibit $\Sigma_0^{+-}(\vec{p})$. Again the solid lines are the Hartree-Fock results and dashed lines are the results of the reaction matrix calculation of Ref.7. The small crosses, circles and dots represent the Hartree-Fock results based upon the use of V_{eff} of Eqs.(3.1)-(3.16). Again, in Fig.5 and Fig.6, we show the contributions of the individual mesons. As discussed previously, we have separated pseudo-omega exchange into contributions which correct the omega and phi fields. Similarly, pseudo-sigma exchange is separated into terms which correct the sigma and pion contributions. The calculation is made with the coupling constants used previously and listed in Table 4.1. It is of interest to note that the separation of the pseudoparticle exchange effects into ω and

ϕ channels and σ and π channels, which was made in the case of Σ^{++}, also works in the case of Σ^{-+}(see Figs.5 and 6).

In Fig.7 we present results for $\Sigma_0^{--}(\vec{p})$. The small inaccuracies in the fit obtained to the dashed curves (see the solid circles, open circles, and crosses) are not significant since $\Sigma_0^{--}(\vec{p})$ appears as a correction to a large denominator (of the order of 2000 MeV) in the effective potential, U_{eff}, which we define below. In Fig.8 we show the contribution of the various mesons. Again, the solid lines are the results obtained using the Hartree-Fock approximation and the dashed lines are the results including correlation effects.[7] The triangles, squares, crosses, solid circles and open circles are the result for meson plus pseudo-meson exchange for σ, ω, π, ϕ and δ fields. Here, unlike the results obtained for Σ^{++} and Σ^{-+}, we see that the individual mesonic contributions (dashed lines) are not very well reproduced by the pseudoparticle model. However, this is not particularly important since the summed contributions reproduce Σ^{--} rather well (see Fig.7).

For the potential HM2, we have a similar discussion and similar results, except that we use only two pseudoparticles: pseudo-sigma and pseudo-omega . At the density of nuclear matter, the attractive contribution from pseudo-omega exchange, with coupling constant $\delta g^2_\omega/(4\pi)=6.52$(see Table 3.2), is divided into two parts, one part $[(\delta g^2_\omega/4\pi)_1= 5.63]$ ascribed to correct the result of ω exchange and another part $[(\delta g^2_\omega/4\pi)_2=0.89]$ ascribed to correct the result of ρ exchange - see Table 4.2. We separate $(\delta g^2_\sigma/4\pi)=-1.15$ into two

terms: $(\delta g^2_\sigma/4\pi)_1$=4.34 to provide attraction to give the correct result for correlated pion exchange (dashed line) and $(\delta g^2_\sigma/4\pi)_2$=-5.49 to provide repulsion to yield the correct result for correlated sigma exchange (dashed line) --see Table 4.2 and Figs.10-11.

Table 4.2

Coupling constants and meson masses for the pseudoparticles for the potential HM2 for $k_F = k_F^{NM} = 1.36$ fm^{-1}. (A factor of m^2/M^2 is included so that the strengths of the potentials arising from particle and pseudoparticle exchange at zero momentum transfer can be compared.)

pseudoparticle	Mass (GeV)	$\frac{\delta g^2}{4\pi}$	$\left(\frac{\delta g^2}{4\pi}\right)_1$	$\left(\frac{\delta g^2}{4\pi}\right)_2$	$\left(\frac{\delta g^2}{4\pi}\right)\left(\frac{m^2}{M^2}\right)$
pseudo-sigma	1.00	-1.15	4.34	-5.49	-0.31
pseudo-omega	1.00	6.52	5.63	0.89	4.00

4.1.2 The Effective Potential

We saw, in Ref.7, that if one reduced the Dirac equation to an equivalent Schroedinger form, the effective potential has the structure

$$U_{eff}(\vec{p}) \cong \frac{m_N}{E_N(\vec{p})}\Sigma^{++}(\vec{p}) + \left(\frac{m_N}{E_N(\vec{p})}\right)^2 \frac{\Sigma^{+-}(\vec{p})\Sigma^{-+}(\vec{p})}{2m_N + \frac{m_N}{E_N(\vec{p})}\left[\Sigma^{++}(\vec{p}) - \Sigma^{--}(\vec{p})\right]} \qquad (4.1)$$

for $|\vec{p}| \leq k_F$. More precisely, the quasiparticle energy in nuclear matter is $\varepsilon(\vec{p}) = (\vec{p}^2 + m^2_N)^{\frac{1}{2}} + U_{eff}(\vec{p})$. The quantities, $\Sigma^{++}(\vec{p})$, $\Sigma^{+-}(\vec{p})$, and $\Sigma^{--}(\vec{p})$ differ from $\Sigma_0{}^{++}(\vec{p})$, $\Sigma_0{}^{+-}(\vec{p})$, and $\Sigma_0{}^{--}(\vec{p})$ in being defined in terms of the correct density matrix for the system, that is, the density matrix expressed in terms of the spinors $f(\vec{q},s)$ — see Eq.(2.13). Note that if $\Sigma^{++}(\vec{p})$, $\Sigma^{+-}(\vec{p})$, and $\Sigma^{--}(\vec{p})$ are replaced by $\Sigma_0{}^{++}(\vec{p})$, $\Sigma_0{}^{+-}(\vec{p})$, and $\Sigma_0{}^{--}(\vec{p})$, one makes only a small error in the calculation of $U_{eff}(\vec{p})$, and we use that approximation here.

We now proceed to present results for $U_{eff}(\vec{p})$, calculated using the relativistic Brueckner-Hartree-Fock (RBHF) theory,[7] and compare these results with our calculations using V_{eff} of Eqs.(3.1)-(3.16). This comparison is made in Figs.21-25. As can be seen from these figures, the fit is remarkably accurate for $|\vec{p}| \leq 2$ fm^{-1}, given the simplicity of the model used to specify V_{eff}. Some of the small disagreement with the reaction matrix calculation (solid lines) is due to the fact that while we have calculated V_{eff} using the approximation, $\Sigma^{++} \simeq \Sigma_0{}^{++}$, the reaction matrix calculations, shown as solid lines, do not include that approximation.

4.2 The Migdal Parameters

4.2.1 The Definition of the Migdal Parameters

As discussed in Refs.7 and 25, we may extract the Landau-Migdal parameters of the interaction in the relativistic theory by considering the forward-scattering amplitude for two particles of momentum $\vec{p}_1$ and $\vec{p}_2$ at the Fermi surface, that is $|\vec{p}_1| = |\vec{p}_2| = k_F$(see Fig.4.1.) The scattering amplitude depends on θ, the angle between $\vec{p}_1$ and $\vec{p}_2$. (Note that θ is not the scattering angle.)

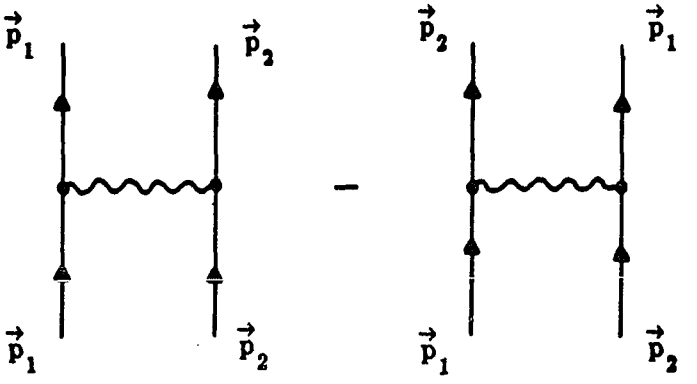

Direct and exchange interaction for the forward scattering of two particles at the Fermi surface ($|\vec{p}_1|=|\vec{p}_2|= k_F$).

Fig.4.1

This amplitude may be written, with $E_N(\vec{p}) = (\vec{p}^2 + m^2_N)^{\frac{1}{2}}$, as

$$\mathfrak{F}(\vec{p}_1,\vec{p}_2)=\left(\frac{m_N}{E_N(\vec{p}_1)}\right)\left(\frac{m_N}{E_N(\vec{p}_2)}\right)\langle\bar{f}(\vec{p}_1 s_1')\bar{f}(\vec{p}_2 s_2')|\hat{M}(1-p_{12})|f(\vec{p}_1 s_1)f(\vec{p}_2 s_2)\rangle, \tag{4.2}$$

where

$$f^{+}(\vec{p},s)f(\vec{p},s) = E_N(\vec{p})/m_N \quad . \tag{4.3}$$

The calculation of this amplitude is discussed in detail in Ref.7, where an expansion of the $f(\vec{p},s)$ in terms of the spinors $u(\vec{p},s)$ and $w(\vec{p},s)$ is used,

$$f(\vec{p},s)= \frac{1}{[1+\alpha^2(p)]^{1/2}} \left(u(\vec{p},s)+\alpha(\vec{p})\sum_{s'}<s'|\vec{\sigma}\cdot\hat{p}|s>w(\vec{p},s')\right) , \tag{4.4}$$

At this point we consider only the leading term,[7,25]

$$\mathcal{F}^{NR}(\vec{p}_1,\vec{p}_2)=\left(\frac{m_N}{E_N(k_F)}\right)^2 <\bar{u}(\vec{p}_1 s_1')\bar{u}(\vec{p}_2 s_2')|\hat{M}(1-p_{12})|u(\vec{p}_1 s_1)u(\vec{p}_2 s_2)> , \tag{4.5}$$

which appears in an expansion in the small parameter $\alpha(\vec{p})$.

We may write the scattering amplitude as follows:

$$\mathcal{F}(\vec{p}_1,\vec{p}_2)= f(\vec{p}_1,\vec{p}_2)+f'(\vec{p}_1,\vec{p}_2)\vec{\tau}_1\cdot\vec{\tau}_2+[g(\vec{p}_1,\vec{p}_2)+g(\vec{p}_1,\vec{p}_2)\vec{\tau}_1\cdot\vec{\tau}_2]\vec{\sigma}_1\cdot\vec{\sigma}_2 + \frac{1}{k_F^2}\left(h(\vec{p}_1,\vec{p}_2)+h'(\vec{p}_1,\vec{p}_2)\vec{\tau}_1\cdot\vec{\tau}_2\right)S_{12}(\vec{p}) \quad , \tag{4.6}$$

where we have introduced the tensor operator $S_{12}(\vec{p})$. Here

$$S_{12}(\vec{p})= \frac{3(\vec{\sigma}_1\cdot\vec{p})(\vec{\sigma}_2\cdot\vec{p})}{\vec{p}^2} - \vec{\sigma}_1\cdot\vec{\sigma}_2 \ , \tag{4.7}$$

and

$$\vec{p} = (\vec{p}_1 - \vec{p}_2)/2 \quad , \tag{4.8}$$

Note that f, f', g, g', h, and h' are functions of θ. These functions may be expanded in terms of Legendre polynomials:

$$f(k_F,\cos\theta)=\sum_l f_l(k_F)P_l(\cos\theta) \ , \tag{4.9}$$

$$f'(k_F,\cos\theta)=\sum_l f'_l(k_F)P_l(\cos\theta), \tag{4.10}$$

$$g(k_F,\cos\theta)=\sum_l g_l(k_F)P_l(\cos\theta) \quad , \tag{4.11}$$

$$g'(k_F,\cos\theta)=\sum_l g'_l(k_F)P_l(\cos\theta), \tag{4.12}$$

$$h(k_F,\cos\theta)=\sum_l h_l(k_F)P_l(\cos\theta) \quad , \tag{4.13}$$

$$h'(k_F,\cos\theta)=\sum_l h'_l(k_F)P_l(\cos\theta). \tag{4.14}$$

Actually, for a short-range force, only the first few terms of these expansions will be significant. Using the functions given above and expansions of these functions in Legendre functions, we get $f_0,f_1,\ldots$; f'_0, $f'_1,\ldots$; $g_0,g_1,\ldots$; $g'_0,g'_1,\ldots$,etc. . We then use the following notation to define various Migdal parameters. In the non-relativistic case, the density of states at Fermi surface is

$$N_0^{NR} = \frac{2k_F m_N}{\pi^2\hbar^2} \quad , \tag{4.15}$$

and the Migdal parameters are

$$F_l^{NR} = N_0^{NR} f_l^{NR}. \quad , \tag{4.16}$$

$$F'^{NR}_l = N_0^{NR} f'^{NR}_l. \quad , \tag{4.17}$$

$$G_l^{NR} = N_0^{NR} g_l^{NR}. \quad , \tag{4.18}$$

$$G'^{NR}_l = N_0^{NR} g'^{NR}_l. \quad , \tag{4.19}$$

$$(l = 0,\ 1,\ 2,\ \ldots.) \quad .$$

In the relativistic case, the density of states at the Fermi surface is

$$\tilde{N}_0 = \frac{2k_F \tilde{E}(k_F)}{\pi^2 \hbar^2} \quad , \quad \tilde{E}(k_F) = (\vec{p}^2 + \tilde{m}^2)^{1/2} \quad , \tag{4.20}$$

and the Migdal parameters are

$$\tilde{F}_l = \tilde{N}_0 \, \tilde{f}_l \quad , \tag{4.21}$$

$$\tilde{F}'_l = \tilde{N}_0 \, \tilde{f}'_l \quad , \tag{4.22}$$

$$\tilde{G}_l = \tilde{N}_0 \, \tilde{g}_l \quad , \tag{4.23}$$

$$\tilde{G}'_l = \tilde{N}_0 \, \tilde{g}'_l \quad , \tag{4.24}$$

$$(l = 0, 1, 2, \ldots.) \ ,$$

where $\tilde{f}_l$, $\tilde{f}'_l$, $\tilde{g}_l$, $\tilde{g}'_l$ are determined by the $f(\vec{p},s)$ and Eq.(4.26). (See Section 6.5.)

4.2.2 The Calculation of the Migdal Parameters

We could fix the parameters of V_{eff} by requiring that the Migdal parameters calculated from the amplitude

$$\mathfrak{F}^{NR}_{eff}(\vec{p}_1,\vec{p}_2) = \left(\frac{m_N}{E_N(k_F)}\right)^2 \langle \bar{u}(\vec{p}_1 s'_1)\bar{u}(\vec{p}_2 s'_2) | V_{eff}(1-p_{12}) | u(\vec{p}_1 s_1)u(\vec{p}_2 s_2) \rangle \tag{4.25}$$

are reasonably close to those obtained from $\mathfrak{F}^{NR}(\vec{p}_1,\vec{p}_2)$. However, we will here calculate the Migdal parameters using the effective interaction specified in the previous chapter. Of course, the actual Migdal parameters of the relativistic BHF theory are to be obtained

using Eq.(4.2). As discussed in Ref.7, the use of the $f(\vec{p},s)$, rather than the $u(\vec{p},s)$, makes for major changes in the Migdal parameter F_0. Therefore, ideally one should calculate the Migdal parameters for the amplitude

$$\mathfrak{F}_{eff}(\vec{p}_1,\vec{p}_2)=\left(\frac{m_N}{E_N(k_F)}\right)^2 <\bar{f}(\vec{p}_1 s_1')\bar{f}(\vec{p}_2 s_2')|V_{eff}(1-p_{12})|f(\vec{p}_1 s_1)f(\vec{p}_2 s_2)> , \tag{4.26}$$

and compare the results with those parameters obtained for $\mathfrak{F}(\vec{p}_1,\vec{p}_2)$

and compare the results with those parameters obtained for $\mathfrak{F}(\vec{p}_1,\vec{p}_2)$
of Eq.(4.2). We will do that in Section 4.2.4.

Using the Fierz transformation technique (see Appendix C) and some rules that we developed (see Appendix D) to treat the exchange terms, for each value of the isospin we can express the on-shell nucleon-nucleon (nucleon-nucleus) scattering amplitude in terms of five independent amplitudes:

$$\begin{aligned}(\vec{p}_1,\vec{p}_2|M^{on}_{\alpha'\beta'\alpha\beta}|\vec{p}_1\vec{p}_2)= {} & M_S[\,\mathbb{I}(1)]_{\alpha',\alpha}[\,\mathbb{I}(2)]_{\beta',\beta} + M_V[\gamma^\mu(1)]_{\alpha',\alpha}[\gamma_\mu(2)]_{\beta',\beta} \\ & + M_T[\sigma^{\mu\nu}(1)]_{\alpha',\alpha}[\sigma_{\mu\nu}(2)]_{\beta',\beta} + M_P[\gamma^5(1)]_{\alpha',\alpha}[\gamma_5(2)]_{\beta',\beta} \\ & + M_A[\gamma^5\gamma^\mu(1)]_{\alpha',\alpha}[\gamma_5\gamma_\mu(2)]_{\beta',\beta} \quad . \end{aligned} \tag{4.27}$$

Then, for a one-boson-exchange potential, we obtain the functions in Eq.(4.6).

As a simple example, let us consider the scattering amplitude for the forward scattering of two quasi-particles at the Fermi surface, which arises from the exchange of a ω meson ($|\vec{p}_1| = |\vec{p}_2| = k_F$). The fully on-shell amplitude is

$$\bar{u}_\alpha(\vec{p}_1' s_1')\bar{u}_\beta(\vec{p}_2' s_2')(\vec{p}_1', \vec{p}_2'|M^{on}_{\alpha\beta\alpha',\beta'}|\vec{p}_1, \vec{p}_2)u_{\alpha'}(\vec{p}_1 s_1)u_{\beta'}(\vec{p}_2 s_2), \quad (4.28)$$

where in M^{on} we have $\vec{p}'^2_1 = \vec{p}'^2_2 = \vec{p}^2_1 = \vec{p}^2_2 = k^2_F = m^2_N$. For the ω exchange interaction, we find

$$(\vec{p}_1, \vec{p}_2|M^{on}_{\alpha'\beta'\alpha\beta}|\vec{p}_1\vec{p}_2) = -\frac{g^2_\omega F^2(0)}{-m^2_\omega}[\gamma^\mu(1)]_{\alpha'\alpha}[\gamma_\mu(2)]_{\beta'\beta}\delta_{\alpha_T'\alpha_T}(1)\delta_{\beta_T'\beta_T}(2)$$

$$-\frac{-g^2_\omega F^2_\omega(t)}{(p_1-p_2)^2-m^2_\omega+i\epsilon}[\gamma^\mu(1)]_{\beta'\alpha}[\gamma_\mu(2)]_{\alpha'\beta}\delta_{\beta_T'\alpha_T}(1)\delta_{\alpha_T'\beta_T}(2), \quad (4.29)$$

with

$$t = (p_1 - p_2)^2 = -2k_F^2(1 - x),$$

where $F^2_\omega(0)$ and $F^2_\omega(t)$ are cut-off factors. (See Section 1.3 and Tables 1.1-1.3.) Using the rules developed in Appendix C to rearrange the indices of the exchange term, we have

$$\delta_{\beta_T'\alpha_T}(1)\delta_{\alpha_T'\beta_T}(2) = \tfrac{1}{2}\delta_{\alpha_T'\alpha_T}(1)\delta_{\beta_T'\beta_T}(2) + \tfrac{1}{2}[\vec{\tau}(1)]_{\alpha_T'\alpha_T}\cdot[\vec{\tau}(2)]_{\beta_T'\beta_T}, \quad (4.30)$$

and

$$[\gamma^{\mu}(1)]_{\beta',\alpha}[\gamma_{\mu}(2)]_{\alpha',\beta} = \mathbb{I}_{\alpha',\alpha}(1)\mathbb{I}_{\beta',\beta}(2) - \tfrac{1}{2}[\gamma^{\mu}(1)]_{\alpha',\alpha}[\gamma_{\mu}(2)]_{\beta',\beta}$$
$$- \tfrac{1}{2}[\gamma^{5}(1)\gamma^{\mu}(1)]_{\alpha',\alpha}[\gamma_{5}(2)\gamma_{\mu}(2)]_{\beta',\beta}$$
$$-[\gamma^{5}(1)]_{\alpha',\alpha}[\gamma_{5}(2)]_{\beta',\beta} \qquad . \tag{4.31}$$

We write $A_{\omega}=-g^{2}{}_{\omega}/(2k_{F}{}^{2})$, $B_{\omega}=1+m^{2}{}_{\omega}/(2k_{F}{}^{2})$, $x=\cos\theta$, so that

$$(\vec{p}_1,\vec{p}_2|M^{on}_{\alpha',\beta',\alpha\beta}|\vec{p}_1,\vec{p}_2)$$

$$= \tfrac{1}{2}\frac{A_{\omega}F^{2}(t)}{B_{\omega}-x}[\mathbb{I}(1)]_{\alpha',\alpha}[\mathbb{I}(2)]_{\beta',\beta}\delta_{\alpha_T'\alpha_T}(1)\delta_{\beta_T'\beta_T}(2)$$

$$+ \tfrac{1}{2}\frac{A_{\omega}F_{\omega}^{2}(t)}{B_{\omega}-x}[\mathbb{I}(1)]_{\alpha',\alpha}[\mathbb{I}(2)]_{\beta',\beta}\vec{\tau}_{\alpha_T'\alpha_T}(1)\cdot\vec{\tau}_{\beta_T'\beta_T}(2)$$

$$+ \left(\frac{g_{\omega}^{2}F_{\omega}^{2}(0)}{m_{\omega}^{2}} - \tfrac{1}{4}\frac{A_{\omega}F_{\omega}^{2}(t)}{B_{\omega}-x}\right)[\gamma^{\mu}(1)]_{\alpha',\alpha}[\gamma_{\mu}(2)]_{\beta',\beta}\delta_{\alpha_T'\alpha_T}(1)\delta_{\beta_T'\beta_T}(2)$$

$$- \tfrac{1}{4}\frac{A_{\omega}F_{\omega}^{2}(t)}{B_{\omega}-x}[\gamma^{\mu}(1)]_{\beta',\alpha}[\gamma_{\mu}(2)]_{\alpha',\beta}\vec{\tau}_{\alpha_T'\alpha_T}(1)\bullet\vec{\tau}_{\beta_T'\beta_T}(2)$$

$$- \tfrac{1}{2}\frac{A_{\omega}F^{2}(t)}{B_{\omega}-x}[\gamma^{5}(1)]_{\alpha',\alpha}[\gamma_{5}(2)]_{\beta',\beta}\delta_{\alpha_T'\alpha_T}(1)\delta_{\beta_T'\beta_T}(2)$$

$$- \tfrac{1}{2}\frac{A_{\omega}F_{\omega}^{2}(t)}{B_{\omega}-x}[\gamma^{5}(1)]_{\alpha',\alpha}[\gamma_{5}(2)]_{\beta',\beta}\vec{\tau}_{\alpha_T'\alpha_T}(1)\cdot\vec{\tau}_{\beta_T'\beta_T}(2)$$

$$- \tfrac{1}{4}\frac{A_{\omega}F_{\omega}^{2}(t)}{B_{\omega}-x}[\gamma^{5}(1)\gamma^{\mu}(1)]_{\alpha',\alpha}[\gamma_{5}(2)\gamma_{\mu}(2)]_{\beta',\beta}\delta_{\alpha_T'\alpha_T}(1)\delta_{\beta_T'\beta_T}(2)$$

$$- \frac{1}{4} \frac{A_\omega F_\omega^2(t)}{B_\omega - x} [\gamma^5(1)\gamma^\mu(1)]_{\beta',\alpha} [\gamma_5(2)\gamma_\mu(2)]_{\alpha',\beta} \vec{\tau}_{\alpha_T'\alpha_T}(1) \cdot \vec{\tau}_{\beta_T'\beta_T}(2) \quad . \tag{4.32}$$

Using the rules developed in Appendix D, we have

$$\begin{aligned} &\bar{u}_\alpha(\vec{p}_1' s_1') \bar{u}_\beta(\vec{p}_2' s_2') (\vec{p}_1', \vec{p}_2' | M^{on}_{\alpha\beta\alpha',\beta'} | \vec{p}_1, \vec{p}_2)_\omega u_{\alpha'}(\vec{p}_1 s_1) u_{\beta'}(\vec{p}_2 s_2) \\ &= f_\omega(x) + f_\omega'(x) \vec{\tau}_1 \cdot \vec{\tau}_2 + [g_\omega(x) + g_\omega'(x) \vec{\tau}_1 \cdot \vec{\tau}_2] \vec{\sigma}_1 \cdot \vec{\sigma}_2 \\ &+ \frac{1}{k_F^2} [h_\omega(x) + h_\omega'(x) \vec{\tau}_1 \cdot \vec{\tau}_2] S_{12}(\vec{p}) \quad , \end{aligned} \tag{4.33}$$

where

$$f_\omega(x) = \frac{1}{2} \frac{A_\omega F_\omega^2(t)}{B_\omega - x} + \left(\frac{g_\omega^2 F_\omega^2(0)}{m_\omega^2} - \frac{1}{4} \frac{A_\omega F_\omega^2(t)}{B_\omega - x} \right) \left(\left(\frac{E}{m_N}\right)^2 - \left(\frac{k_F}{m_N}\right)^2 x \right) \quad ,$$

$$f_\omega'(x) = \frac{1}{2} \frac{A_\omega F_\omega^2(t)}{B_\omega - x} - \frac{1}{4} \frac{A_\omega F_\omega^2(t)}{B_\omega - x} \left(\left(\frac{E}{m_N}\right)^2 - \left(\frac{k_F}{m_N}\right)^2 x \right) \quad ,$$

$$g_\omega(x) = g_\omega'(x) = \frac{1}{4} \frac{A_\omega F_\omega^2(t)}{B_\omega - x} \left(1 + \frac{1}{3} \left(\frac{k_F}{m_N}\right)^2 (1-x) \right) \quad .$$

Using the same procedures we can determine the functions f(x), f'(x), g(x), g'(x), etc. for the exchange of other mesons.

σ exchange:

Let $A_\sigma = g^2_\sigma/(2k_F^2)$ and $B_\sigma = 1+m_\sigma^2/(2k_F^2)$. Then

$$f_\sigma(x) = \frac{1}{8}\frac{A_\sigma F_\sigma^2(t)}{B_\sigma - x} + \frac{1}{8}\frac{A_\sigma F_\sigma^2(t)}{B_\sigma - x}\left((\frac{E}{m_N})^2 - (\frac{k_F}{m_N})^2 x\right) - \frac{g_\sigma^2 F_\sigma^2(0)}{m_\sigma^2} \quad ,$$

$$f'_\sigma(x) = \frac{1}{8}\frac{A_\sigma F_\sigma^2(t)}{B_\sigma - x} + \frac{1}{8}\frac{A_\sigma F_\sigma^2(t)}{B_\sigma - x}\left((\frac{E}{m_N})^2 - (\frac{k_F}{m_N})^2 x\right) \quad ,$$

$$g_\sigma(x) = g'_\omega(x) = \frac{1}{8}\frac{A_\sigma F_\sigma^2(t)}{B_\sigma - x}\left((\frac{E}{m_N})^2 + 1 + \frac{2}{3}(\frac{k_F}{m_N})^2(1-x)\right) \quad ,$$

and

$$g'_\sigma(x) = g_\sigma(x) \quad .$$

ρ exchange:

Let $A_\rho = g^2_\rho/(2k_F^2)$, $B_\rho = 1+m_\rho^2/(2k_F^2)$ and $2a = (f_\rho/g_\rho)$. Using the Gordon decomposition (see Appendix E), we find

$$f_\rho(x) = -\frac{3}{2}\frac{A_\rho F_\rho^2(t)}{B_\rho - x}\left[a_1 + a_2[(\frac{E}{m_N})^2 - (\frac{k_F}{m_N})^2 x]\right) \quad ,$$

$$f'_\rho(x) = \frac{1}{2}\frac{A_\rho F_\rho^2(t)}{B_\rho - x}\left(a_1 + a_2[(\frac{E}{m_N})^2 - (\frac{k_F}{m_N})^2 x]\right) \quad ,$$

$$g_\rho(x) = -\frac{3}{2}\frac{A_\rho F_\rho^2(t)}{B_\rho - x}\left(a_3[2+\frac{4}{3}(\frac{k_F}{m_N})^2(1-x)] - a_4[1+\frac{1}{3}(\frac{k_F}{m_N})^2(1-x)]\right) \quad ,$$

$$g'_\rho(x) = -\frac{1}{3}\, g_\rho(x) \quad ,$$

$$a_1 = 1 + 3a + 3a^2 + \frac{1}{2}(\frac{ak_F}{m_N})^2(1-x) \quad ,$$

$$a_2 = -\frac{1}{2} - 3a - 3a^2 + \frac{1}{2}(\frac{ak_F}{m_N})^2(1-x) \quad ,$$

$$a_3 = -\frac{1}{2}a - \frac{1}{2}a^2 + \frac{1}{4}(\frac{ak_F}{m_N})^2(1-x) \quad ,$$

$$a_4 = -\frac{1}{2} - a - a^2 - \frac{1}{2}(\frac{ak_F}{m_N})^2(1-x) \quad .$$

π <u>exchange</u> (pseudovector coupling):

Let $A_\pi = g^2{}_\pi/(2k_F{}^2)$ and $B_\pi = 1 + m_\pi{}^2/(2k_F{}^2)$. Then

$$f_\pi(x) = \frac{3}{8}\frac{A_\pi F_\pi^2(t)}{B_\pi - x}(\frac{k_F}{m_N})^2(1-x) \quad ,$$

$$f'_\pi(x) = -\frac{1}{3}\, f_\pi(x) \quad ,$$

$$g_\pi(x) = f'_\pi(x) \quad ,$$

and

$$g'_\pi(x) = -\frac{1}{3}\, g_\pi(x) \quad .$$

ϕ exchange:

Let $A_\phi = g^2{}_\phi/(2k_F{}^2)$ and $B_\phi = 1+m_\phi{}^2/(2k_F{}^2)$. Then

$$f_\phi(x) = \frac{1}{2}\,\frac{A_\phi F_\phi^2(t)}{B_\phi - x} + \left(\frac{g_\phi^2 F_\phi^2(0)}{m_\phi^2} - \frac{1}{4}\,\frac{A_\phi F_\phi^2(t)}{B_\phi - x}\right)\left(\left(\frac{E}{m_N}\right)^2 - \left(\frac{k_F}{m_N}\right)^2 x\right) \quad ,$$

$$f'_\phi(x) = \frac{1}{2}\,\frac{A_\phi F_\phi^2(t)}{B_\phi - x} - \frac{1}{4}\,\frac{A_\phi F_\phi^2(t)}{B_\phi - x}\left(\left(\frac{E}{m_N}\right)^2 - \left(\frac{k_F}{m_N}\right)^2 x\right) \quad ,$$

$$g_\phi(x) = g'_\phi(x) = \frac{1}{4}\,\frac{A_\phi F_\phi^2(t)}{B_\phi - x}\left(1 + \frac{1}{3}\left(\frac{k_F}{m_N}\right)^2 (1-x)\right) \quad .$$

η exchange (pseudovector coupling):

Let $A_\eta = g^2{}_\eta/(2k_F{}^2)$ and $B_\eta = 1+m_\eta{}^2/(2k_F{}^2)$. Then

$$f_\eta(x) = \frac{1}{8}\,\frac{A_\eta F_\eta^2(t)}{B_\eta - x}\left(\frac{k_F}{m_N}\right)^2 (1-x) \quad ,$$

$$f'_\eta(x) = f_\eta(x) \quad ,$$

$$g_\eta(x) = -\tfrac{1}{3} f_\eta(x) \quad ,$$

and

$$g'_\eta(x) = -\tfrac{1}{3} f_\eta(x) \quad .$$

δ exchange:

Let $A_\delta = g^2{}_\delta/(2k_F{}^2)$ and $B_\delta = 1 + m_\delta{}^2/(2k_F{}^2)$. Then

$$f_\delta(x) = \frac{3}{8} \frac{A_\delta F_\delta^2(t)}{B_\delta - x} \left(2 + (\frac{k_F}{m_N})^2 (1-x)\right) \quad ,$$

$$f'_\delta(x) = -\frac{g_\delta^2 F_\delta^2(0)}{m_\delta^2} - \tfrac{1}{3} f_\delta(x) \quad ,$$

$$g_\delta(x) = f_\delta(x) \quad ,$$

$$g'_\delta(x) = -\tfrac{1}{3} f_\delta(x) \quad .$$

Using $f(\vec{p},s)$ and the rules developed in Appendices C-E, for the exchange of various mesons, we can determine the functions $\tilde{f}(x)$, $\tilde{f}'(x)$, $\tilde{g}(x)$, $\tilde{g}'(x)$, etc.- see Section 6.5.

4.2.3 Numerical Results

The Migdal parameters for the amplitude $\mathcal{F}^{NR}(\vec{p}_1,\vec{p}_2)$ were given in Ref.7 for the interactions HEA and HM2. Our calculational results are listed in Table 1 - Table 22. We will first compare the Migdal parameters obtained for the amplitudes $\mathcal{F}^{NR}(\vec{p}_1,\vec{p}_2)$ and $\mathcal{F}^{NR}_{eff}(\vec{p}_1,\vec{p}_2)$. In Table 1 (for the potential HEA) and Table 7 (for the potential HM2) we present results for the Migdal parameters calculated for various values of k_F. The first line presents the results of the Hartree-Fock approximation for the interaction $V^{(1)}_{eff}=U$. The second line gives the result for $V^{(2)}_{eff}=\Delta U$ and the third line is the result for $V_{eff}=U+\Delta U$. The fourth line gives the values of the Migdal parameters obtained from $\mathcal{F}^{NR}(\vec{p}_1,\vec{p}_2)$.[7,25] It is to be stressed that, with a few exceptions, the interaction V_{eff}, which makes for a good fit to $\Sigma_0^{++}(\vec{p})$, $\Sigma_0^{+-}(\vec{p})$, $\Sigma_0^{--}(\vec{p})$, and $U_{eff}(\vec{p})$, leads to quite reasonable values for the Migdal parameters.

Some further details of our calculations are presented in Table 2 - Table 6 (for the potential HEA) and in Table 8 - Table 10 (for the potential HM2). The first seven rows present the Hartree-Fock results for $V_{eff}=U_\eta$, $V_{eff}=U_\pi$, $V_{eff}=U_\sigma$, etc. The result for $V_{eff}=U$ is

then given in the eighth row. (We note that there is a great deal of cancellation among the various contributions to each Migdal parameter.) In the next three rows we have the contributions from $V_{eff}=\Delta U_{\sigma}$, $V_{eff}=\Delta U_{\omega}$ and $V_{eff}=\Delta U_{\delta}$. The sum of these contributions, that is, the result for $V_{eff}=\Delta U$, is given as ΔU. Finally, the result for $V_{eff}=U+\Delta U$ is given. That result is then to be compared to the result of reaction matrix calculations. The last row gives the percentage error in this comparsion. On the whole, given the large amount of cancellation in these sums, the result obtained is quite good.

In Tables 11-12 we present the results of the various approximations, which we mentioned in Section 3.3, for the potential HEA for k_F= 1.36 fm^{-1}. These can be compared to the results of the reaction matrix calculations. We see that only Approximation 1 and Approximation 2 give quite reasonable values. This is why we stated in Sections 3.1 and 3.4: "the choice for the coupling constants of the pseudoparticles is not unique", but "the range of choice is limited".

4.2.4 Consideration of a Relativistic System.

We now turn to the comparion of $\mathcal{F}_{eff}(\vec{p}_1,\vec{p}_2)$ and $\mathcal{F}(\vec{p}_1,\vec{p}_2)$ of Eqs.(4.6) and (4.2). The Migdal parameters obtained from the amplitude $\mathcal{F}(\vec{p}_1,\vec{p}_2)$ have already been given in Ref.7. We may

calculate $\mathcal{F}_{eff}(\vec{p}_1,\vec{p}_2)$ using Eq.(2.13) for $f(\vec{p},s)$ and Eq.(2.12) for $\widetilde{m}(\vec{p})$.

When using Eq.(2.13), we can usually neglect the rather weak momentum dependence of m(p); however, we have kept the density dependence of this quantity in our calculation. For the calculation of the Migdal parameters, we have to use the formulas in Section 6.5. We should also use $\widetilde{m}=\widetilde{m}(k_F)$ in Eq.(2.12), since we are dealing with particles at the Fermi surface. As we have seen in Ref.7, the result for F_0 is particularly sensitive to the details of the calculation, since this quantity goes through zero at some density slightly above that of nuclear matter.

In Table 13 (for the potential HEA), and Table 19 (for the potential HM2) we present our results for the Migdal parameters of the RBHF model. We see from these tables that our effective interaction does a good job in reproducing the Migdal parameters obtained from the full G-matrix analysis. As has been noted previously, the relativistic theory gives a value of $F_0 \geq -1.0$ at $k_F=1.36 fm^{-1}$, which is necessary if the system is to have a positive compressibility parameter at nuclear densities.

In Tables 14-18 (for the potential HEA) and Tables 20-22 (for the potential HM2), we present details of our calculation. This material is similar to that presented in Table 2 except that we are now using the spinors $f(\vec{p},s)$ instead of the $u(\vec{p},s)$ [see Eqs.(4.2)-(4.20)]. We also provide, in Table 4.3, the values of $A(k_F)$ and $\widetilde{m}(k_F)=m_N+A(k_F)$ used to generate the numbers given in Tables 13-22.

We stress that these Migdal parameters are not those of the fully-self-consistent RBHF theory. One can find the Migdal parameters of the fully-self-consistent RBHF theory, as given by our pseudoparticle model, in Chapter 6.

Table 4.3

Values of $A(k_F)$ and $\tilde{m}(k_F)$ used to calculate the Migdal parameters of Tables 13-22(k_F=1.36 fm^{-1}). Values of the parameters to be used at other densities for the potentials HEA and HM2 are also shown.

k_F (fm^{-1})	A (MeV)	$\tilde{m}$ (fm^{-1})	$[\tilde{m}(k_F)/\tilde{E}(k_F)]^{1/2}$
1.60	-480	2.325	0.908
1.40	-365	2.908	0.949
1.36	-345	3.010	0.955
1.20	-255	3.466	0.972
1.00	-151	3.993	0.985

Chapter 5

Dynamics of Nuclear Saturation

5.1 Binding Energy

We recall Eq.(4.4), where the quantity $\alpha(\vec{p})$ was given by

$$\alpha(\vec{p}) = \frac{\frac{m_N}{E_N(\vec{p})}\Sigma^{+-}(\vec{p})}{p^0 + E_N(\vec{p}) - \frac{m_N}{E_N(\vec{p})}\Sigma^{--}(\vec{p})} \tag{5.1}$$

$$\simeq \frac{\frac{m_N}{E_N(\vec{p})}\Sigma^{+-}(\vec{p})}{2E_N(\vec{p}) - \frac{m_N}{E_N(\vec{p})}[\Sigma^{--}(\vec{p}) - \Sigma^{++}(\vec{p})]} \quad . \tag{5.2}$$

In terms of these quantities we could calculate the energy of nuclear matter by using Eqs.(2.17)-(2.19). In the quasiparticle model we replace the reaction matrix, $\hat{M}$, appearing in Eqs.(2.17)-(2.19), with the potential $V_{eff}=U+\Delta U$. Here U represents the Born terms of the OBE model (including exchange) and ΔU represents the Born terms arising from the exchange of pseudoparticles, as described in detail in Chapter 3. Therefore, we will be using the approximation,

$$E(\vec{p})=\sum_{s'}\int\frac{d\vec{q}}{(2\pi)^3}\left(\frac{m_N}{E_N(\vec{q})}\right)\langle\vec{p},\bar{f}(\vec{q},s')|(U+\Delta U)(1-p_{12})|\vec{p},f(\vec{q},s')\rangle\theta(k_F-|\vec{q}|) \quad . \tag{5.3}$$

To calculate the binding energy per particle we use the following expression:

$$\frac{E_B}{A} = \frac{\mathcal{E}_{kin}}{A} + \frac{\mathcal{E}_{pot}}{A} \quad , \tag{5.4}$$

where

$$\frac{\mathcal{E}_{kin}}{A} \equiv \frac{3}{k_F^3} \int_0^{k_F} p^2 dp \left(\frac{1 - \alpha^2(p)}{1 + \alpha^2(p)} E_N(p) - m_N \right) \quad , \tag{5.5}$$

and

$$\frac{\mathcal{E}_{pot}}{A} \equiv \frac{3}{k_F^3} \int_0^{k_F} p^2 dp \left(\frac{m_N}{E_N(\vec{p})}\right) \frac{1}{2[1 + \alpha^2(\vec{p})]^2} \left\{ \left(1+4\alpha^2(\vec{p})\right) \Sigma^{++}(\vec{p}) \right.$$

$$\left. -2\alpha^2(\vec{p}) \Sigma^{--}(\vec{p}) + \frac{8\alpha^2(\vec{p})}{m_N} E_N^2(\vec{p}) \right\} . \tag{5.6}$$

with $p = |\vec{p}|$. These equations follow from inserting Eq.(4.4) into Eq.(2.18) and are slightly more accurate versions of Eqs.(2.4.4) and Eq.(2.4.8) of Ref.7. Then we calculate the binding energy, B.E.=$(Am_N-E)/A$, using Appendix 9 of Ref.7, the equations in Section 2.5, and Eqs.(5.4)-(5.6). These calculations are not fully self-consistent, but represent the first iteration of a self-consistent scheme. We report fully - self-consistent calculations for the pseudoparticle model in Chapter 6.

5.2 Results of Computation for the Potential HEA

The matrix elements of the self-energy and various saturation curves were calculated using the RBHF theory and the results were

presented in Ref.25. Our results are shown in Figs. 26-31. In Fig.26 the curve labelled a' is the saturation curve for HEA, calculated in our pseudoparticle model using the potential ΔU given in Chapter 3. We find K_∞ = 211 MeV and k_F = 1.21 fm^{-1} at the saturation point. (This value of K_∞ is quite close to that calculated from the value of Migdal parameter, F_0, in Ref.25. There it was found that K_∞ = 175 MeV. Here we calculated K_∞ directly from the value of the binding energy per particle, B.E./A , obtained as a function of nuclear matter density , using the pseudoparticle method.)

The pseudoparticle coupling constants determined in Chapter 3 were density dependent. If we fix their values to those found for k_F= 1.36 fm^{-1} in Chapter 3, we obtain the saturation curve labelled a' in Fig.27. Note the small increase in the incompressibility and in k_F reported in Table 23 for this density-independent approximation (Approximation 2). The values obtained for the Fermi momentum k_F and for K_∞ are also given in Table 23.

In Fig.28 we present the saturation curves labelled 1, 2, 3, 4, 5, corresponding to the Approximations 1, 2, 3, 4, 5, presented in Table 3.3 for the potential HEA (density-dependent approximations). These results are compared to the results of reaction matrix calculations. (Refs.7,25.) We see that all these approximations yield similar saturation curves. When considering the results for the Migdal parameters we are led to prefer Approximation 1 or Approximation 2 of Table 3.3.

Table 5.1

Pseudoparticle coupling constants and modified pseudoparticle coupling constants for the potential HEA and HM2 for $k_F = k_F^{NM} = 1.36\ fm^{-1}$.

	HEA		HM2	
	Pseudo-particle Coupling Constants	Modified Pseudo-particle Coupling Constants	Pseudo-particle Coupling Constants	Modified Pseudo-particle Coupling Constants
$\delta g^2_\sigma/4\pi$	-2.81	-2.81	-1.15	-1.15
$\delta g^2_\omega/4\pi$	14.2	17.5	6.52	7.35
$\delta g^2_\delta/4\pi$	5.54	5.54	0.00	0.00

Thus far, our choice of V_{eff} has been based upon a fit to matrix elements obtained in reaction-matrix calculations (in the RBHF theory) for the potential HEA. We now consider an arbitrary change of ΔU such that the saturation curves are made to pass through the rectangle in Figs. 26-27. The rectangle denotes the region of generally accepted values for the saturation density and binding energy of nuclear matter. In Chapter 3, ΔU described the exchange of a pseudo-sigma, pseudo-omega and pseudo-delta particle in the

case of the potential HEA. The coupling constant for the pseudo-omega particle was $\delta g^2_\omega/(4\pi)=14.2$. If we arbitrarily increase $\delta g^2_\omega/(4\pi)$ to 17.5 (see Table 5.1), we obtain the curve labelled b' in Fig.26, in a non-self-consistent approximation. (See Table 23 - Approximation 3.) If we further neglect the density dependence of the pseudoparticle coupling constants, and again use $\delta g^2_\omega/(4\pi)=17.5$, we obtain the curve labelled b' in Fig.27. (See Table 23 - Approximation 4.)

5.3 Results of Computation for the Potential HM2

In Table 5.1 we also summarize some features of ΔU for the potential HM2. If we use the density-dependent pseudoparticle coupling constants, we obtain the saturation curve a' in Fig.29 -see Table 24 (Approximation 1). The density-independent result is labelled a' and is shown in Fig.30 -see Table 24 (Approximation 2). When we use the modified pseudoparticle coupling constants given in Table 5.1, we obtain the saturation curves labelled b' of Figs.29-30, corresponding to density-dependent and density-independent cases, respectively. These curves pass through the rectangle in Figs.29-30.

We remark that for the potential HEA and the potential HM2, the use of (either modified or unmodified) density-independent coupling constants for the pseudoparticles can lead to a larger value of saturation density and to a larger value of the incompressibility parameter, K_∞.

5.4 Results of Computation for the Potential BMR2

We present a separate discussion of the potential BMR2 introduced in Ref.20 (see also Section 1.3), since we have not calculated the RBHF reaction matrices in this case. We have added two pseudoparticles or three pseudoparticles (see Table 5.2, $M_\sigma = M_\omega = 1$ GeV, $M_\delta = 1.25$ GeV.) to the interaction BMR2 and have calculated the saturation curves in the relativistic Hartree-Fock approximation. The results of that calculation are shown in Fig.31. In all these calculation we used density-independent pseudoparticle coupling constants, i.e. we have used the pseudoparticle coupling constants for $k_F = k_F^{NM} = 1.36$ fm^{-1}. These correspond to the "modified case" for the potential HEA and HM2. We find that in adding two pseudoparticles in order to obtain saturation at the correct energy and density in the Hartree-Fock approximation, the value of the incompressibility parameter is large (K_∞ is around 450 MeV) but it is still reasonable. Much larger values of K_∞ can be found in the simple sigma plus omega model, such as that described in Ref.8 and in Section 6.3. We remark that the general trend obtained in previous calculations is seen here: An attempt to obtain the correct saturation properties without taking into account the details of the saturation dynamics as described in RBHF reaction-matrix calculations leads to large values of K_∞

Table 5.2

Pseudoparticle coupling constants[a] for the potential BMR2 for $k_F = k_F^{NM} = 1.36$ fm^{-1}. Also given are the Fermi momentum, k_F, at saturation and the incompressibility parameter, K_∞, for Approximations 1 through 7.

BMR2	$\frac{1}{4\pi}\delta g_\sigma^2$	$\frac{1}{4\pi}\delta g_\omega^2$	$\frac{1}{4\pi}\delta g_\delta^2$	k_F (fm^{-1})	B.E./A (MeV)	K_∞ (MeV)
Approx.1	- 6.35	14.40	0.00	1.37	-15.19	448
Approx.2	- 5.5[b]	14.40[b]	8.54[b]	1.35	-15.19	439
Approx.3	-10.4	7.25	8.54	1.30	-14.95	443
Approx.4	-10.5	7.25	8.54	1.30	-15.22	441
Approx.5	-10.6	7.25	8.54	1.31	-15.49	481
Approx.6	- 5.5	14.54	8.54	1.35	-15.49	471
Approx.7	- 5.5	14.26	8.54	1.36	-14.90	441

a). $M_\sigma = M_\omega = 1$GeV, $M_\delta = 1.25$ GeV.

b). The sign is such as to increase the attraction in the σ channel.

c). The sign is such as to decrease the repulsion due to ω exchange.

d). The sign is such as to decrease the repulsion due to δ exchange.

Chapter 6

Fully-Self-Consistent Pseudoparticle Model

Full self-consistency requires that the various matrix elements of $\Sigma(p)$ are calculated using the spinors $f(\vec{p},s)$ obtained from the self-consistent solution of Eq.(2.8). The equations of Appendix 9 of Ref.7 were appropriately modified to carry out the fully-self-consistent calculations. The modified equations and the results of fully-self-consistent calculations are reported here.

6.1 Green's Function

Inserting Eq.(2.27) into Eq.(2.8) we find

$$[\vec{\gamma}\cdot\vec{p}+m_N+A(p)+\gamma^0 B(p)+\frac{\vec{\gamma}\cdot\vec{p}}{m_N}C(p)]f(\vec{p},s)=\gamma^0 p^0 f(\vec{p},s) \quad , \tag{6.1}$$

where A(p), B(p) and C(p) parameterize the self-energy. The Green's function is

$$G(p^0,\vec{p}) = \frac{1}{\not{p}-m_N-A(p)-\gamma^0 B(p)-\frac{\vec{\gamma}\cdot\vec{p}}{m_N}C(p)+i\epsilon} \quad . \tag{6.2}$$

Keeping only the positive-energy spinors we have

$$G(p^0,\vec{p}) = \sum \frac{m_N}{E_N(\vec{p})} \left(\frac{f(p^0,\vec{p},s)\overline{f}(p^0,\vec{p},s)}{p^0-\epsilon(p^0,\vec{p})-i\epsilon}\,\theta(k_F-|\vec{p}|) \right.$$

$$\left. + \frac{f(p^0,p,s)\overline{f}(p^0,\vec{p},s)}{p^0-\epsilon(p^0,\vec{p})+i\epsilon}\,\theta(|\vec{p}|-k_F) \right) , \quad (6.3)$$

where $\widetilde{m}(\vec{p}) = [m_N+A(p)]/[1+C(p)/m_N]$, $\widetilde{E}(\vec{p}) = [\,\vec{p}^{\,2} + \widetilde{m}^2(\vec{p})\,]^{\frac{1}{2}}$, and $\varepsilon_{\vec{p}} = B(p) + [1+ C(p)/m_N]\widetilde{E}(\vec{p})$ is the pole position. For a fermion of spin 1/2 the propagator is

$$\left(\frac{i}{\not{p}-m_N-\Sigma(p)+i\epsilon}\right) = \frac{i(\tilde{\not{p}}+\tilde{m})}{\tilde{p}^2-\tilde{m}^2+i\epsilon}\,\frac{1}{1+C(p)/m_N} \quad . \quad (6.4)$$

Now due to the effect of the nuclear medium, the nucleon in nuclear matter is not on mass-shell. In a general Feynman diagram, we use the following replacement

$$\frac{1}{\not{p}-m_N-\Sigma(p)+i\epsilon} \longrightarrow -2\pi i\frac{\tilde{m}}{\tilde{E}(\vec{p})}\,\delta\left(p^0-B(p)-[1+\frac{C(p)}{m_N}]\tilde{E}(\vec{p})\right)\Lambda_+(\vec{p}) \quad , \quad (6.5)$$

and

$$\Lambda_+(\vec{p}) = \sum_s f(\vec{p},s)\overline{f}(\vec{p},s) \quad . \quad (6.6)$$

We obtain a set of new formulas (see the next section) which are used to perform the relativistic calculation of the nucleon self-energy in the Hartree-Fock approximation. The new formulas contain a factor of $1/(1+C(p)/m_N)$ and depend upon the parameters $\tilde{p}^0$ and $\tilde{m}$.

Note the definition

$$\tilde{p} = (\tilde{p}^0,\vec{p}) = [\,\tilde{E}(\vec{p}),\vec{p}\,] = \left(\frac{p^0-B(p)}{1+C(p)/m_N}\,,\,\vec{p}\,\right) . \quad (6.7)$$

6.2 Relativistic Calculation of the Nucleon Self-Energy

In this section we present the calculation of the nucleon self-energy, $\Sigma(p)$, obtained by using $f(\vec{p},s)$ in the nuclear-matter density matrix for the contributions of the σ, ω, π, ρ, ,ϕ, δ and η fields. All these new equations are modified versions of the equations of Appendix 9 of Ref.7.

We recall Section 2.5 and Eq.(2.27). In the case of nuclear matter, where N = Z, we need to evaluate the Feynman diagrams shown in Fig.6.1.

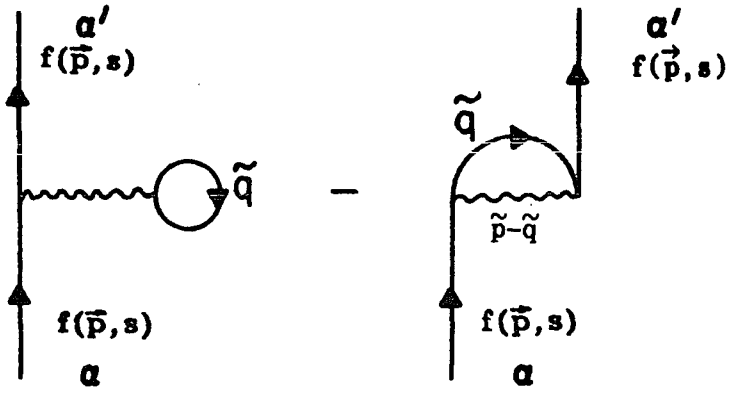

Fig.6.1

According to the argument in Section 6.1, we now add a new Feynman rule for relativistic nuclear physics: when calculating the scattering amplitude -iM , for each internal fermion line, we should use a factor $i(\not{p}-m+i\varepsilon)^{-1}[1+C(p)/m_N]^{-1}$. We obtain the following formulas which replace those of Appendix 9 of Ref.7 in the calculation of the self-energy $\Sigma(p)$.

Contribution of σ -field:

$$\Sigma^{\sigma}_{\substack{\alpha',\alpha \\ \alpha'_T\alpha_T}}(p) = (-1)\delta_{\alpha'_T\alpha_T}\int \frac{d\vec{q}}{(2\pi)^3}\left(\frac{\tilde{m}}{\tilde{E}(\vec{q})}\right)\left(\frac{g_\sigma^2}{m_\sigma^2}\right)\Bigg\{ F_\sigma^2(0)\delta_{\alpha',\alpha}\,T_r\left(\frac{\tilde{q}+\tilde{m}}{2\tilde{m}}\right)T_r\mathbb{I}^{iso}$$

$$+ \frac{F_\sigma^2(\tilde{p}-\tilde{q})}{1-\frac{(\tilde{p}-\tilde{q})^2}{m_\sigma^2}}\left(\frac{\tilde{q}+\tilde{m}}{2\tilde{m}}\right)_{\alpha',\alpha}\Bigg\}\left(\frac{1}{1+\frac{C(p)}{m_N}}\right) \quad ,$$

$$A_\sigma(p) = 4\int \frac{d\vec{q}}{(2\pi)^3}\left(\frac{\tilde{m}}{\tilde{E}(\vec{q})}\right)\left(-\frac{g_\sigma^2}{m_\sigma^2}\right)\left(F_\sigma^2(0) - \frac{F_\sigma^2(\tilde{p}-\tilde{q})}{8\left(1-\frac{(\tilde{p}-\tilde{q})^2}{m_\sigma^2}\right)}\right)\left(\frac{1}{1+\frac{C(p)}{m_N}}\right) \quad ,$$

$$B_\sigma(p) = 4\int \frac{d\vec{q}}{(2\pi)^3}\left(\frac{\tilde{q}^0}{\tilde{E}(\vec{q})}\right)\left(-\frac{g_\sigma^2}{m_\sigma^2}\right)\left(-\frac{F_\sigma^2(\tilde{p}-\tilde{q})}{8\left(1-\frac{(\tilde{p}-\tilde{q})^2}{m_\sigma^2}\right)}\right)\left(\frac{1}{1+\frac{C(p)}{m_N}}\right) \quad ,$$

$$C_\sigma(p) = 4\int \frac{d\vec{q}}{(2\pi)^3}\left(\frac{\vec{q}\cdot\vec{p}}{\tilde{E}(\vec{q})\vec{p}^2}\right)\left(-\frac{g_\sigma^2}{m_\sigma^2}\right)\left(\frac{F_\sigma^2(\tilde{p}-\tilde{q})}{1-\frac{(\tilde{p}-\tilde{q})^2}{m_\sigma^2}}\right)\left(\frac{m_N}{1+\frac{C(p)}{m_N}}\right) \quad .$$

Contribution of ω -field:

$$\Sigma^{\omega}_{\substack{\alpha',\alpha \\ \alpha'_T\alpha}}(p) = \delta_{\alpha'_T\alpha_T}\int \frac{d\vec{q}}{(2\pi)^3}\left(\frac{\tilde{m}}{\tilde{E}(\vec{q})}\right)\left(\frac{g_\omega^2}{m_\omega^2}\right)\Big\{(\gamma_\mu)_{\alpha',\alpha}F_\omega^2(o)T_r\left(\gamma^\mu\left(\frac{\tilde{\not q}+\tilde{m}}{2\tilde{m}}\right)\right)T_r\mathbb{I}^{iso}$$

$$- \left(\frac{F_\omega^2(\tilde{p}-\tilde{q})}{1-\frac{(\tilde{p}-\tilde{q})^2}{m_\omega^2}}\right)\left(\gamma_\mu\left(\frac{\tilde{\not q}+\tilde{m}}{2\tilde{m}}\right)\gamma^\mu\right)_{\alpha',\alpha}\Big\}\left(\frac{1}{1+\frac{C(p)}{m_N}}\right) ,$$

$$A_\omega(p) = 4\int \frac{d\vec{q}}{(2\pi)^3}\left(\frac{\tilde{m}}{\tilde{E}(\vec{q})}\right)\left(\frac{g_\omega^2}{m_\omega^2}\right)\left(-\frac{F_\omega^2(\tilde{p}-\tilde{q})}{2\left(1-\frac{(\tilde{p}-\tilde{q})^2}{m_\omega^2}\right)}\right)\left(\frac{1}{1+\frac{C(p)}{m_N}}\right) ,$$

$$B_\omega(p) = 4\int \frac{d\vec{q}}{(2\pi)^3}\left(\frac{\tilde{m}}{\tilde{E}(\vec{q})}\right)\left(\frac{g_\omega^2}{m_\omega^2}\right)\left(F_\omega^2(o)+\frac{F_\omega^2(\tilde{p}-\tilde{q})}{4\left(1-\frac{(\tilde{p}-\tilde{q})^2}{m_\omega^2}\right)}\right)\left(\frac{1}{1+\frac{C(p)}{m_N}}\right) ,$$

$$C_\omega(p) = 4\int \frac{d\vec{q}}{(2\pi)^3}\left(\frac{\vec{q}\cdot\vec{p}}{\tilde{E}(\vec{q})\vec{p}^2}\right)\left(\frac{g_\omega^2}{m_\omega^2}\right)\left(-\frac{F_\omega^2(\tilde{p}-\tilde{q})}{4\left(1-\frac{(\tilde{p}-\tilde{q})^2}{m_\omega^2}\right)}\right)\left(\frac{m_N}{1+\frac{C(p)}{m_N}}\right) .$$

Contribution of ρ -field:

$$\Sigma^{\rho}_{\substack{\alpha',\alpha \\ \alpha_T'\alpha_T}}(p) = \delta_{\alpha_T'\alpha_T}\int \frac{d\vec{q}}{(2\pi)^3}\left(\frac{\tilde{m}}{\tilde{E}(\vec{q})}\right)\left(-\frac{g_\rho^2}{m_\rho^2}\right)\left(\frac{F_\rho^2(\tilde{p}-\tilde{q})}{1-\frac{(\tilde{p}-\tilde{q})^2}{m_\rho^2}}\right)$$

$$x\left(J_\mu(\tilde{p}-\tilde{q})\left(\frac{\tilde{q}+\tilde{m}}{2\tilde{m}}\right)J^\mu(\tilde{p}-\tilde{q})\right)_{\alpha'\alpha}\Bigg)\left(\frac{1}{1+\frac{C(p)}{m_N}}\right) .$$

Here

$$J_\mu(k) = \gamma_\mu + \frac{i\sigma^{\mu\nu}}{2m_N}k_\nu\left(\frac{f_\rho}{g_\rho}\right) = \gamma_\mu - a\left[\gamma^\mu\frac{k}{2m_N} - \frac{k}{2m_N}\gamma^\mu\right] ,$$

with $a = f_\rho/2g_\rho$, note that the quantity

$$\chi(\tilde{b}) = J_\mu(-\tilde{b})\left(\frac{\tilde{q}+\tilde{m}}{2\tilde{m}}\right)J^\mu(\tilde{b}) ,$$

where $\tilde{b} = \tilde{q} - \tilde{p}$, can be written as

$$\chi(\tilde{b}) = \left(2 - \frac{\tilde{q}}{\tilde{m}}\right) + a\left(\frac{3(\tilde{b}\cdot\tilde{q})}{m_N\tilde{m}} - \frac{3\tilde{b}}{m_N}\right)$$

$$+a^2\left(\frac{3\tilde{b}^2}{2m_N^2} + \frac{\tilde{q}\,\tilde{b}^2}{2m_N^2\tilde{m}} - \frac{2(\tilde{q}\cdot\tilde{b})\,\tilde{b}}{m_N^2\,\tilde{m}}\right) .$$

Here $\tilde{q}^0 = \tilde{E}(\vec{q})$.

$$A_\rho(p) = -3\int \frac{d\vec{q}}{(2\pi)^3}\left(\frac{\tilde{m}}{\tilde{E}(\vec{q})}\right)\left(\frac{g_\rho^2}{m_\rho^2}\right)\left(-\frac{F_\rho^2(\tilde{p}-\tilde{q})}{\left(1-\frac{(\tilde{p}-\tilde{q})^2}{m_\rho^2}\right)}\right)\left(\frac{1}{1+\frac{C(p)}{m_N}}\right)$$

$$x\left(2 - \frac{3a(\tilde{p}-\tilde{q})\cdot\tilde{q}}{m_N\tilde{m}} + \frac{3a^2(\tilde{p}-\tilde{q})^2}{2m_N^2}\right) ,$$

$$B_\rho(p) = 4\int \frac{d\vec{q}}{(2\pi)^3}\left(\frac{\tilde{m}}{\tilde{E}(\vec{q})}\right)\left(\frac{g_\rho^2}{m_\rho^2}\right)\left(\frac{F_\rho^2(\tilde{p}-\tilde{q})}{\left(1-\frac{(\tilde{p}-\tilde{q})^2}{m_\rho^2}\right)}\right)\left(\frac{1}{1+\frac{C(p)}{m_N}}\right)$$

$$\times\left\{\frac{\tilde{q}^0}{\tilde{m}} - \frac{3a(\tilde{p}^0-\tilde{q}^0)}{m_N} + a^2\left(\frac{2(\tilde{q}\cdot\tilde{p}-\tilde{q}^2)(\tilde{p}^0-\tilde{q}^0)}{m_N^2\,\tilde{m}} - \frac{(\tilde{p}-\tilde{q})^2\tilde{q}^0}{2m_N^2\,\tilde{m}}\right)\right\},$$

$$C_\rho(p) = -3\int \frac{d\vec{q}}{(2\pi)^3}\left(\frac{\tilde{m}}{\tilde{E}(\vec{q})}\right)\left(\frac{g_\rho^2}{m_\rho^2}\right)\left(\frac{F_\rho^2(\tilde{p}-\tilde{q})}{4\left(1-\frac{(\tilde{p}-\tilde{q})^2}{m_\rho^2}\right)}\right)\left(\frac{m_N}{1+\frac{C(p)}{m_N}}\right)$$

$$\times\left\{\frac{\vec{q}\cdot\vec{p}}{\tilde{m}\,\vec{p}^2}+\left(-3a+\frac{2a^2(\tilde{p}\cdot\tilde{q}-\tilde{q}^2)}{m_N\,\tilde{m}}\right)\left(\frac{(\vec{p}^2-\vec{p}\cdot\vec{q})}{m_N\,\vec{p}^2}\right)-\frac{a^2(\tilde{p}-\tilde{q})^2(\vec{p}\cdot\vec{q})}{2\,m_N^2\,\tilde{m}\,\vec{p}^2}\right\}.$$

Contribution of π -field:

$$\Sigma^{\pi(pv)}_{\substack{\alpha',\alpha\\ \alpha_T'\alpha_T}}(p) = (-3)\delta_{\substack{\alpha',\alpha\\ T\ T}}\int\frac{d\vec{q}}{(2\pi)^3}\left(\frac{\tilde{m}}{\tilde{E}(\vec{q})}\right)\left(\frac{g_\pi^2}{m_\pi^2}\right)\left(\frac{F_\pi^2(\tilde{p}-\tilde{q})}{1-\frac{(\tilde{p}-\tilde{q})^2}{m_\pi^2}}\right)\left(\frac{1}{1+\frac{C(p)}{m_N}}\right)$$

$$\times\frac{1}{8m_N^2}\left((\tilde{m}^2+m_N^2)-2(\tilde{p}\cdot\tilde{q})\left(1+\frac{\tilde{\not{p}}}{\tilde{m}}\right)+2\tilde{\not{p}}\tilde{m}+\frac{\tilde{\not{q}}}{\tilde{m}}(m_N^2-\tilde{m}^2)\right),$$

$$A_\pi^{(pv)}(p) = 3\int\frac{d\vec{q}}{(2\pi)^3}\left(\frac{\tilde{m}}{\tilde{E}(\vec{q})}\right)\left(\frac{g_\pi^2}{m_\pi^2}\right)\left(\frac{F_\pi^2(\tilde{p}-\tilde{q})}{1-\frac{(\tilde{p}-\tilde{q})^2}{m_\pi^2}}\right)\left(\frac{1}{1+\frac{C(p)}{m_N}}\right)$$

$$\times\frac{1}{8m_N^2}\left(2(\tilde{p}\cdot\tilde{q})-(m_N^2+\tilde{m}^2)\right),$$

$$B_\pi^{(pv)}(p) = 3\int \frac{d\vec{q}}{(2\pi)^3}\left(\frac{\tilde{m}}{\tilde{E}(\vec{q})}\right)\left(\frac{g_\pi^2}{m_\pi^2}\right)\left(\frac{F_\pi^2(\tilde{p}-\tilde{q})}{1-\frac{(\tilde{p}-\tilde{q})^2}{m_\pi^2}}\right)\left(\frac{1}{1+\frac{C(P)}{m_N}}\right)$$

$$\times \frac{1}{8m_N^2\tilde{m}}\left(2\tilde{p}^0(\tilde{p}\cdot\tilde{q})-2\tilde{p}^0\tilde{m}^2+\tilde{q}^0(\tilde{m}^2-m_N^2)\right),$$

$$C_\pi^{(pv)}(p) = -3\int \frac{d\vec{q}}{(2\pi)^3}\left(\frac{\tilde{m}}{\tilde{E}(\vec{q})}\right)\left(\frac{g_\pi^2}{m_\pi^2}\right)\left(\frac{F_\pi^2(\tilde{p}-\tilde{q})}{1-\frac{(\tilde{p}-\tilde{q})^2}{m_\pi^2}}\right)\left(\frac{m_N}{1+\frac{C(p)}{m_N}}\right)$$

$$\times \frac{1}{8m_N^2\tilde{m}}\left(2(\tilde{p}.\tilde{q}-\tilde{m}^2)-\frac{(m_N^2-\tilde{m}^2)(\vec{p}\cdot\vec{q})}{\vec{p}^2}\right).$$

Contribution of ϕ -field:

$$\Sigma^{\varphi}_{\substack{\alpha',\alpha\\ \alpha_T'\alpha}}(p) = \delta_{\alpha_T'\alpha_T}\int \frac{d\vec{q}}{(2\pi)^3}\left(\frac{\tilde{m}}{\tilde{E}(\vec{q})}\right)\left(\frac{g_\varphi^2}{m_\varphi^2}\right)\left\{(\gamma_\mu)_{\alpha',\alpha}F_\omega^2(o)T_r\left(\gamma^\mu\left(\frac{\tilde{q}+\tilde{m}}{2\tilde{m}}\right)\right)T_r\mathbb{I}^{iso}\right.$$

$$\left. - \left(\frac{F_\varphi^2(\tilde{p}-\tilde{q})}{1-\frac{(\tilde{p}-\tilde{q})^2}{m_\varphi^2}}\right)\left(\gamma_\mu\left(\frac{\tilde{q}+\tilde{m}}{2\tilde{m}}\right)\gamma^\mu\right)_{\alpha',\alpha}\right\}\left(\frac{1}{1+\frac{C(p)}{m_N}}\right).$$

$$A_\varphi(p) = 4\int \frac{d\vec{q}}{(2\pi)^3}\left(\frac{\tilde{m}}{\tilde{E}(\vec{q})}\right)\left(\frac{g_\varphi^2}{m_\varphi^2}\right)\left(-\frac{F_\varphi^2(\tilde{p}-\tilde{q})}{2\left(1-\frac{(\tilde{p}-\tilde{q})^2}{m_\varphi^2}\right)}\right)\left(\frac{1}{1+\frac{C(p)}{m_N}}\right),$$

$$B_\varphi(p) = 4\int \frac{d\vec{q}}{(2\pi)^3}\left(\frac{\tilde{m}}{\tilde{E}(\vec{q})}\right)\left(\frac{g_\varphi^2}{m_\varphi^2}\right)\left(F_\varphi^2(o)+\frac{F_\varphi^2(\tilde{p}-\tilde{q})}{4\left(1-\frac{(\tilde{p}-\tilde{q})^2}{m_\varphi^2}\right)}\right)\left(\frac{1}{1+\frac{C(p)}{m_N}}\right),$$

$$C_{\varphi}(p) = 4\int \frac{d\vec{q}}{(2\pi)^3}\left(\frac{\vec{q}\cdot\vec{p}}{\tilde{E}(\vec{q})\vec{p}^2}\right)\left(\frac{g_{\varphi}^2}{m_{\varphi}^2}\right)\left(-\frac{F_{\varphi}^2(\tilde{p}-\tilde{q})}{4\left(1-\frac{(\tilde{p}-\tilde{q})^2}{m_{\varphi}^2}\right)}\right)\left(\frac{m_N}{1+\frac{C(p)}{m_N}}\right) .$$

Contribution of δ -field:

$$\Sigma^{\delta}_{\substack{\alpha',\alpha\\ \alpha'_T\alpha}}(p) = 3\delta_{\substack{\alpha',\alpha\\ T\ T}}\int\frac{d\vec{q}}{(2\pi)^3}\left(\frac{\tilde{m}}{\tilde{E}(\vec{q})}\right)\left(\frac{g_{\delta}^2}{m_{\delta}^2}\right)\left(\frac{F_{\delta}^2(\tilde{p}-\tilde{q})}{1-\frac{(\tilde{p}-\tilde{q})^2}{m_{\delta}^2}}\right)\left(\frac{\tilde{q}+\tilde{m}}{2\tilde{m}}\right)_{\alpha'\alpha}\left(\frac{1}{1+\frac{C(p)}{m_N}}\right) .$$

$$A_{\delta}(p) = \frac{3}{2}\int\frac{d\vec{q}}{(2\pi)^3}\left(\frac{\tilde{m}}{\tilde{E}(\vec{q})}\right)\left(\frac{g_{\delta}^2}{m_{\delta}^2}\right)\left(\frac{F_{\delta}^2(\tilde{p}-\tilde{q})}{[1-\frac{(\tilde{p}-\tilde{q})^2}{m_{\delta}^2}]}\right)\left(\frac{1}{1+\frac{C(p)}{m_N}}\right) ,$$

$$B_{\delta}(p) = \frac{3}{2}\int\frac{d\vec{q}}{(2\pi)^3}\left(\frac{\tilde{q}^0}{\tilde{E}(\vec{q})}\right)\left(\frac{g_{\delta}^2}{m_{\delta}^2}\right)\left(\frac{F_{\delta}^2(\tilde{p}-\tilde{q})}{1-\frac{(\tilde{p}-\tilde{q})^2}{m_{\delta}^2}}\right)\left(\frac{1}{1+\frac{C(p)}{m_N}}\right) ,$$

$$C_{\delta}(p) = -\frac{3}{2}\int\frac{d\vec{q}}{(2\pi)^3}\left(\frac{\vec{q}\cdot\vec{p}}{\tilde{E}(\vec{q})\vec{p}^2}\right)\left(\frac{g_{\delta}^2}{m_{\delta}^2}\right)\left(\frac{F_{\delta}^2(\tilde{p}-\tilde{q})}{1-\frac{(\tilde{p}-\tilde{q})^2}{m_{\delta}^2}}\right)\left(\frac{m_N}{1+\frac{C(p)}{m_N}}\right) .$$

Contribution of η -field:

$$\Sigma^{\eta(pv)}_{\substack{\alpha',\alpha \\ \alpha_T',\alpha_T}}(p) = (-1)\delta_{\alpha_T',\alpha_T}\int \frac{d\vec{q}}{(2\pi)^3}\left(\frac{\tilde{m}}{\tilde{E}(\vec{q})}\right)\left(\frac{g_\eta^2}{m_\eta^2}\right)\left(\frac{F_\eta^2(\tilde{p}-\tilde{q})}{1-\frac{(\tilde{p}-\tilde{q})^2}{m_\eta^2}}\right)\left(\frac{1}{1+\frac{C(p)}{m_N}}\right)$$

$$\times \frac{1}{8m_N^2}\left((\tilde{m}^2+m_N^2)-2(\tilde{p}\bullet\tilde{q})\left(1+\frac{\tilde{p}}{\tilde{m}}\right)+2\tilde{p}\tilde{m}+\frac{\tilde{q}}{\tilde{m}}(m_N^2-\tilde{m}^2)\right) .$$

$$A^{(pv)}_\eta(p) = 4\int \frac{d\vec{q}}{(2\pi)^3}\left(\frac{\tilde{m}}{\tilde{E}(\vec{q})}\right)\left(\frac{g_\eta^2}{m_\eta^2}\right)\left(\frac{F_\eta^2(\tilde{p}-\tilde{q})}{\left(1-\frac{(\tilde{p}-\tilde{q})^2}{m_\eta^2}\right)}\right)\left(\frac{1}{1+\frac{C(p)}{m_N}}\right)$$

$$\times \frac{1}{8m_N^2}\left(2(\tilde{p}\bullet\tilde{q})-(\tilde{m}^2+m_N^2)\right) ,$$

$$B^{(pv)}_\eta(p) = 4\int \frac{d\vec{q}}{(2\pi)^3}\left(\frac{\tilde{q}^0}{\tilde{E}(\vec{q})}\right)\left(\frac{g_\eta^2}{m_\eta^2}\right)\left(\frac{F_\eta^2(\tilde{p}-\tilde{q})}{\left(1-\frac{(\tilde{p}-\tilde{q})^2}{m_\eta^2}\right)}\right)\left(\frac{1}{1+\frac{C(p)}{m_N}}\right)$$

$$\times \frac{1}{8m_N^2\tilde{m}}\left(2\tilde{p}^0(\tilde{p}\bullet\tilde{q})-2\tilde{p}^0\tilde{m}^2+\tilde{q}^0(\tilde{m}^2-m_N^2)\right) ,$$

$$C^{(pv)}_\eta(p) = 4\int \frac{d\vec{q}}{(2\pi)^3}\left(\frac{\tilde{m}}{\tilde{E}(\vec{q})}\right)\left(-\frac{g_\eta^2}{m_\eta^2}\right)\left(\frac{F_\eta^2(\tilde{p}-\tilde{q})}{1-\frac{(\tilde{p}-\tilde{q})^2}{m_\eta^2}}\right)\left(\frac{m_N}{1+\frac{C(p)}{m_N}}\right)$$

$$\times \frac{1}{8m_N^2\tilde{m}}\left(2(\tilde{p}\bullet\tilde{q}-\tilde{m}^2)-\frac{(m_N^2-\tilde{m}^2)}{\vec{p}^2}(\vec{p}\bullet\vec{q})\right) .$$

6.3 Relativistic Dynamics of Nuclear Saturation

Upon inserting

$$f(p,s) = \sqrt{\frac{E_N(\vec{p})}{2m_N}\frac{\tilde{\varepsilon}(\vec{p})}{\tilde{E}(\vec{p})}}\begin{pmatrix} \chi_s \\ \frac{\vec{\sigma}\cdot\vec{p}}{\tilde{\varepsilon}(\vec{p})}\chi_s \end{pmatrix} , \qquad (2.13)$$

into Eq.(2.18), we see that Eq.(5.5) and Eq.(5.6) can be written as:

$$\frac{\mathcal{E}_{kin}}{A} \equiv \frac{3}{k_F^3}\int_0^{k_F} p^2 dp \left(\tilde{E}(\vec{p}) - m_N - \frac{\tilde{m}}{\tilde{E}(\vec{p})}(m_N - \tilde{m})\right) , \qquad (6.8)$$

with $p = |\vec{p}|$ and

$$\frac{\mathcal{E}_{pot}}{A} \equiv \frac{1}{2}\frac{3}{k_F^3}\int_0^{k_F} p^2 dp \left(\frac{\tilde{m}}{\tilde{E}(\vec{p})}A(p)+B(p)+\frac{C(p)\vec{p}^2}{\tilde{E}(\vec{p})}\right) . \qquad (6.9)$$

If we follow the same procedures as those described in Section 5.1 and use the formulas listed in Section 6.2, we can perform a fully-self-consistent calculation of $\Sigma(p)$. This calculation is shown in Fig.6.2.

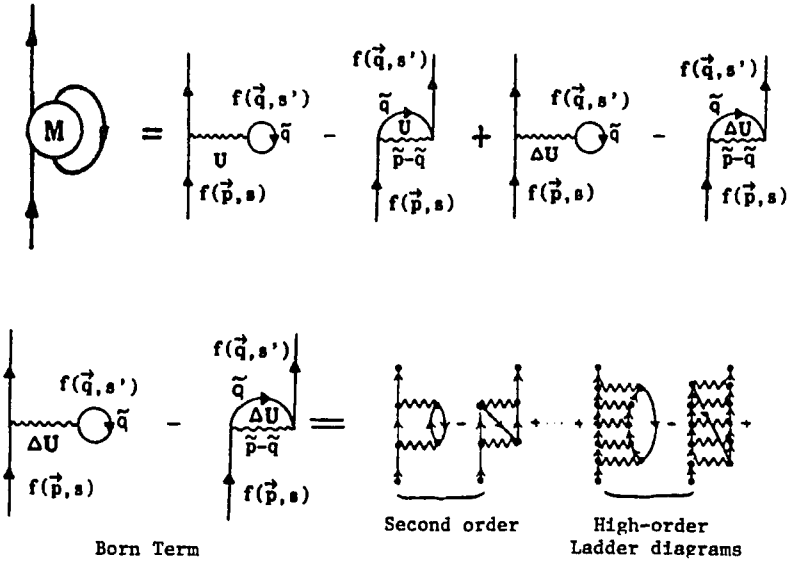

Fig.6.2

If we compare this figure with Fig.3.3, we see that we should change the spinor $u(\vec{p},s)$ to $f(\vec{p},s)$. Another important difference in the self-consistent calculation is that we must now solve the following equation:

$$\tilde{m} = m_N + A(\tilde{m}) \quad . \tag{6.10}$$

This is an integral equation which may be solved by iteration. Equation (6.10), which has the schematic form

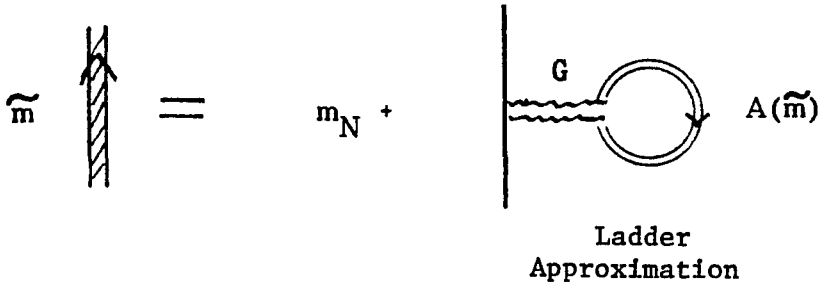

Fig.6.3

must be solved at each nuclear density in a self-consistent manner to obtain A(p).

An illustrative example (σ-ω model)

As a simple example let us consider Walecka's σ-ω model and only use the Relativistic Hartree Approximation (RHA). We then only calculate the first term in Fig.6.1. In that approximation there are only two terms to consider: the σ contribution to A(p) and the ω contribution to B(p). We obtain

$$A = -4\int\frac{d\vec{q}}{(2\pi)^3}\frac{g_\sigma^2}{m_\sigma^2}\frac{\tilde{m}(A)}{\tilde{E}(\vec{q})} = -\frac{g_\sigma^2}{m_\sigma^2}\rho_s \ , \tag{6.11}$$

$$B = \frac{g_\omega^2}{m_\omega^2}\rho_B \ , \tag{6.12}$$

where

$$\rho_s = \frac{2\tilde{m}(A)}{\pi^2}\left(\frac{k_F}{2}\sqrt{k_F^2+\tilde{m}^2(A)} + \frac{\tilde{m}^2(A)}{2}\ln\frac{\tilde{m}(A)}{[k_F^2+\tilde{m}^2(A)]^{1/2}+k_F}\right), \tag{6.13}$$

$$\rho_B = \frac{2k_F^3}{3\pi^2} \ ; \ (k_F = \text{Fermi momentum}) \ . \tag{6.14}$$

We use the following density-independent coupling constants:

$$C_s = g_\sigma(m^2{}_N/m^2{}_\sigma) = 267.1 \ , \tag{6.15}$$

$$C_v = g_\omega(m^2{}_N/m^2{}_\omega) = 195.9 \ , \tag{6.16}$$

to evaluate A(p) and $\tilde{m}[A(p)]$. We then insert $\tilde{m}$ into Eqs.(6.8) and (6.9) to obtain the saturation curves. The results, including comparison between non-self-consistent and fully - self-consistent calculations are listed in Table 25.

For each iteration we use the absolute value $|\ A_{output} - A_{input}\ |$ to specify the accuracy of the solution. The results reported in Table 25 show the effect of modifying the required iteration accuracy. From Table 25 we see that the results obtained by using many iterations are very close to the result of Walecka (Ref.8).

6.4 Relativistic Dynamics of Nuclear Saturation: Numerical Results

For the potentials HEA, HM2 and BMR2, we solve Eq.(6.10) by iteration. Choosing an iteration accuracy for each nuclear density, we evaluate A(p), B(p), C(p) and the self-consistent value of $\widetilde{m}[A(p), C(p)]$. Then, inserting these values into Eqs.(6.8)-(6.9), we calculate various saturation curves. The results are shown in Figs.26-27 and Figs.29-32. Figs.33-35 exhibit the results of using different iteration accuracy specifications. (Also see Tables 26-28.)

Results for the potential HEA

In Fig.26, the curve labelled a is the fully-self-consistent saturation curve for the potential HEA calculated in our pseudoparticle model using the potential ΔU as given in Chapter 3. Values of the incompressibility parameter obtained in these calculations are given under the heading Approximation 1 in Table 23. These values are quite close to the value calculated from the value of the Migdal parameter, F_0, in Ref.25. There it was found that K_∞= 175 MeV. Here we calculated K_∞=177 MeV directly from the binding energy curves:

$$K_\infty = 9\rho_B^2 \frac{\partial^2(\rho_B E_B/A)}{\partial^2 \rho_B} = k_F^2 \frac{\partial^2(E_B/A)}{\partial^2 \rho_B} \quad . \tag{6.17}$$

If we fix the values of the coupling constants to those found for $k_F = 1.36\ fm^{-1}$ in Chapter 3, we obtain the saturation curve labelled a in Fig.27. When we arbitrarily increase $\delta g^2_\omega/(4\pi)$ to 17.5(see Section 5.2), we obtain the fully self-consistent curves labelled b in Figs. 26-27. (See Table 23 -- Approximations 3-4.)

Results for the Potential HM2

For the potential HM2, we obtain the fully self-consistent saturation curves labelled a and b in Figs.29-30. The values obtained for the Fermi momentum, k_F, and for K_∞, are given in Table 24. In Fig.32, the curves labelled D and N denote the self-consistent results for the binding energy per nucleon for the potential, $\bar{V}_{eff} = \bar{U} + \Delta\bar{U}$, introduced in Chapter 3. The potential is an effective interaction simulating the G-matrix results for the interaction HM2. Here we use the modified pseudoparticle coupling constants $\delta g^2_\sigma = -1.15$, $\delta g^2_\omega = 6.98$, for $k_F = k_F^{NM} = 1.36\ fm^{-1}$. ($M_\sigma$ = 1 GeV, M_ω = 1 GeV). Curve N denotes the results for density-independent pseudoparticle coupling constants while curve D denotes the results for density-dependent pseudoparticle coupling constants. The density dependence used is that given in Eqs.(3.16)-(3.17).

Results for the potential BMR2

For the same Approximations 1-7 (see Section 5.4), the results of the fully-self-consistent calculations are listed in Table 6.1. (Also see Fig.31.)

Table 6.1

Pseudoparticle coupling constants for the potential BMR2 for $k_F = k_F^{NM} = 1.36$ fm^{-1}. Also given are the fully-self-consistent results: the Fermi momentum, k_F, at saturation and the incompressibility parameter, K_∞, for Approximations 1 through 7.

BMR2	$\frac{1}{4\pi}\delta g_\sigma^2$	$\frac{1}{4\pi}\delta g_\omega^2$	$\frac{1}{4\pi}\delta g_\delta^2$	k_F (fm^{-1})	B.E./A (MeV)	K_∞ (MeV)
Approx.1	- 6.35	14.40	0.00	1.39	-15.33	493
Approx.2	- 5.50	14.40	8.54	1.39	-15.97	483
Approx.3	-10.40	7.25	8.54	1.33	-15.58	467
Approx.4	-10.50	7.25	8.54	1.33	-15.30	467
Approx.5	-10.60	7.25	8.54	1.34	-15.87	517
Approx.6	-5.50	14.54	8.54	1.39	-15.97	493
Approx.7	-5.50	14.26	8.54	1.39	-15.33	493

6.5 Calculation of the Migdal Parameters of the Fully-Self -Consistent RBHF Theory

For various potentials, if one determines the self-consistent solution of Eq.(6.10), $\widetilde{m}[A(k_F),C(k_F)]$, we can obtain the Migdal parameters of the fully-self-consistent RBHF theory.

As a simple example let us consider the scattering amplitude for forward scattering of two quasi-particles at the Fermi surface, which arises from the exchange of a ω meson. The fully on-shell amplitude is

$$\overline{f}_\alpha(\vec{p}_1's_1')\overline{f}_\beta(\vec{p}_2's_2')\langle\vec{p}_1',\vec{p}_2'|M^{on}_{\alpha\beta\alpha',\beta'}|\vec{p}_1,\vec{p}_2\rangle_\omega f_{\alpha'}(\vec{p}_1s_1)f_{\beta'}(\vec{p}_2s_2) \quad , (6.18)$$

where in M^{on} we have $\vec{p}^2{}_1 = \vec{p}^2{}_2 = k^2{}_F = m^2{}_N$. We have

$$\overline{f}_\alpha(\vec{p}_1's_1')\overline{f}_\beta(\vec{p}_2's_2')\langle\vec{p}_1',\vec{p}_2'|M^{on}_{\alpha\beta\alpha',\beta'}|\vec{p}_1,\ \vec{p}_2\rangle_\omega f_{\alpha'}(\vec{p}_1s_1)f_{\beta'}(\vec{p}_2s_2)$$

$$= \tilde{f}_\omega(x) + \tilde{f}'_\omega(x)\vec{\tau}_1\cdot\vec{\tau}_2 + [\ \tilde{g}_\omega(x) + \tilde{g}'_\omega(x)\vec{\tau}_1\cdot\vec{\tau}_2\ ]\vec{\sigma}_1\cdot\vec{\sigma}_2$$

$$+ \frac{1}{k_F^2}[\ \tilde{h}_\omega(x) + \tilde{h}'_\omega(x)\vec{\tau}_1\cdot\vec{\tau}_2\ ]S_{12}(\vec{p}) \quad , \qquad (6.19)$$

where

$$\tilde{f}_\omega(x) = \frac{1}{2}\frac{A_\omega F^2_\omega(t)}{B_\omega - x} + \left(\frac{g^2_\omega F^2_\omega(0)}{m^2_\omega} - \frac{1}{4}\frac{A_\omega F^2_\omega(t)}{B_\omega - x}\right)\left(\left(\frac{\tilde{E}}{\tilde{m}}\right)^2 - \left(\frac{k_F}{\tilde{m}}\right)^2 x\right) \quad ,$$

$$\tilde{f}'_{\omega}(x) = \frac{1}{2}\frac{A_{\omega}F^2_{\omega}(t)}{B_{\omega}-x} - \frac{1}{4}\frac{A_{\omega}F^2_{\omega}(t)}{B_{\omega}-x}\left((\frac{\tilde{E}}{\tilde{m}})^2-(\frac{k_F}{\tilde{m}})^2x\right) \quad ,$$

$$\tilde{g}_{\omega}(x) = \tilde{g}'_{\omega}(x) = \frac{1}{4}\frac{A_{\omega}F^2_{\omega}(t)}{B_{\omega}-x}\left(1+\frac{1}{3}(\frac{k_F}{\tilde{m}})^2(1-x)\right) \quad .$$

Using the same procedures we can determine the functions $\tilde{f}(x)$, $\tilde{f}'(x)$, $\tilde{g}(x)$, $\tilde{g}'(x)$, etc. for the exchange of other mesons.

σ <u>exchange</u>:

Let $A_{\sigma}=g^2{}_{\sigma}/(2k_F{}^2)$ and $B_{\sigma}=1+m_{\sigma}{}^2/(2k_F{}^2)$. Then

$$\tilde{f}_{\sigma}(x) = \frac{1}{8}\frac{A_{\sigma}F^2_{\sigma}(t)}{B_{\sigma}-x} + \frac{1}{8}\frac{A_{\sigma}F^2_{\sigma}(t)}{B_{\sigma}-x}\left((\frac{\tilde{E}}{\tilde{m}})^2-(\frac{k_F}{\tilde{m}})^2x\right) - \frac{g^2_{\sigma}F^2_{\sigma}(0)}{m^2_{\sigma}} \quad ,$$

$$\tilde{f}'_{\sigma}(x) = \frac{1}{8}\frac{A_{\sigma}F^2_{\sigma}(t)}{B_{\sigma}-x} + \frac{1}{8}\frac{A_{\sigma}F^2_{\sigma}(t)}{B_{\sigma}-x}\left((\frac{\tilde{E}}{\tilde{m}})^2-(\frac{k_F}{\tilde{m}})^2x\right) \quad ,$$

$$\tilde{g}_{\sigma}(x) = \tilde{g}'_{\sigma}(x) = \frac{1}{8}\frac{A_{\sigma}F^2_{\sigma}(t)}{B_{\sigma}-x}\left((\frac{\tilde{E}}{\tilde{m}})^2+1+\frac{2}{3}(\frac{k_F}{\tilde{m}})^2(1-x)\right) \quad .$$

ρ <u>exchange</u>:

Let $A_{\rho}=g^2{}_{\rho}/(2k_F{}^2)$, $B_{\rho}=1+m_{\rho}{}^2/(2k_F{}^2)$ and $2a=(f_{\rho}/g_{\rho})$. Using the Gordon decomposition (see Appendix E), we find

$$\tilde{f}_\rho(x) = -\frac{3}{2}\frac{A_\rho F_\rho^2(t)}{B_\rho - x}\left[a_1' + a_2'\left[\left(\frac{\tilde{E}}{\tilde{m}}\right)^2 - \left(\frac{k_F}{\tilde{m}}\right)^2 x\right]\right] ,$$

$$\tilde{f}_\rho'(x) = \frac{1}{2}\frac{A_\rho F_\rho^2(t)}{B_\rho - x}\left(a_1' + a_2'\left[\left(\frac{\tilde{E}}{\tilde{m}}\right)^2 - \left(\frac{k_F}{\tilde{m}}\right)^2 x\right]\right) ,$$

$$\tilde{g}_\rho(x) = -\frac{3}{2}\frac{A_\rho F_\rho^2(t)}{B_\rho - x}\left(a_3'\left[2+\frac{4}{3}\left(\frac{k_F}{\tilde{m}}\right)^2(1-x)\right] - a_4'\left[1+\frac{1}{3}\left(\frac{k_F}{\tilde{m}}\right)^2(1-x)\right]\right) ,$$

$$\tilde{g}_\rho'(x) = -\frac{1}{3}\tilde{g}_\rho(x) ,$$

$$a_1' = 1 + 3a' + 3a'^2 + \frac{1}{2}\left(\frac{ak_F}{m_N}\right)^2(1-x) ,$$

$$a_2' = -\frac{1}{2} - 3a' - 3a'^2 + \frac{1}{2}\left(\frac{ak_F}{m_N}\right)^2(1-x) ,$$

$$a_3' = -\frac{1}{2}a' - \frac{1}{2}a'^2 + \frac{1}{4}\left(\frac{ak_F}{m_N}\right)^2(1-x) ,$$

$$a_4' = -\frac{1}{2} - a' - a'^2 - \frac{1}{2}\left(\frac{ak_F}{m_N}\right)^2(1-x) ,$$

$$a' = a(\tilde{m}/m_N) \ , \ 2a = (f_\rho/g_\rho) \ .$$

π <u>exchange</u> (pseudovector coupling):

Let $A_\pi = g^2_\pi/(2k_F^2)$ and $B_\pi = 1 + m_\pi^2/(2k_F^2)$. Then

$$\tilde{f}_\pi(x) = \frac{3}{8}\frac{A_\pi F_\pi^2(t)}{B_\pi - x}\left(\frac{k_F}{\tilde{m}}\right)^2(1-x) ,$$

$$\tilde{f}_\pi'(x) = -\frac{1}{3}\tilde{f}_\pi(x) ,$$

$$\tilde{g}_\pi(x) = \tilde{f}'_\pi(x) \quad ,$$

and

$$\tilde{g}'_\pi(x) = -\frac{1}{3}\,\tilde{g}_\pi(x) \quad .$$

ϕ exchange:

Let $A_\phi = g^2{}_\phi/(2k_F{}^2)$ and $B_\phi = 1+m_\phi{}^2/(2k_F{}^2)$. Then

$$\tilde{f}_\phi(x) = \frac{1}{2}\,\frac{A_\phi F_\phi^2(t)}{B_\phi - x} + \left(\frac{g_\phi^2 F_\phi^2(0)}{m_\phi^2} - \frac{1}{4}\,\frac{A_\phi F_\phi^2(t)}{B_\phi - x}\right)\left(\left(\frac{\tilde{E}}{\tilde{m}}\right)^2 - \left(\frac{k_F}{\tilde{m}}\right)^2 x\right) \quad ,$$

$$\tilde{f}'_\phi(x) = \frac{1}{2}\,\frac{A_\phi F_\phi^2(t)}{B_\phi - x} - \frac{1}{4}\,\frac{A_\phi F_\phi^2(t)}{B_\phi - x}\left(\left(\frac{\tilde{E}}{\tilde{m}}\right)^2 - \left(\frac{k_F}{\tilde{m}}\right)^2 x\right) \quad ,$$

$$\tilde{g}_\phi(x) = \tilde{g}'_\phi(x) = \frac{1}{4}\,\frac{A_\phi F_\phi^2(t)}{B_\phi - x}\left(1 + \frac{1}{3}\left(\frac{k_F}{\tilde{m}}\right)^2 (1-x)\right) \quad .$$

η exchange (pseudovector coupling):

Let $A_\eta = g^2{}_\eta/(2k_F{}^2)$ and $B_\eta = 1+m_\eta{}^2/(2k_F{}^2)$. Then

$$\tilde{f}_\eta(x) = \frac{1}{8}\,\frac{A_\eta F_\eta^2(t)}{B_\eta - x}\left(\frac{k_F}{\tilde{m}}\right)^2 (1-x) \quad ,$$

$$\tilde{f}'_\eta(x) = \tilde{f}_\eta(x) \quad ,$$

$$\tilde{g}_\eta(x) = -\frac{1}{3}\tilde{f}_\eta(x) \quad ,$$

and

$$\tilde{g}'_\eta(x) = -\frac{1}{3}\tilde{f}_\eta(x) \quad .$$

δ exchange:

Let $A_\delta = g^2{}_\delta/(2k_F{}^2)$ and $B_\delta = 1+m_\delta{}^2/(2k_F{}^2)$. Then

$$\tilde{f}_\delta(x) = \frac{3}{8}\frac{A_\delta F_\delta^2(t)}{B_\delta - x}\left(2+(\frac{k_F}{\tilde{m}})^2(1-x)\right) \quad ,$$

$$\tilde{f}'_\delta(x) = -\frac{g_\delta^2 F_\delta^2(0)}{m_\delta^2} - \frac{1}{3}\tilde{f}_\delta(x) \quad ,$$

$$\tilde{g}_\delta(x) = \tilde{f}_\delta(x) \quad ,$$

$$\tilde{g}'_\delta(x) = -\frac{1}{3}\tilde{f}_\delta(x) \quad .$$

6.6 Migdal Parameters of the Fully-Self-Consistent RBHF Theory: Numerical Results

For the amplitude $\mathcal{F}_{eff}(\vec{p}_1,\vec{p}_2)$, we have evaluated the Migdal parameters of the fully-self-consistent RBHF theory. Use the formulas in Section 6.2, we sum all the contributions of the mesons of

the OBEP, find the self-consistent solution of Eq.(6.10), $\widetilde{m}[A(k_F),C(k_F)]$, then we use the formulas in Section 6.5 to find the functions $\widetilde{f}_l$, $\widetilde{f}'_l$, $\widetilde{g}_l$, $\widetilde{g}'_l$, etc.. In Table 29 (for the potential HEA), and in Table 30 (for the potential HM2), we present details of our calculation and the comparison with the semi-self-consistent calculations (see Section 4.2.4) and with the G-matrix results, for various nuclear densities.

Chapter 7

Summary and Outlook

In this work we have shown how, using a simple calculational scheme, we could fit the Migdal parameters and various matrix elements of the nucleon self-energy, $\Sigma(p)$, which had been calculated in the relativistic-Brueckner-Hartree-Fock (RBHF) theory. From the text we see that it was quite simple to fit the nucleon self-energy and Migdal parameters, which had been calculated for two "realistic" nucleon-nucleon interactions (HEA and HM2) in a rather complicated reaction matrix calculation for (relativistic) nuclear matter. (These potentials differ mainly in the strength of the tensor force. For example, the potential HM2 has strong tensor coupling of the rho meson to the nucleon and therefore a weak nucleon-nucleon tensor force.) For example, consider a one-boson-exchange potential which includes a description of the exchange of σ, ω, π, ρ, η, ϕ, and δ "mesons". One can calculate the Born terms for the exchange of these mesons and add the Born terms for the exchange of a pseudo-sigma and a pseudo-omega particle with a large mass, with either a real or imaginary coupling constant. The essential point is that the exchange of the particles and pseudoparticles of our simple model can be treated in the Born approximation, and the reaction matrices of the full theory can be well approximated. As may be seen in this work, the pseudoparticle method works quite well in reproducing the reaction matrices of the RBHF theory for densities of $(1/4)\rho_{NM}$ to

about $(5/4)\rho_{NM}$, where ρ_{NM} is the density of nuclear matter. (This detailed fit requires that the pseudoparticle coupling constants have some relatively weak density dependence.) In this work we also present the nuclear matter saturation curves for the potentials HEA, HM2 and BMR2 using our pseudoparticle model. This simple model reproduces the saturation curves calculated with the full relativistic Brueckner-Hartree-Fock theory quite well. Within the context of the pseudoparticle approximation to the full RBHF theory, we obtained quite reasonable values for the incompressibility parameter. The values are quite similar to those obtained earlier using the full RBHF analysis.

We have to stress that, although the relativistic model of nuclear physics has achieved a number of successes, much work remains to be done. It would be useful to extend the RBHF theory to provide a (parameter-free) model of finite nuclei. Further, the construction of the relativistic optical potential at low energies remains an outstanding problem. The use of relativistic wave functions to study nuclear spectroscopy and inelastic scattering should also receive significant attention.

The goal of this work was to obtain a simple effective interaction which could be used for relativistic-Hartree-Fock calculations of finite nuclei. That is, we wished to avoid the difficult problem of calculating reaction matrices for finite nuclei. For calculations in finite nuclei it is much easier to use density-independent approximations. Therefore, the most directly relevant model would

be given by the solid curves of Figs.26 and 30, for the potentials HEA and HM2, respectively, or curve N of Fig.32 (HM2). If one wishes to use a model which reproduces generally accepted values of binding energy and saturation density, the relevant models are represented by curve b of Fig.26 and curve N of Fig.32. Of course, our methods may be used to construct pseudoparticle approximations for other boson-exchange-models of the nuclear force.

Our group has begun to test the pseudoparticle model of the nuclear interaction in finite systems. We have calculated the properties of finite nuclei: ^{12}C, ^{16}O and ^{40}Ca in a relativistic Hartree-Fock approximation using the quasipotentials constructed in this work. The study of finite nuclei is different from the study of nuclear matter. The wave function is not a plane wave, and we must use the general form of the relativistic optical potential for the case of an off-mass-shell nucleon [Eq.(2.26)]. We must also consider states characterized by angular momentum. For ^{12}C, ^{16}O and ^{40}Ca, for the potential HM2, we did not add any new adjustable parameters. We did not change the form factors and we did not make any change in the quasipotentials constructed in this work. We then obtained quite good results for the binding energy, single-particle energy levels and the charge density distribution. The use of the quasipotentials constructed in this work to calculate the properties of finite nuclei in a relativistic Hartree-Fock approximation is still under study at the Center for Nuclear Theory of Brooklyn College. We hope to report on results of numerical calculations in the near future.

The Brooklyn College group believes that the nucleon is well represented as a nontopological soliton and the motion of the rest frame of this soliton is described by a four-component Dirac spinor. In nuclear matter this spinor is to be determined by solving Eq.(2.8). In Eq.(2.8) there is a strong scalar field, A(p), arising from meson exchange. This field changes the mass parameter in the spinor from the free-space value. That is the essential feature underlying the success of the relativistic theories of nuclear structure.

In recent years, the Brooklyn group has developed a unified approach to hadron and nuclear structure based upon the recognization that the scalar field used in determining hadron structure in "covariant soliton dynamics" may be related to the scalar fields used in the description of nuclear structure.

The description of nuclear structure via the use of effective Lagrangians has been extremely successful. Effective Lagrangians describing quarks coupled to a scalar field (which is considered to be an order parameter of a gluon condensate in a zero-momentum mode) have been of use in describing hadron structure. We expect further success for this approach and we believe that a new and more fundamental theory will emerge which will represent a unification of nuclear and hadron physics.

Table 1

Migdal parameters for the potential HEA calculated for the case where the nucleon spinor is $u(\vec{p},s)$ with $|\vec{p}| = k_F$(see text). The first line is calculated with $V_{eff} = \Delta U$ and the third line gives the results obtained for $V_{eff} = U + \Delta U$. The fourth line is the result of a reaction matrix calculation. (Note that the Migdal parameters given here are not those of the relativistic BHF theory.)

$k_F(fm^{-1})$	F_0	F_1	F'_0	F'_1	G_0	G_1	G'_0	G'_1
1.36	3.132	-1.532	2.928	0.182	0.829	0.477	-0.348	0.024
	-5.462	0.335	3.455	0.308	-0.443	0.062	1.425	0.282
	-2.330	-1.197	0.527	0.490	0.386	0.539	1.077	0.306
	-2.095	-1.251	0.551	0.539	0.365	0.511	1.178	0.246
1.00	1.900	-0.897	-2.180	0.212	0.838	0.343	-0.206	0.052
	-4.507	0.169	3.052	0.164	-0.365	0.039	1.306	0.148
	-2.607	-0.728	0.827	0.376	0.473	0.382	1.100	0.200
	-2.439	-0.841	0.897	0.475	0.362	0.349	1.097	0.190
1.20	2.546	-1.232	-2.611	0.211	0.839	0.427	-0.291	0.047
	-5.090	0.256	3.323	0.243	-0.413	0.051	1.394	0.220
	-2.544	-0.976	0.712	0.454	0.426	0.478	1.144	0.267
	-2.266	-1.069	0.694	0.534	0.370	0.441	1.140	0.231
1.40	3.824	-1.608	-30011	0.172	0.824	0.490	-0.360	0.016
	-5.543	0.356	3.478	0.324	-0.449	0.064	1.428	0.298
	-2.259	-1.252	0.477	0.496	0.375	0.554	1.068	0.314
	-2.046	-1.302	0.517	0.538	0.363	0.526	1.187	0.249
1.60	4.076	-2.016	-3.339	0.091	0.790	0.536	-0.418	-0.037
	-5.903	0.461	3.555	0.402	-0.472	0.074	1.432	0.377
	-1.827	-1.555	0.216	0.493	0.318	0.610	1.005	0.340
	-1.756	-1.592	0.361	0.529	0.348	0.583	1.235	0.255

Table 2

Various contributions to the Migdal Parameters for the potential HEA. The first seven rows give the contribution of the Born terms for each of the mesons indicated. The contributions from pseudoparticle exchange (ΔU_σ, ΔU_ω and ΔU_δ) are given as well as their sum (ΔU). The total is the result for $V_{eff} = U + \Delta U$ and is compared to reaction matrix results of reference 7. Here $k_F = 1.36$ fm^{-1}.

	F_0	F_1	F'_0	F'_1	G_0	G_1	G'_0	G'_1
U_η	0.068	-0.050	0.068	-0.050	-0.023	0.017	-0.023	0.017
U_π	1.234	-0.266	-0.411	0.089	-0.411	0.089	0.137	-0.030
U_σ	-9.211	0.732	1.773	0.732	1.773	0.732	1.773	0.732
U_δ	1.928	0.326	-3.693	-0.109	1.928	0.326	-0.643	-0.109
U_ω	7.558	-1.261	-1.352	-0.588	-1.537	-0.536	-1.537	-0.536
U_ρ	0.347	-0.818	0.922	0.194	-0.634	-0.076	0.212	0.025
U_ϕ	1.208	-0.195	-0.235	-0.086	-0.267	-0.075	-0.267	-0.075
U(Sum)	3.132	-1.532	-2.928	0.182	0.829	0.477	-0.348	0.024
ΔU_σ	-1.312	0.056	0.354	0.056	0.354	0.056	0.354	0.056
ΔU_ω	-2.749	0.444	0.531	0.197	0.604	0.171	0.604	0.171
ΔU_δ	-1.401	-0.165	2.570	0.055	-1.401	-0.165	0.467	0.055
ΔU	-5.462	0.335	3.455	0.308	-0.443	0.062	1.425	0.282
$V_{eff}=U+\Delta U$	-2.330	-1.197	0.527	0.490	0.386	0.539	1.077	0.306
G matrix results	-2.095	-1.251	0.551	0.539	0.365	0.511	1.178	0.246
Error (%)	11.22	4.32	4.36	9.09	5.75	5.48	8.57	24.39

Table 3

Same as Table 2, except that $k_F = 1.00\ fm^{-1}$.

	F_0	F_1	F'_0	F'_1	G_0	G_1	G'_0	G'_1
U_η	0.035	-0.030	0.035	-0.030	-0.012	0.010	-0.012	0.010
U_π	0.869	-0.304	-0.289	0.102	-0.289	0.102	0.096	-0.034
U_σ	-6.769	0.415	1.598	0.415	1.598	0.415	1.598	0.415
U_δ	1.581	0.152	-2.851	-0.051	1.581	0.152	-0.527	-0.051
U_ω	5.319	-0.580	-1.232	-0.304	-1.323	-0.265	-1.323	-0.265
U_ρ	0.013	-0.463	0.767	0.122	-0.509	-0.036	0.170	0.012
U_ϕ	0.852	-0.087	-0.208	-0.042	-0.208	-0.035	-0.208	-0.035
U(Sum)	1.900	-0.897	-2.180	0.212	0.838	0.343	-0.206	0.052
ΔU_σ	-1.092	0.030	0.323	0.030	0.323	0.030	0.323	0.030
ΔU_ω	-2.162	0.221	0.526	0.107	0.565	0.091	0.565	0.091
ΔU_δ	-1.253	-0.082	2.203	0.027	-1.253	-0.082	0.418	0.027
ΔU	-4.507	0.169	3.052	0.164	-0.365	0.039	1.306	0.148
$V_{eff}=U+\Delta U$	-2.607	-0.728	0.872	0.376	0.473	0.382	1.100	0.200
G matrix results	-2.439	-0.841	0.897	0.475	0.362	0.349	1.097	0.190
Error (%)	6.89	13.44	2.79	20.84	30.66	9.46	0.27	5.50

Table 4

Same as Table 2, except that $k_F = 1.20$ fm^{-1}.

	F_0	F_1	F'_0	F'_1	G_0	G_1	G'_0	G'_1
U_η	0.054	-0.041	0.054	-0.041	-0.018	0.014	-0.018	0.014
U_π	1.081	-0.292	-0.360	0.098	-0.360	0.098	0.120	-0.033
U_σ	-8.139	0.591	1.718	0.591	1.718	0.591	1.718	0.591
U_δ	1.791	0.243	-3.335	-0.081	1.791	0.243	-0.597	-0.081
U_ω	6.542	-0.927	-1.319	-0.457	-1.459	-0.408	-1.459	-0.408
U_ρ	0.171	-0.665	0.858	0.166	-0.583	-0.056	0.195	0.019
U_ϕ	1.046	-0.141	-0.227	-0.065	-0.250	-0.055	-0.250	-0.055
U(Sum)	2.546	-1.232	-2.611	0.211	0.839	0.427	-0.291	0.047
ΔU_σ	-1.229	0.044	0.346	0.044	0.346	0.044	0.346	0.044
ΔU_ω	-2.505	0.339	0.539	0.157	0.597	0.134	0.597	0.134
ΔU_δ	-1.356	-0.127	2.438	0.042	-1.356	-0.127	0.451	0.042
ΔU	-5.090	0.256	3.323	0.243	-0.413	0.051	1.394	0.220
$V_{eff}=U+\Delta U$	-2.544	-0.976	0.712	0.454	0.426	0.478	1.144	0.267
G matrix results	-2.266	-1.069	0.694	0.534	0.370	0.441	1.140	0.231
Error (%)	12.27	8.70	2.59	14.98	15.14	8.39	0.35	15.58

Table 5

Same as Table 2, except that k_F = 1.40 fm^{-1}.

	F_0	F_1	F'_0	F'_1	G_0	G_1	G'_0	G'_1
U_η	0.073	-0.052	0.073	-0.052	-0.024	0.016	-0.024	0.016
U_π	1.270	-0.257	-0.423	0.086	-0.423	0.086	0.141	-0.029
U_σ	-9.474	0.767	1.783	0.767	1.783	0.767	1.783	0.767
U_δ	1.958	0.350	-3.779	-0.117	1.958	0.350	-0.653	-0.117
U_ω	7.815	-1.352	-1.356	-0.621	-1.553	-0.569	-1.553	-0.569
U_ρ	0.393	-0.854	0.937	0.200	-0.646	-0.081	0.215	0.027
U_ϕ	1.249	-0.210	-0.236	-0.091	-0.271	-0.079	-0.271	-0.079
U(Sum)	3.824	-1.608	-3.001	0.172	0.824	0.490	-0.360	0.016
ΔU_σ	-1.329	0.060	0.355	0.060	0.355	0.060	0.355	0.060
ΔU_ω	-2.806	0.472	0.526	0.206	0.604	0.180	0.604	0.180
ΔU_δ	-1.408	-0.176	2.597	0.058	-1.408	-0.176	0.469	0.058
ΔU	-5.543	0.356	3.478	0.324	-0.449	0.064	1.428	0.298
$V_{eff}=U+\Delta U$	-2.259	-1.252	0.477	0.496	0.375	0.554	1.068	0.314
G matrix results	-2.046	-1.302	0.517	0.538	0.363	0.526	1.187	0.249
Error (%)	10.41	3.84	7.74	7.81	3.31	5.32	10.03	26.10

Table 6

Same as Table 2, except that $k_F = 1.60$ fm^{-1}.

	F_0	F_1	F'_0	F'_1	G_0	G_1	G'_0	G'_1
U_η	0.093	-0.061	0.093	-0.061	-0.031	0.020	-0.031	0.020
U_π	1.434	-0.207	-0.478	0.069	-0.478	0.069	0.159	-0.023
U_σ	-10.754	0.930	1.805	0.930	1.805	0.930	1.805	0.930
U_δ	2.081	0.469	-4.181	-0.156	2.081	0.469	-0.694	-0.156
U_ω	9.131	-1.850	-1.350	-0.785	-1.606	-0.738	-1.606	-0.738
U_ρ	0.632	-1.007	1.010	0.212	-0.697	-0.108	0.233	0.036
U_ϕ	1.459	-0.290	-0.238	-0.118	-0.284	-0.106	-0.284	-0.106
U(Sum)	4.076	-2.016	-3.339	0.091	0.790	0.536	-0.418	-0.037
ΔU_σ	-1.408	0.076	0.355	0.076	0.355	0.076	0.355	0.076
ΔU_ω	-3.072	0.613	0.498	0.250	0.594	0.225	0.594	0.225
ΔU_δ	-1.421	-0.227	2.699	0.076	-1.421	-0.227	0.474	0.076
ΔU	-5.903	0.461	3.555	0.402	-0.472	0.074	1.423	0.377
$V_{eff}=U+\Delta U$	-1.827	-1.555	0.216	0.493	0.318	0.610	1.005	0.340
G matrix results	-1.756	-1.592	0.361	0.529	0.348	0.583	1.235	0.255
Error (%)	4.04	2.32	40.17	6.81	8.62	4.63	18.62	33.33

Table 7

Migdal parameters for the potential HM2 calculated for the case where the nucleon spinor is $u(\vec{p},s)$ with $|\vec{p}| = k_F$(see text). The first line is calculated with $V_{eff} = \Delta U$ and the third line gives the results obtained for $V_{eff} = U + \Delta U$. The fourth line is the result of a reaction matrix calculation. (Note that the Migdal parameters given here are not those of the relativistic BHF theory.)

$k_F(fm^{-1})$	F_0	F_1	F'_0	F'_1	G_0	G_1	G'_0	G'_1
1.36	0.362	-1.853	-0.174	0.693	-0.529	0.664	0.574	0.205
	-2.702	0.271	0.648	0.146	0.726	0.111	0.726	0.111
	-2.341	-1.582	0.474	0.839	0.197	0.775	1.300	0.316
	-2.470	-1.467	0.779	0.695	0.249	0.592	1.375	0.279
1.00	-0.390	-1.038	0.090	0.458	-0.149	0.433	0.542	0.134
	-1.969	0.121	0.545	0.069	0.579	0.051	0.579	0.051
	-2.359	-0.917	0.635	0.527	0.430	0.484	1.121	0.185
	-2.816	-0.925	1.114	0.532	0.336	0.401	1.265	0.198
1.20	-0.027	-1.462	-0.048	0.595	-347	0.565	0.567	0.180
	-2.376	0.196	0.609	0.109	0.666	0.081	0.666	0.081
	-2.403	-1.266	0.561	0.704	0.319	0.646	1.233	0.261
	-2.632	-1.214	0.909	0.636	0.301	0.513	1.322	0.250

Table 8

Various contributions to the Migdal Parameters for the potential HM2. The first seven rows give the contribution of the Born terms for each of the mesons indicated. The contributions from pseudoparticle exchange (ΔU_σ and ΔU_ω) are given as well as their sum (ΔU). The total is the result for $V_{eff} = U + \Delta U$ and is compared to reaction matrix results of reference 7. Here $k_F = 1.36$ fm^{-1}.

	F_0	F_1	F'_0	F'_1	G_0	G_1	G'_0	G'_1
U_η	0.024	-0.019	0.024	-0.019	-0.008	0.006	-0.008	0.006
U_π	1.461	-0.407	-0.487	0.136	-0.487	0.136	0.162	-0.045
U_σ	-9.877	0.701	2.117	0.701	2.117	0.701	2.117	0.701
U_δ	0.260	0.033	-0.470	-0.011	0.260	0.033	-0.087	-0.011
U_ω	7.460	-0.966	-1.587	-0.479	-1.811	-0.387	-1.811	-0.387
U_ρ	1.033	-1.195	0.228	0.366	-0.600	0.176	0.200	-0.059
U(Sum)	0.362	-1.853	-0.174	0.693	-0529	0.664	0.574	0.205
ΔU_σ	-0.363	0.013	0.107	0.013	0.107	0.013	0.107	0.013
ΔU_ω	-2.340	0.258	0.541	0.134	0.618	0.098	0.618	0.098
ΔU	-2.702	0.271	0.648	0.146	0.726	0.111	0.726	0.111
$V_{eff}=U+\Delta U$	-2.341	-1.582	0.474	0.839	0.197	0.775	1.300	0.316
G matrix results	-2.470	-1.467	0.779	0.695	0.249	0.592	1.375	0.279
Error (%)	5.22	7.84	39.26	20.70	20.90	30.90	5.45	13.30

Table 9

Same as Table 8, except that $k_F = 1.00\ fm^{-1}$.

	F_0	F_1	F'_0	F'_1	G_0	G_1	G'_0	G'_1
U_η	0.012	-0.010	0.012	-0.010	-0.004	0.003	-0.004	0.003
U_π	0.994	-0.379	-0.331	0.126	-0.331	0.126	0.110	-0.042
U_σ	-7.330	0.390	1.850	0.390	1.850	0.390	1.850	0.390
U_δ	0.210	0.015	-0.366	-0.005	0.210	0.015	-0.070	-0.005
U_ω	5.347	-0.438	-1.374	-0.236	-1.477	-0.185	-1.477	-0.185
U_ρ	0.377	-0.617	0.299	0.192	-0.396	-0.083	0.132	-0.028
U(Sum)	-0.390	-1.038	0.090	0.458	-0.149	0.433	0.542	0.134
ΔU_σ	-0.277	0.006	0.086	0.006	0.086	0.006	0.086	0.006
ΔU_ω	-1.692	0.115	0.458	0.063	0.493	0.045	0.493	0.045
ΔU	-1.969	0.121	0.545	0.069	0.579	0.051	0.579	0.051
$V_{eff}=U+\Delta U$	-2.359	-0.917	0.635	0.527	0.430	0.484	1.121	0.185
G matrix results	-2.816	-0.925	1.114	0.532	0.336	0.401	1.265	0.198
Error (%)	16.20	0.86	43.00	0.94	28.00	20.70	11.40	6.57

Table 10

Same as Table 8, except that k_F = 1.20 fm^{-1}.

	F_0	F_1	F'_0	F'_1	G_0	G_1	G'_0	G'_1
U_η	0.018	-0.015	0.018	-0.015	-0.006	0.005	-0.006	0.005
U_π	1.259	-0.400	-0.420	0.133	-0.420	0.133	0.140	-0.045
U_σ	-8.766	0.562	2.022	0.562	2.022	0.562	2.022	0.562
U_δ	0.240	0.024	-0.426	-0.008	0.240	0.024	-0.080	-0.008
U_ω	6.510	-0.705	-1.512	-0.364	-1.677	-0.290	-1.677	-0.290
U_ρ	0.712	-0.928	0.270	0.286	-0.505	0.131	0.168	-0.044
U(Sum)	-0.027	-1.462	-0.048	0.595	-0.347	0.565	0.567	0.180
ΔU_σ	-0.326	0.009	0.100	0.009	0.100	0.009	0.100	0.009
ΔU_ω	-2.050	0.187	0.511	0.099	0.567	0.072	0.567	0.072
ΔU	-2.376	0.196	0.609	0.109	0.666	0.081	0.666	0.081
$V_{eff}=U+\Delta U$	-2.403	-1.266	0.561	0.704	0.319	0.646	1.233	0.261
G matrix results	-2.632	-1.214	0.909	0.636	0.301	0.513	1.322	0.250
Error (%)	8.70	4.28	38.30	10.70	5.98	25.90	6.72	4.40

Table 11

Migdal parameters for various approximations (which we described in Section 3.4) for the potential HEA calculated for the case where the nucleon spinor is $u(\vec{p},s)$, with $k_F = 1.36$ fm^{-1}. The first line is a result of a reaction matrix calculation.

HEA	F_0	F_1	F'_0	F'_1	G_0	G_1	G'_0	G'_1
G matrix	-2.095	-1.251	0.551	0.539	0.365	0.511	1.178	0.246
approx.1	-2.330	-1.196	0.528	0.491	0.386	0.541	1.078	0.309
approx.2	-2.303	-1.225	0.667	0.486	0.273	0.523	1.082	0.305
approx.3	-2.586	-0.638	-0.152	0.388	1.334	0.674	1.014	0.322
approx.4	-2.319	-1.170	-0.268	0.478	1.083	0.617	1.067	0.301
approx.5	-2.319	-1.166	-0.635	0.470	1.417	0.651	1.067	0.296
approx.6	-2.319	-1.162	0.601	0.501	0.277	0.537	1.060	0.315
approx.7	-2.327	-1.137	-0.250	0.487	1.038	0.619	1.055	0.307
approx.8	-2.375	-0.957	-0.762	0.522	1.351	0.688	0.994	0.331

Table 12

Migdal parameters for various approximations (which we described in Section 3.4) for the potential HEA calculated for the case where the nucleon spinor is $f(\vec{p},s)$, with k_F= 1.36 fm^{-1}. The first line is a result of a reaction matrix calculation.

HEA	F_0	F_1	F'_0	F'_1	G_0	G_1	G'_0	G'_1
G matrix	-0.904	-1.992	0.634	0.358	0.381	0.423	1.051	0.223
approx.1	-0.909	-2.133	0.701	0.243	0.377	0.381	0.978	0.176
approx.2	-0.872	-2.172	0.831	0.236	0.268	0.369	0.981	0.171
approx.3	-0.958	-1.947	-0.408	0.275	1.277	0.465	0.919	0.198
approx.4	-0.787	-2.216	0.002	0.220	1.035	0.412	0.965	0.163
approx.5	-0.723	-2.273	-0.318	0.205	1.350	0.424	0.963	0.155
approx.6	-0.963	-2.041	0.754	0.264	0.275	0.388	0.962	0.188
approx.7	-0.844	-2.138	0.008	0.237	0.993	0.420	0.955	0.173
approx.8	-1.043	-1.825	-0.491	0.300	1.300	0.483	0.902	0.214

Table 13

Migdal parameters for the potential HEA calculated for the case where the nucleon spinor is $f(\vec{p},s)$ with $|\vec{p}| = k_F$(see text). The first line is calculated with $V_{eff} = \Delta U$ and the third line gives the results obtained for $V_{eff} = U + \Delta U$. The fourth line is a result of a reaction matrix calculation. (Note that the Migdal parameters given here are not those of the relativistic BHF theory.)

$k_F(fm^{-1})$	F_0	F_1	F'_0	F'_1	G_0	G_1	G'_0	G'_1
1.36	4.440	-2.861	-2.386	-0.044	0.783	0.266	-0.387	-0.055
	-5.349	0.729	3.088	0.288	-0.407	0.116	1.364	0.231
	-0.909	-2.132	0.702	0.244	0.376	0.382	0.977	0.176
	-0.904	-1.992	0.634	0.358	0.381	0.423	1.051	0.223
1.00	2.070	-1.094	-2.109	0.178	0.817	0.310	-0.225	0.041
	-4.490	0.228	2.944	0.165	-0.359	0.045	1.296	0.140
	-2.420	-0.866	0.885	0.343	0.458	0.355	1.071	0.181
	-2.236	-0.971	0.900	0.446	0.364	0.336	1.074	0.188
1.20	3.161	-1.857	-2.371	0.104	0.818	0.323	-0.312	0.010
	-5.040	0.443	3.147	0.237	-0.398	0.076	1.365	0.196
	-1.879	-1.414	0.776	0.341	0.420	0.399	1.053	0.206
	-1.705	-1.424	0.723	0.450	0.376	0.401	1.080	0.222
1.40	4.816	-3.167	-2.360	-0.092	0.771	0.241	-0.405	-0.076
	-5.410	0.814	3.051	0.296	-0.407	0.127	1.357	0.236
	-0.594	-2.353	0.691	0.204	0.364	0.368	0.952	0.160
	-0.613	-2.187	0.622	0.319	0.382	0.419	1.034	0.219
1.60	7.376	-5.392	-1.868	-0.467	0.669	0.005	-51018	-0.244
	-5.592	1.431	2.651	0.317	-0.385	0.206	1.274	0.239
	1.784	-3.961	0.783	-0.150	0.284	0.211	0.764	-0005
	1.865	-3.737	0.690	-0.036	0.392	0.298	0.828	0.159

Table 14

Various contributions to the Migdal Parameters for the potential HEA. The first seven rows give the contribution of the Born terms for each of the mesons indicated. The contributions from pseudoparticle exchange (ΔU_σ, ΔU_ω and ΔU_δ) are given as well as their sum (ΔU). The total is the result for $V_{eff} = U + \Delta U$ and is compared to reaction matrix results of reference 7. Here $k_F = 1.36$ fm^{-1}.

	F_0	F_1	F'_0	F'_1	G_0	G_1	G'_0	G'_1
U_η	0.062	-0.045	0.062	-0.045	-0.021	0.015	-0.021	0.015
U_π	1.109	-0.239	-0.370	0.080	-0.370	0.080	0.123	-0.027
U_σ	-8.194	0.602	1.673	0.602	1.673	0.602	1.673	0.602
U_δ	1.826	0.212	-3.349	-0.071	1.826	0.212	-0.609	-0.071
U_ω	7.836	-2.147	-1.073	-0.637	-1.488	-0.519	-1.488	-0.519
U_ρ	0.544	-0.902	0.856	0.125	-0.579	-0.052	0.193	0.017
U_ϕ	1.257	-0.342	-0.185	-0.098	-0.258	-0.072	-0.258	-0.072
U(Sum)	4.440	-2.861	-2.386	-0.044	0.783	0.266	-0.387	-0.055
ΔU_σ	-1.161	0.036	0.336	0.036	0.336	0.036	0.336	0.036
ΔU_ω	-2.860	0.779	0.420	0.223	0.585	0.166	0.585	0.166
ΔU_δ	-1.328	-0.086	2.332	0.029	-1.328	-0.086	0.443	0.029
ΔU	-5.349	0.729	3.088	0.288	-0.407	0.116	1.364	0.231
$V_{eff}=U+\Delta U$	-0.909	-2.132	0.702	0.244	0.376	0.382	0.977	0.176
G matrix results	-0.904	-1.992	0.634	0.358	0.381	0.423	1.051	0.223
Error (%)	0.55	7.03	10.73	31.84	1.31	9.69	7.04	21.07

Table 15

Same as Table 14, except that k_F = 1.00 fm^{-1}.

	F_0	F_1	F'_0	F'_1	G_0	G_1	G'_0	G'_1
U_η	0.035	-0.029	0.035	-0.029	-0.012	0.010	-0.012	0.010
U_π	0.855	-0.297	-0.285	0.099	-0.285	0.099	0.095	-0.033
U_σ	-6.638	0.397	1.584	0.397	1.584	0.397	1.584	0.397
U_δ	1.567	0.138	-2.806	-0.046	1.567	0.138	-0.522	-0.046
U_ω	5.362	-0.704	-1.189	-0.317	-1.315	-0.264	-1.315	-0.264
U_ρ	0.029	-0.491	0.753	0.119	-0.500	-0.035	0.167	0.012
U_ϕ	0.860	-0.108	-0.201	-0.045	-0.222	-0.035	-0.222	-0.035
U(Sum)	2.070	-1.094	-2.109	0.178	0.817	0.310	-0.225	0.041
ΔU_σ	-1.070	0.026	0.320	0.026	0.320	0.026	0.320	0.026
ΔU_ω	-2.179	0.273	0.507	0.115	0.562	0.090	0.562	0.090
ΔU_δ	-1.241	-0.071	2.167	0.024	-1.241	-0.071	0.414	0.024
ΔU	-4.490	0.228	2.994	0.165	-0.359	0.045	1.296	0.140
$V_{eff}=U+\Delta U$	-2.420	-0.866	0.885	0.343	0.458	0.355	1.071	0.181
G matrix results	-2.236	-0.971	0.900	0.446	0.364	0.336	1.074	0.188
Error (%)	8.23	10.81	1.67	23.09	25.82	5.65	0.28	3.72

Table 16

Same as Table 14, except that $k_F = 1.20$ fm^{-1}.

	F_0	F_1	F'_0	F'_1	G_0	G_1	G'_0	G'_1
U_η	0.051	-0.039	0.051	-0.039	-0.017	0.013	-0.017	0.013
U_π	1.026	-0.277	-0.342	0.092	-0.342	0.092	0.114	-0.031
U_σ	-7.691	0.532	1.670	0.532	1.670	0.532	1.670	0.532
U_δ	1.745	0.191	-3.182	-0.064	1.745	0.191	-0.582	-0.064
U_ω	6.676	-1.330	-1.185	-0.489	-1.436	-0.401	-1.436	-0.401
U_ρ	0.284	-0.726	0.820	0.144	-0.556	-0.049	0.185	0.016
U_ϕ	1.070	-0.208	-0.203	-0.072	-0.246	-0.055	-0.246	-0.055
U(Sum)	3.161	-1.857	-2.371	0.104	0.818	0.323	-0.312	0.010
ΔU_σ	-1.159	0.034	0.337	0.034	0.337	0.034	0.337	0.034
ΔU_ω	-2.559	0.499	0.483	0.173	0.587	0.132	0.587	0.132
ΔU_δ	-1.322	-0.090	2.327	0.030	-1.322	-0.090	0.441	0.030
ΔU	-5.040	0.443	3.147	0.237	-0.398	0.076	1.365	0.196
$V_{eff}=U+\Delta U$	-1.879	-1.414	0.776	0.341	0.420	0.399	1.053	0.206
G matrix results	-1.705	-1.424	0.723	0.450	0.376	0.401	1.080	0.222
Error (%)	10.21	0.70	7.33	24.22	11.70	0.50	2.50	7.20

Table 17

Same as Table 14, except that k_F = 1.40 fm^{-1}.

	F_0	F_1	F'_0	F'_1	G_0	G_1	G'_0	G'_1
U_η	0.064	-0.046	0.064	-0.046	-0.021	0.015	-0.021	0.015
U_π	1.121	-0.227	-0.374	0.076	-0.374	0.076	0.125	-0.025
U_σ	-8.265	0.613	1.665	0.613	1.665	0.613	1.665	0.613
U_δ	1.838	0.213	-3.370	-0.071	1.838	0.213	-0.613	-0.071
U_ω	8.140	-2.398	-1.031	-0.672	-1.495	-0.548	-1.495	-0.548
U_ρ	0.612	-0.939	0.864	0.112	-0.582	-0.051	0.194	0.017
U_ϕ	1.306	-0.383	-0.178	-0.104	-0.260	-0.077	-0.260	-0.077
U(Sum)	4.816	-3.167	-2.360	-0.092	0.771	0.241	-0.405	-0.076
ΔU_σ	-1.153	0.035	0.334	0.035	0.334	0.035	0.334	0.035
ΔU_ω	-2.934	0.861	0.399	0.234	0.582	0.174	0.582	0.174
ΔU_δ	-1.323	-0.082	2.318	0.027	-1.323	-0.082	0.441	0.027
ΔU	-5.410	0.814	3.051	0.296	-0.407	0.127	1.357	0.236
$V_{eff}=U+\Delta U$	-0.594	-2.353	0.691	0.204	0.364	0.368	0.952	0.160
G matrix results	-0.613	-2.187	0.622	0.319	0.382	0.419	1.034	0.219
Error (%)	3.10	7.59	11.09	31.05	4.71	12.17	7.93	26.94

Table 18

Same as Table 14, except that $k_F = 1.60$ fm^{-1}.

	F_0	F_1	F'_0	F'_1	G_0	G_1	G'_0	G'_1
U_η	0.070	-0.046	0.070	-0.046	-0.023	0.015	-0.023	0.015
U_π	1.083	-0.156	-0.361	0.052	-0.361	0.052	0.120	-0.017
U_σ	-7.933	0.548	1.554	0.548	1.554	0.548	1.554	0.548
U_δ	1.816	0.156	-3.241	-0.052	1.816	0.156	-0.605	-0.052
U_ω	9.806	-4.196	-0.676	-0.828	-1.484	-0.683	-1.484	-0.683
U_ρ	0.954	-1.053	0.902	-0.041	-0.571	-0.021	0.190	0.007
U_ϕ	1.580	-0.681	-0.117	-0.136	-0.262	-0.098	-0.262	-0.098
U(Sum)	7.376	-5.392	-1.868	-0.467	0.669	0.005	-0.510	-0.244
ΔU_σ	-1.022	0.023	0.310	0.023	0.310	0.023	0.310	0.023
ΔU_ω	-3.326	1.433	0.245	0.286	0.549	0.208	0.549	0.208
ΔU_δ	-1.244	-0.025	2.096	0.008	-1.244	-0.025	0.415	0.008
ΔU	-5.592	1.431	2.651	0.317	-0.385	0.206	1.274	0.2.39
$V_{eff}=U+\Delta U$	1.784	-3.961	0.783	-0.150	0.284	0.211	0.764	-0.005
G matrix results	1.865	-3.737	0.690	-0.036	0.392	0.298	0.828	0.159
Error (%)	4.34	5.99	13.48	316.67	27.55	29.19	7.73	

Table 19

Migdal parameters for the potential HM2 calculated for the case where the nucleon spinor is $f(\vec{p},s)$ with $|\vec{p}| = k_F$(see text). The first line is calculated with $V_{eff} = \Delta U$ and the third line gives the results obtained for $V_{eff} = U + \Delta U$. The fourth line is a result of a reaction matrix calculation. (Note that the Migdal parameters given here are not those of the relativistic BHF theory.)

$k_F(fm^{-1})$	F_0	F_1	F'_0	F'_1	G_0	G_1	G'_0	G'_1
1.36	1.755	-2.977	0.095	0.402	-0.506	0.516	-0.490	0.075
	-2.773	0.577	0.527	0.181	0.700	0.102	0.700	0.102
	-1.018	-2.400	0.621	0.583	0.194	0.617	1.190	0.177
	-1.182	-2.218	0.848	0.476	0.306	0.464	1.258	0.214
1.00	-0.183	-1.210	0.122	0.419	-0.145	0.410	0.530	0.117
	-1.980	0.163	0.527	0.075	0.576	0.049	0.576	0.049
	-2.163	-1.047	0.649	0.494	0.429	0.459	1.105	0.166
	-2.609	-1.051	1.114	0.502	0.344	0.382	1.245	0.190
1.20	0.628	-1.997	0.066	0.463	-0.337	0.495	0.528	0.122
	-2.409	0.335	0.553	0.126	0.645	0.077	0.654	0.077
	-1.781	-1.662	0.620	0.591	0.316	0.571	1.181	0.200
	-2.039	-1.571	0.929	0.540	0.325	0.455	1.268	0.224

Table 20

Various contributions to the Migdal Parameters for the potential HM2. The first seven rows give the contribution of the Born terms for each of the mesons indicated. The contributions from pseudoparticle exchange (ΔU_σ and ΔU_ω) are given as well as their sum (ΔU). The total is the result for $V_{eff} = U + \Delta U$ and is compared to reaction matrix results of reference 7. Here $k_F = 1.36$ fm^{-1}.

	F_0	F_1	F'_0	F'_1	G_0	G_1	G'_0	G'_1
U_η	0.022	-0.017	0.022	-0.017	-0.007	0.006	-0.007	0.006
U_π	1.312	-0.365	-0.437	0.122	-0.437	0.122	0.146	-0.041
U_σ	-8.773	0.555	2.000	0.555	2.000	0.555	2.000	0.555
U_δ	0.247	0.018	-0.427	-0.006	0.247	0.018	-0.082	-0.006
U_ω	7.791	-1.919	-1.250	-0.581	-1.753	-0.375	-1.753	-0.375
U_ρ	1.157	-1.248	0.187	0.330	-0.556	-0.191	0.185	-0.064
U(Sum)	1.755	-2.977	0.095	0.402	-0.506	0.516	0.490	0.075
ΔU_σ	-0.320	0.007	0.102	0.007	0.102	0.007	0.102	0.007
ΔU_ω	-2.453	0.571	0.425	0.175	0.598	0.095	0.598	0.095
ΔU	-2.773	0.577	0.527	0.181	0.700	0.102	0.700	0.102
$V_{eff}=U+\Delta U$	-1.018	-2.400	0.621	0.583	0.194	0.617	1.190	0.177
G matrix results	-1.182	-2.218	0.848	0.476	0.306	0.464	1.258	0.214
Error (%)	13.90	8.20	26.83	22.54	36.60	33.00	5.41	17.30

Table 21

Same as Table 20, except that k_F = 1.00 fm^{-1}.

	F_0	F_1	F'_0	F'_1	G_0	G_1	G'_0	G'_1
U_η	0.012	-0.010	0.012	-0.010	-0.004	0.003	-0.004	0.003
U_π	0.977	-0.373	-0.326	0.124	-0.326	0.124	0.109	-0.041
U_σ	-7.187	0.371	1.833	0.370	1.833	0.370	1.833	0.370
U_δ	0.208	0.013	-0.360	-0.004	0.208	0.013	-0.069	-0.004
U_ω	5.396	-0.569	-1.325	-0.254	-1.469	-0.184	-1.469	-0.184
U_ρ	0.412	-0.642	0.287	0.193	0.389	0.082	0.130	-0.027
U(Sum)	-0.183	-1.210	0.122	0.419	-0.146	0.410	0.530	0.117
ΔU_σ	-0.271	0.005	0.086	0.005	0.086	0.005	0.086	0.005
ΔU_ω	-1.708	0.158	0.442	0.069	0.490	0.044	0.049	0.044
ΔU	-1.980	0.163	0.527	0.075	0.576	0.049	0.576	0.049
$V_{eff}=U+\Delta U$	-2.163	-1.047	0.649	0.494	0.429	0.459	1.105	0.166
G matrix results	-2.609	-1.051	1.114	0.502	0.344	0.382	1.245	0.190
Error (%)	17.10	0.38	41.70	1.59	24.70	20.20	11.20	12.60

Table 22

Same as Table 20, except that $k_F = 1.20\ fm^{-1}$.

	F_0	F_1	F'_0	F'_1	G_0	G_1	G'_0	G'_1
U_η	0.017	-0.014	0.017	-0.014	-0.006	0.005	-0.006	0.005
U_π	1.196	-0.380	-0.399	0.127	-0.399	0.127	0.133	-0.042
U_σ	-8.278	0.496	1.967	0.496	1.967	0.496	1.967	0.496
U_δ	0.234	0.018	-0.407	-0.006	0.234	0.018	-0.078	-0.006
U_ω	6.665	-1.138	-1.355	-0.417	-1.650	-0.285	-1.650	-0.285
U_ρ	0.795	-0.978	0.242	0.279	-0.484	0.133	0.161	-0.045
U(Sum)	0.628	-1.997	0.066	0.465	-0.337	0.493	0.528	0.122
ΔU_σ	-0.307	0.007	0.096	0.007	0.096	0.007	0.096	0.007
ΔU_ω	-2.102	0.329	0.457	0.120	0.558	0.071	0.558	0.071
ΔU	-2.409	0.335	0.553	0.126	0.654	0.077	0.654	0.077
$V_{eff}=U+\Delta U$	-1.781	-1.662	0.620	0.591	0.316	0.571	1.181	0.200
G matrix results	-2.039	-1.571	0.929	0.540	0.325	0.455	1.268	0.224
Error (%)	12.70	5.79	33.30	9.44	2.77	25.50	6.86	10.70

Table 23

Fermi momentum, k_F, at saturation and the incompressibility parameter, K_∞, calculated in the pseudoparticle method for the potential HEA. The coupling constants of the pseudoparticles are chosen to be either density-dependent or density independent, as discussed in the text. See Figs. 26-27.

HEA	$k_F(fm^{-1})$	K_∞(MeV)	Pseudoparticle Parameters
Approximation 1			density dependent
Non-self-consistant	1.21	211	(Fig.26-curve a')
Self-consistant	1.21	177	(Fig.26-curve a)
Approximation 2			density independent
Non-self-consistant	1.30	244	(Fig.27-curve a')
Self-consistant	1.32	209	(Fig.27-curve a)
Approximation 3			modified parameters; density dependent
Non-self-consistant	1.29	323	(Fig.26-curve b')
Self-consistant	1.31	287	(Fig.26-curve b)
Approximation 4			modified parameters; density independent
Non-self-consistant	1.41	447	(Fig.27-curve b')
Self-consistant	1.45	427	(Fig.27-curve b)

Table 24

Fermi momentum, k_F, at saturation and the incompressibility parameter, K_∞, calculated in the pseudoparticle method for the potential HM2. The coupling constants of the pseudoparticles are chosen to be either density-dependent or density independent, as discussed in the text. See Figs. 29-30.

HM2	$k_F(fm^{-1})$	K_∞(MeV)	Pseudoparticle Parameters
Approximation 1			density dependent
Non-self-consistant	1.22	143	(Fig.29-curve a')
Self-consistant	1.19	220	(Fig.29-curve a)
Approximation 2			density independent
Non-self-consistant	1.33	289	(Fig.30-curve a')
Self-consistant	1.37	260	(Fig.30-curve a)
Approximation 3			modified parameters; density dependent
Non-self-consistant	1.28	169	(Fig.29-curve b')
Self-consistant	1.23	160	(Fig.29-curve b)
Approximation 4			modified parameters; density independent
Non-self-consistant	1.39	396	(Fig.30-curve b')
Self-consistant	1.37	120	(Fig.30-curve b)

Table 25

Fermi momentum, k_F, binding energy per particle(B.E./A) at saturation and the incompressibility parameter, K_∞, calculated for different iteration accuracy for the σ - ω model. The coupling constants and the iteration accuracy are chosen as discussed in Section 6.3. The last line is a result of the case where the nucleon spinor is $u(\vec{p},s)$.

Iteration Accuracy	$\frac{1}{4\pi}\delta g_\sigma^2$	$\frac{1}{4\pi}\delta g_\omega^2$	k_F (fm^{-1})	B.E./A (MeV)	K_∞ (MeV)
0.01	6.5205	10.848	1.43	-15.760	1949.0
0.001	6.5205	10.848	1.42	-15.758	544.4
0.0003	6.5205	10.848	1.42	-15.752	542.4
0.0001	6.5205	10.848	1.42	-15.751	544.4
none	6.5205	10.843	1.38	-14.609	609.4

Table 26

Fermi momentum, k_F, binding energy per particle(B.E./A) at saturation and the incompressibility parameter, K_∞, calculated for different iteration accuracy for the potential HEA, are listed in (d.d.) and (d.ind.) columns, respectively. The coupling constants of the pseudoparticles are chosen to be either density-dependent (d.d.)or density independent(d.ind.):$\delta g^2_\sigma/4\pi$ = -2.81, $\delta g^2_\omega/4\pi$ = 17.5 and $\delta g^2_\delta/4\pi$ = 5.54, for $k_F = k_F^{NM}$ = 1.36 fm^{-1}. The values of these coupling constants at other values of the density may be obtained using Eqs.3.14-3.15. The first column is the iteration accuracy(I.A.). (See Section 6.3.)

I.A.	k_F (fm^{-1})		B.E./A (MeV)		K_∞ (MeV)	
	d.d.	d.ind.	d.d.	d.ind.	d.d.	d.ind.
0.01	1.31	1.45	-15.248	-15.796	480	418
0.001	1.31	1.45	-15.269	-15.766	304	431
0.0003	1.31	1.45	-15.270	-15.763	290	424
0.0001	1.31	1.45	-15.270	-15.763	287	427

Table 27

Fermi momentum, k_F, binding energy per particle(B.E./A) at saturation and the incompressibility parameter, K_∞, calculated for different iteration accuracy for the potential HM2, are listed in (d.d.) and (d.ind.) columns, respectively. The coupling constants of the pseudoparticles are chosen to be either density-dependent (d.d.)or density independent(d.ind.):$\delta g^2_\sigma/4\pi$ = -1.15 and $\delta g^2_\omega/4\pi$ = 6.98 for $k_F = k_F^{NM}$ = 1.36 fm^{-1}. The values of these coupling constants at other values of the density may be obtained using Eqs.3.16-3.17. The first column is the iteration accuracy(I.A.). (See Section 6.3.)

I.A.	k_F (fm^{-1})		B.E./A (MeV)		K_∞ (MeV)	
	d.d.	d.ind.	d.d.	d.ind.	d.d.	d.ind.
0.01	1.22	1.37	-16.384	-15.299	144	3703
0.001	1.21	1.35	-16.439	-15.200	148	295
0.0003	1.21	1.34	-16.444	-15.204	174	280
0.0001	1.21	1.34	-16.446	-15.205	155	271

Table 28

Fermi momentum, k_F, binding energy per particle(B.E./A) at saturation and the incompressibility parameter, K_∞, calculated for different iteration accuracy for the potential BMR2. The coupling constants of the pseudoparticles are chosen to be density independent: $\delta g^2_\sigma/4\pi = -5.50$, $\delta g^2_\omega/4\pi = 14.20$ and $\delta g^2_\delta/4\pi = 8.54$, for $k_F = k_F^{NM} = 1.36$ fm^{-1}.

Iteration Accuracy	k_F (fm^{-1})	B.E./A (MeV)	K_∞ (MeV)
0.01	1.39	-15.227	496
0.001	1.39	-15.201	496
0.0003	1.31	-15.199	490
0.0001	1.39	-15.199	483

Table 29

Migdal parameters for the potential HEA calculated for the case where the nucleon spinor is $f(\vec{p},s)$ with $|\vec{p}| = k_F$ (see text). The first line is a result of a reaction matrix calculation; the second line gives the results obtained for the semi-self-consistent case (s.s.c.). (See Chapter 4.) The third line is calculated using the fully-self-consistent pseudoparticle method (f.s.c.).

HEA	F_0	F_1	F'_0	F'_1	G_0	G_1	G'_0	G'_1
				1.36 fm^{-1}				
G Matrix	-0.904	-1.992	0.634	0.358	0.381	0.423	1.051	0.223
s.s.c.	-0.909	-2.132	0.702	0.244	0.376	0.382	0.977	0.176
f.s.c.	-0.814	-2.196	0.714	0.226	0.376	0.371	0.971	0.167
				1.00 fm^{-1}				
G Matrix	-2.236	-0.971	0.900	0.446	0.364	0.366	1.074	0.188
s.s.c.	-2.420	-0.866	0.885	0.343	0.458	0.355	1.071	0.181
f.s.c.	-1.933	-0.909	0.583	0.321	0.494	0.347	0.943	0.164
				1.20 fm^{-1}				
G Matrix	-1.705	-1.424	0.723	0.450	0.376	0.401	1.080	0.222
s.s.c.	-1.879	-1.414	0.776	0.341	0.420	0.399	1.053	0.206
f.s.c.	-1.588	-1.463	0.625	0.323	0.440	0.393	0.983	0.194
				1.40 fm^{-1}				
G Matrix	-0.613	-2.187	0.622	0.319	0.382	0.419	1.034	0.219
s.s.c.	-0.594	-2.353	0.691	0.204	0.364	0.368	0.952	0.160
f.s.c.	-0.503	-2.449	0.752	0.178	0.357	0.352	0.958	0.148

Table 30

Migdal parameters for the potential HM2 calculated for the case where the nucleon spinor is $f(\vec{p},s)$ with $|\vec{p}| = k_F$. (see text.) The first line is a result of a reaction matrix calculation; the second line gives the results obtained for the semi-self-consistent case (s.s.c.). (See Chapter 4.) The third line is calculated using the fully-self-consistent pseudoparticle method (f.s.c.).

HM2	F_0	F_1	F'_0	F'_1	G_0	G_1	G'_0	G'_1
				1.36 fm^{-1}				
G Matrix	-1.182	-2.218	0.848	0.476	0.306	0.464	1.258	0.214
s.s.c.	-1.018	-2.400	0.621	0.583	0.194	0.617	1.190	0.176
f.s.c.	-0.951	-2.441	0.630	0.569	0.193	0.609	1.184	0.169
				1.00 fm^{-1}				
G Matrix	-2.609	-1.051	1.114	0.502	0.344	0.382	1.245	0.190
s.s.c.	-2.163	-1.047	0.649	0.494	0.429	0.459	1.105	0.166
f.s.c.	-2.790	-1.012	0.826	0.513	0.621	0.472	1.294	0.179
				1.20 fm^{-1}				
G Matrix	-2.039	-1.571	0.929	0.540	0.325	0.455	1.268	0.224
s.s.c.	-1.781	-1.662	0.620	0.591	0.316	0.571	1.181	0.200
f.s.c.	-1.965	-1.662	0.681	0.593	0.381	0.571	1.242	0.202

Figure 1

Self-energy $\Sigma_0^{++}(\vec{p})$ vs. $|\vec{p}|/k_F$ for the potential HEA.

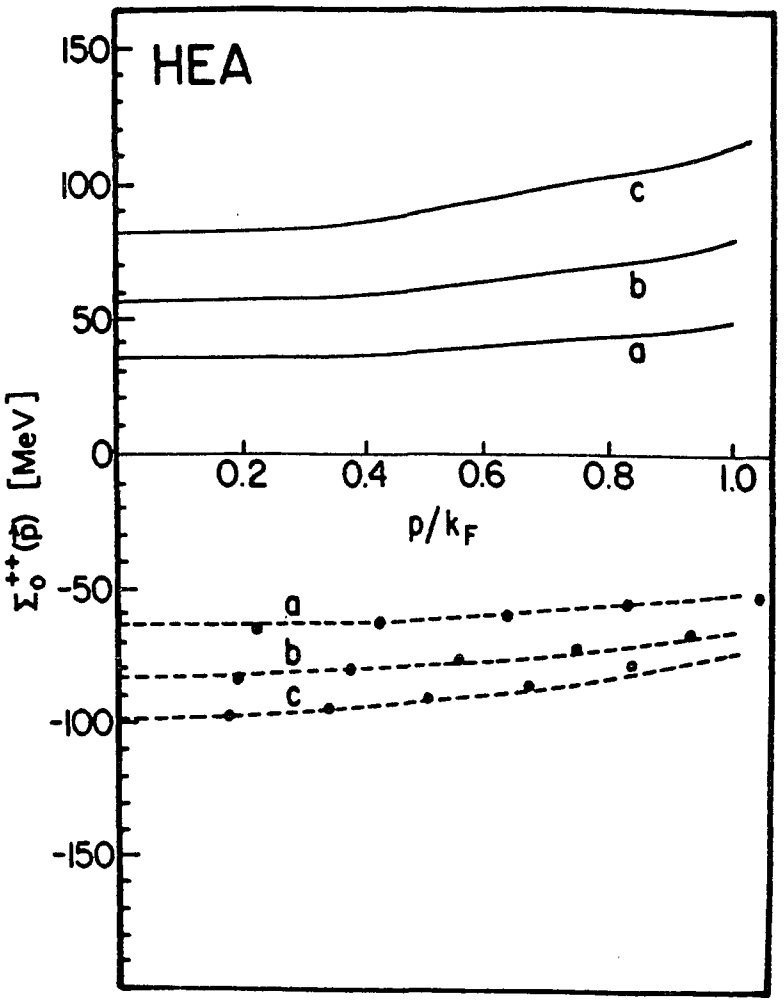

The solid lines denote the Hartree-Fock results and the dashed lines include the effects of correlations. The dots in the lower half of the figure are the results obtained with v_{eff} of Eqs. (3.1)-(3.3), (3.12)-(3.15).

(a) $k_F = 1.2$ fm^{-1}, (b) $k_F = 1.36$ fm^{-1}, (c) $k_F = 1.5$ fm^{-1}.

Figure 2

Contribution of ω and ϕ exchange to the self-energy $\Sigma_0^{++}(\vec{p})$ for the potential HEA.

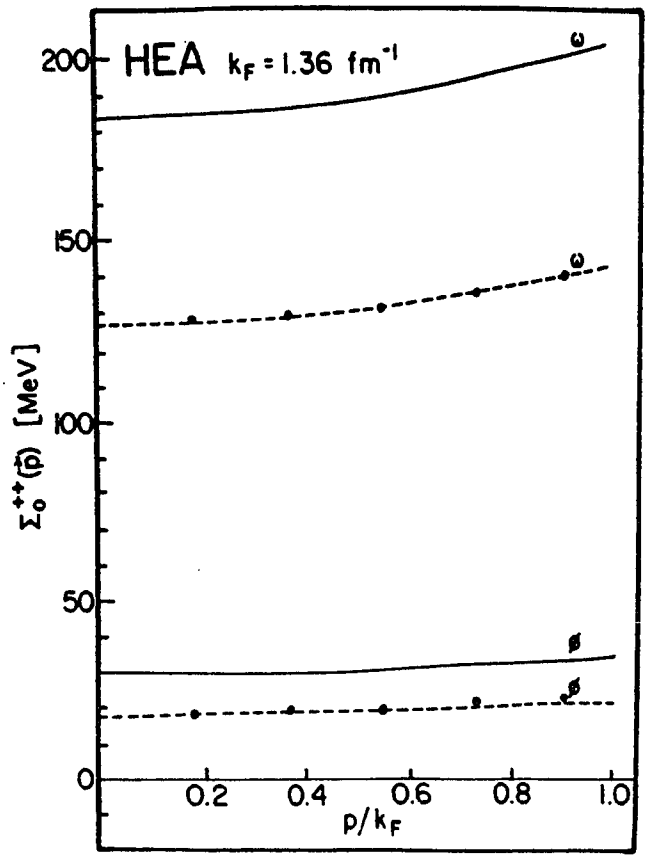

The solid lines exhibit the results as calculated in the Hartree-Fock approximation. The dashed lines show the contribution in the presence of correlations. The upper set of black dots shows the results of ω exchange and a portion of the total pseudo-omega exchange $\{(\delta g^2_\omega/4\pi)_1=12.30\}$ calculated in the Hartree-Fock approximation. The lower set of black dots shows the similar results for ϕ exchange and a portion of pseudo-omega exchange $\{(\delta g^2_\omega/4\pi)_2=1.90\}$ - see Table 4.1. [Note that the <u>total</u> pseudo-omega exchange is calculated with $(\delta g^2_\omega/4\pi)=12.30+1.90 = 14.20$].

Figure 3

Contribution of σ , π and δ exchange to the self-energy $\Sigma_0^{++}(\vec{p})$ for the potential HEA.

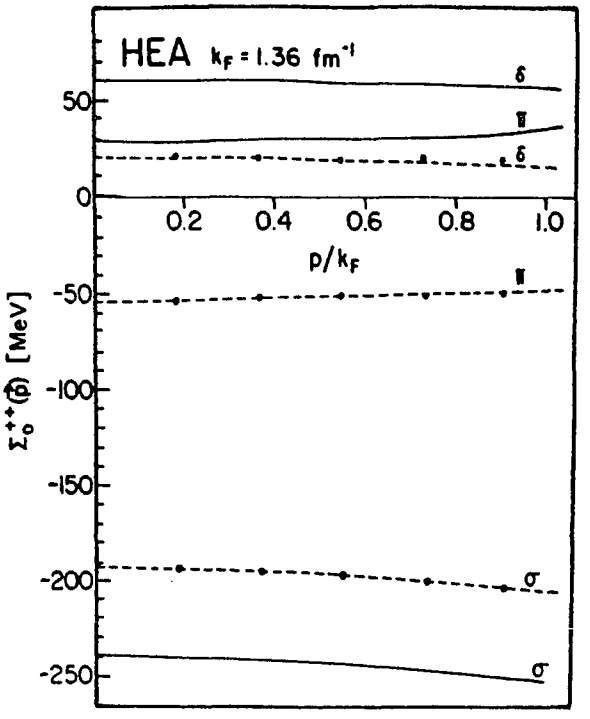

The solid lines exhibit the results as calculated in the Hartree-Fock approximation. The dashed lines are the results in the presence of correlations. The uppermost set of black dots are the results for delta and pseudo-delta exchange($\delta g^2_\delta/4\pi$ = 5.54) calculated in the Hartree-Fock approximation. The lower set of black dots represents sigma and pseudo-sigma exchange [$(\delta g^2_\delta/4\pi)_1$= 3.78 - see Table 4.1] calculated in the Hartree-Fock approximation. In the case of the pion we add a portion of the pseudo-sigma exchange [$(\delta g^2_\sigma/4\pi)_2$= -6.59 - see Table 4.1] which is taken to to be attractive. The total result for pseudo-sigma exchange [$\delta g^2_\sigma/4\pi$= -2.81 - see Table 3.1] is seen to be attractive.

Figure 4

Self-energy $\Sigma_0^{+-}(\vec{p})$ vs. $|\vec{p}|/k_F$ for the potential HEA.

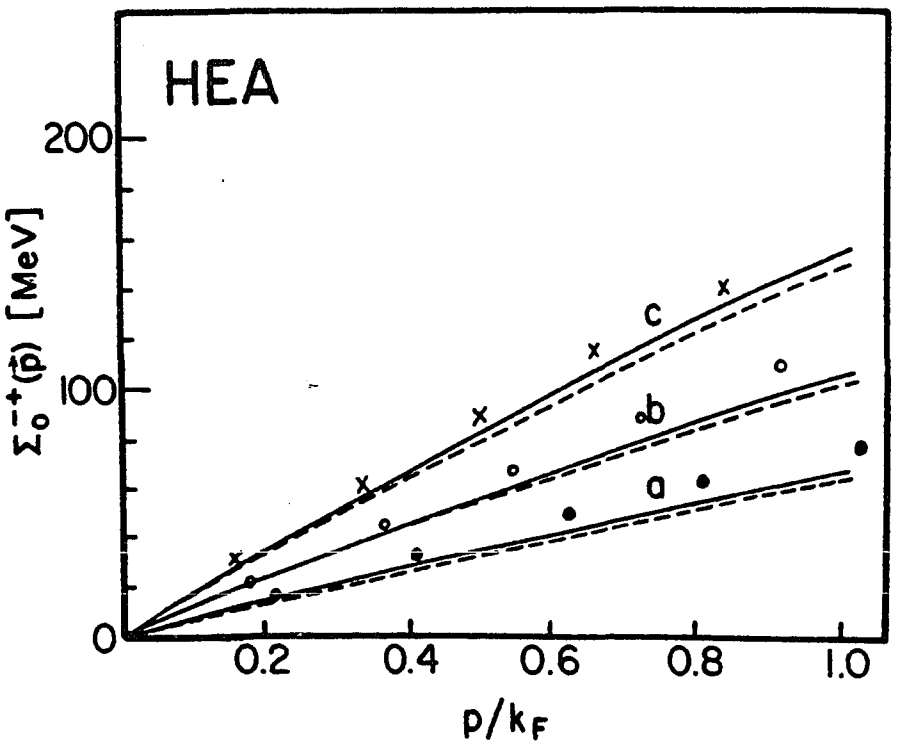

The solid curves are the Hartree-Fock results and the dashed lines include the effects of correlations. [See Ref.7.] The small dots are calculated with V_{eff} of Eqs. (3.1)-(3.3),(3.12-3.15).

(a) $k_F = 1.2$ fm^{-1}, (b) $k_F = 1.36$ fm^{-1}, (c)$k_F = 1.5$ fm^{-1}.

Figure 5

Contribution of σ, ω and ϕ exchange to the self-energy $\Sigma_0^{-+}(\vec{p})$ for the potential HEA.

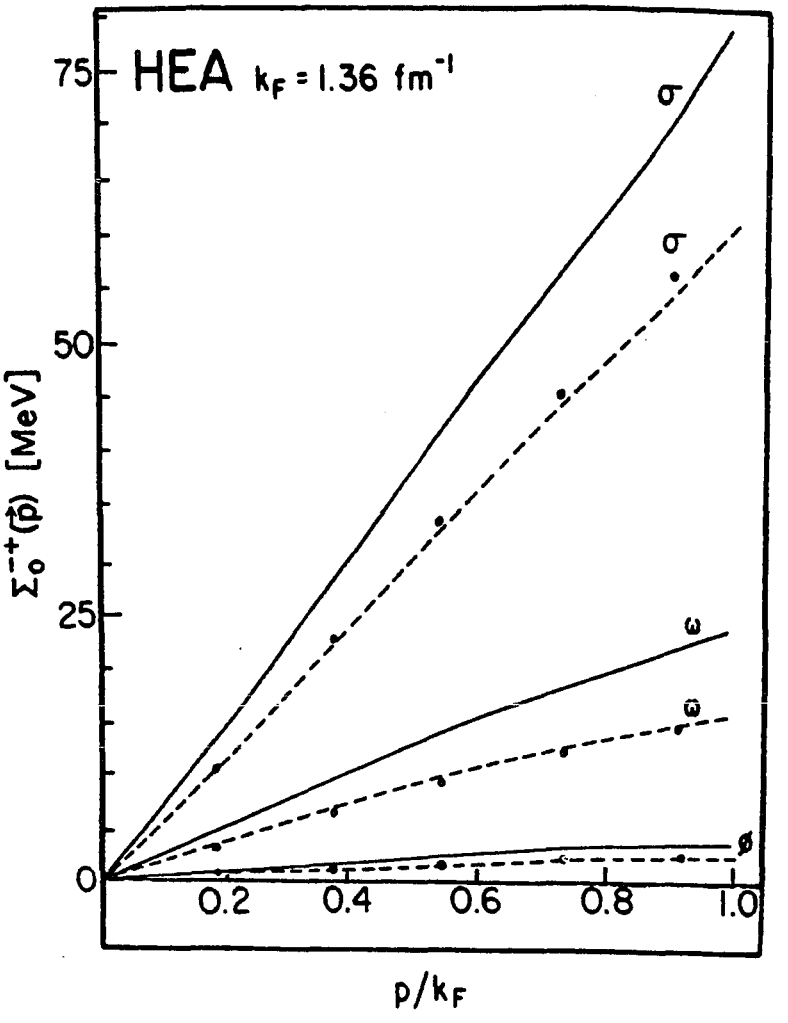

The solid lines denote the Hartree-Fock results and the dashed lines denote the results of the RBHF theory. The dots result from adding pseudo-particle exchange to the Hartree-Fock results. [Here $(\delta g^2_\omega/4\pi)_1 = 12.30$, $(\delta g^2_\omega/4\pi)_2 = 1.90$ and $(\delta g^2_\sigma/4\pi)_1 = 3.78$ - see Table 3.1.]

Figure 6

Contribution of π exchange to the self-energy $\Sigma_0^{-+}(\vec{p})$ for the potential HEA.

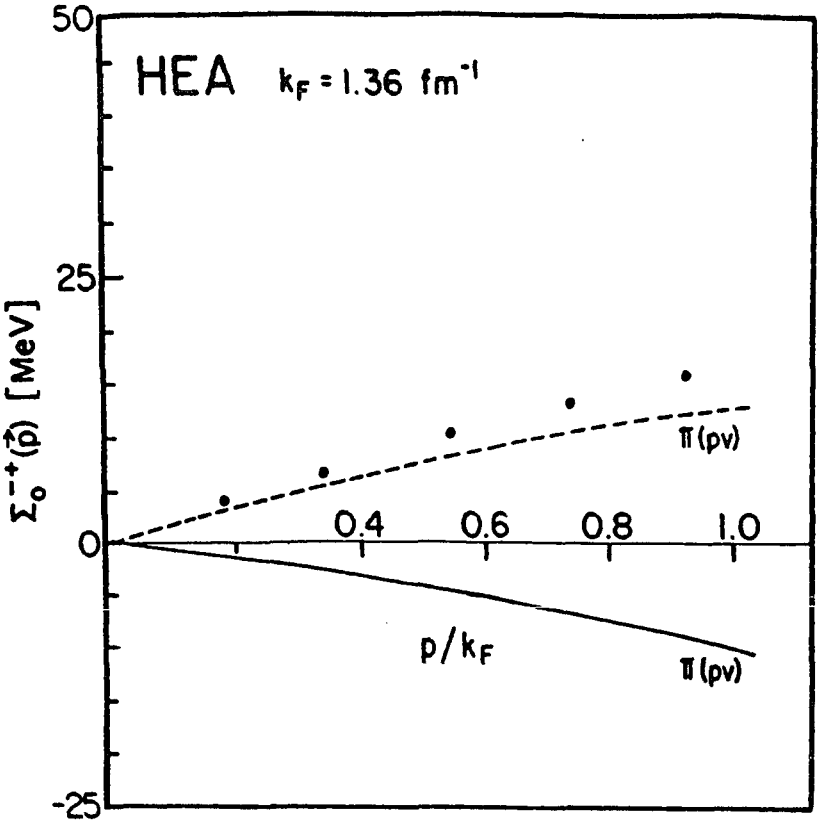

The solid lines exhibit the results as calculated in the Hartree-Fock approximation. The dashed lines exhibit the results as calculated in RBHF theory. Pseudo-vector coupling is used. The black dots are obtained by adding a portion of pseud0-sigma exchange with $(\delta g^2_\sigma/4\pi)_2 = -6.59$. (See Table 4.1.) [Here the negative sign for $(\delta g^2_\sigma/4\pi)$ means that the contribution of the pseudo-sigma particle has the same sign as that obtained for sigma exchange.]

Figure 7

Self-energy $\Sigma_o^{--}(\vec{p})$ vs. $|\vec{p}|/k_F$ for the potential HEA.

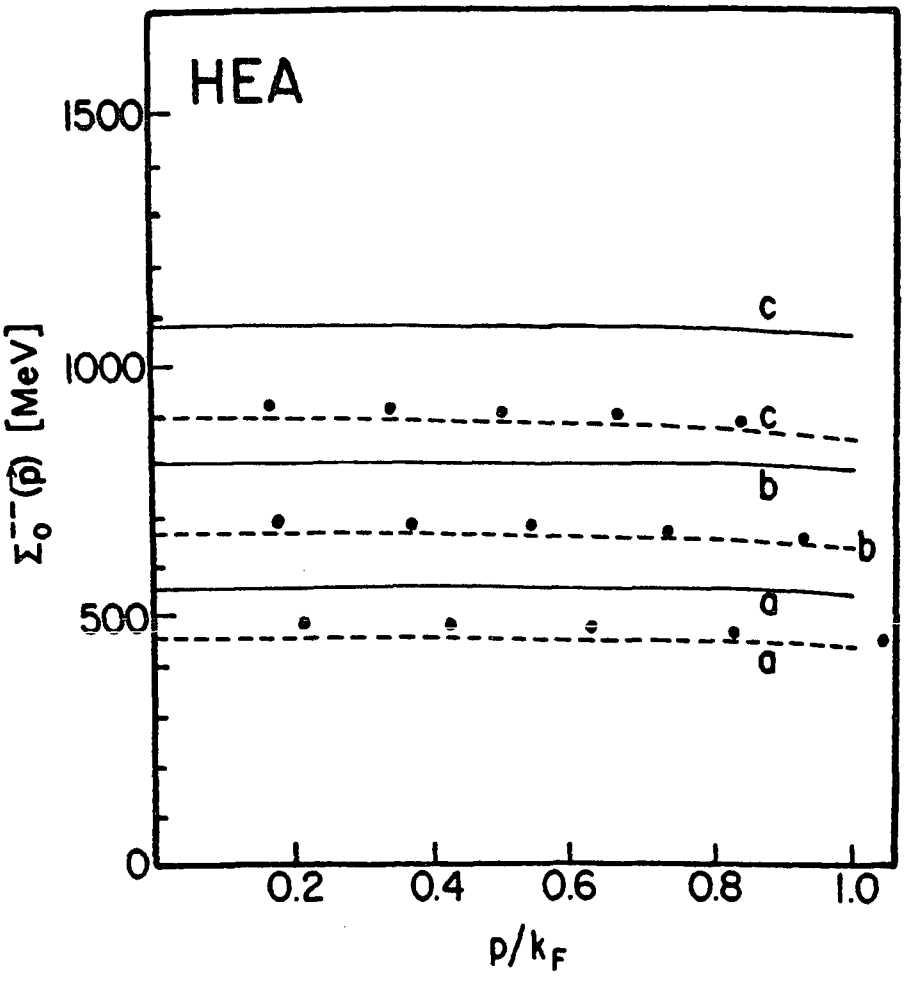

The curves have the same meaning as that described in the caption of Fig.1. Results calculated with V_{eff} are represented by the dots.

Figure 8

Contribution of ω, σ, π, ϕ and δ exchange to the self-energy $\Sigma_0^{--}(\vec{p})$ for the potential HEA.

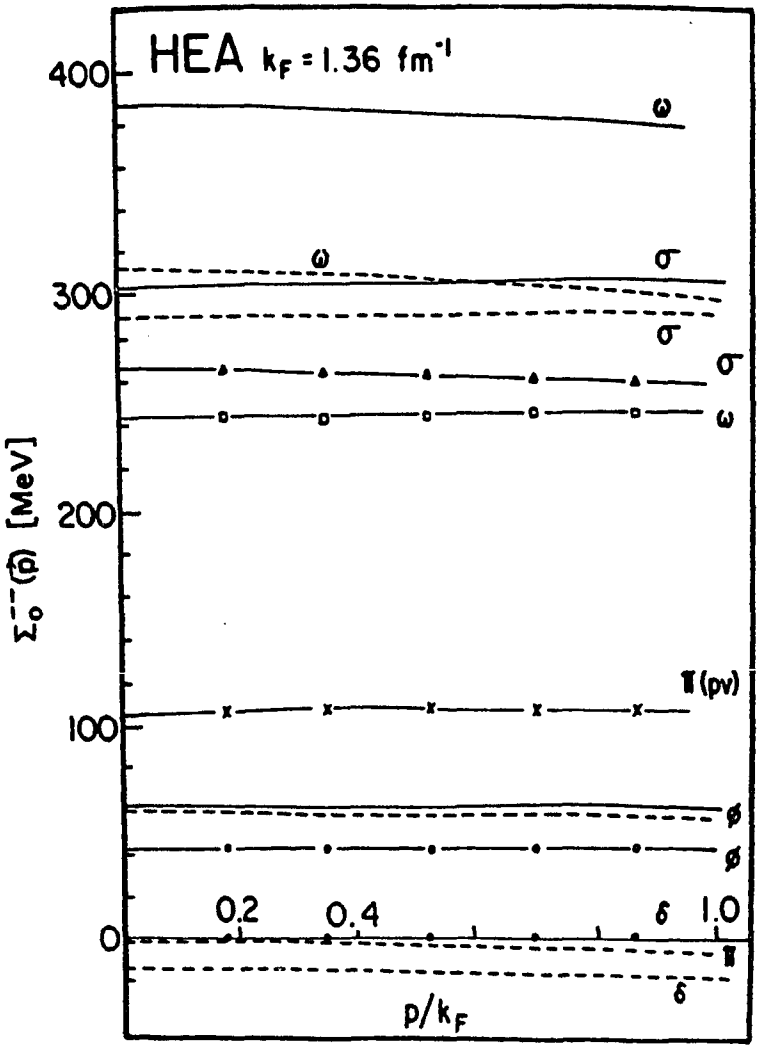

The unbroken solid lines are the Hartree-Fock results and the dashed lines include the effects of correlations[6]. The results of calculations of meson plus pseudo-meson exchange are shown as triangles (sigma), square (omega), crosses (pion), dots (phi) and circles (delta).

Figure 9

Self-energy $\Sigma_0^{++}(\vec{p})$ vs. $|\vec{p}|/k_F$ for the potential HM2.

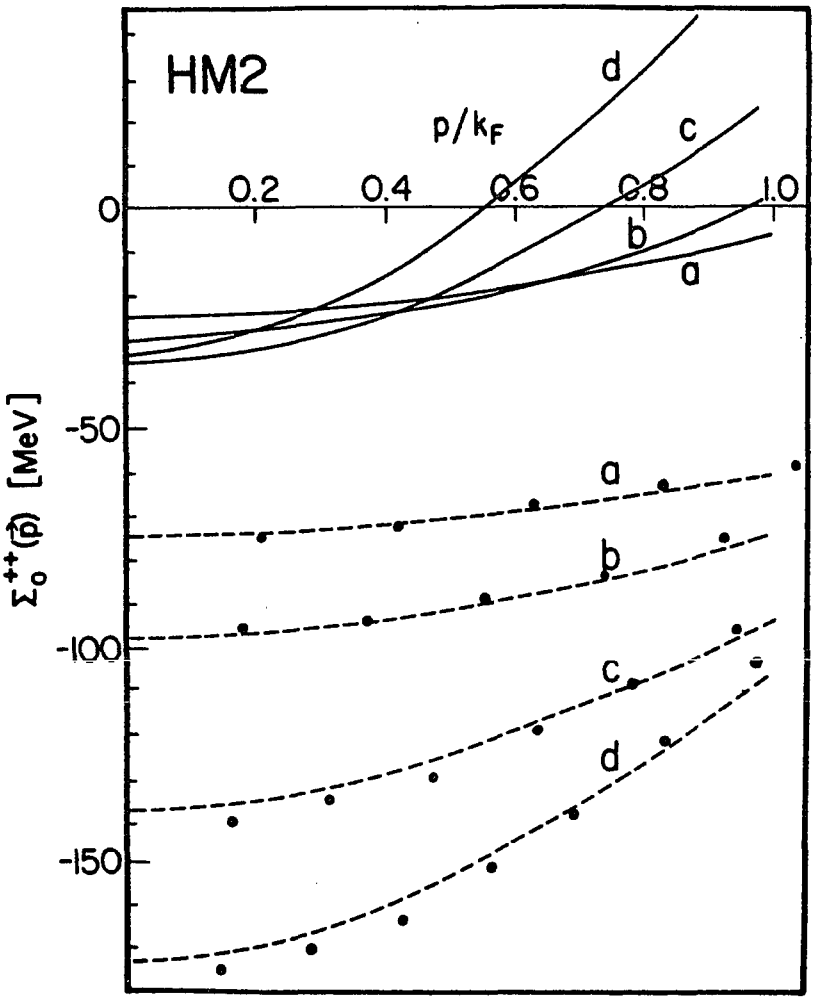

The solid lines denote the Hartree-Fock results and the dashed lines include the effects of correlations. The dots in the lower half of the figure are the results obtained with V_{eff} of Eqs. (3.1)-(3.3), (3.16)-(3.17).

(a) $k_F = 1.2$ fm^{-1}, (b) $k_F = 1.36$ fm^{-1}, (c) $k_F = 1.5$ fm^{-1}, (d) $k_F = 1.6$ fm^{-1}.

Figure 10

Contribution of ω and ρ exchange to the self-energy $\Sigma_0^{++}(\vec{p})$ for the potential HM2.

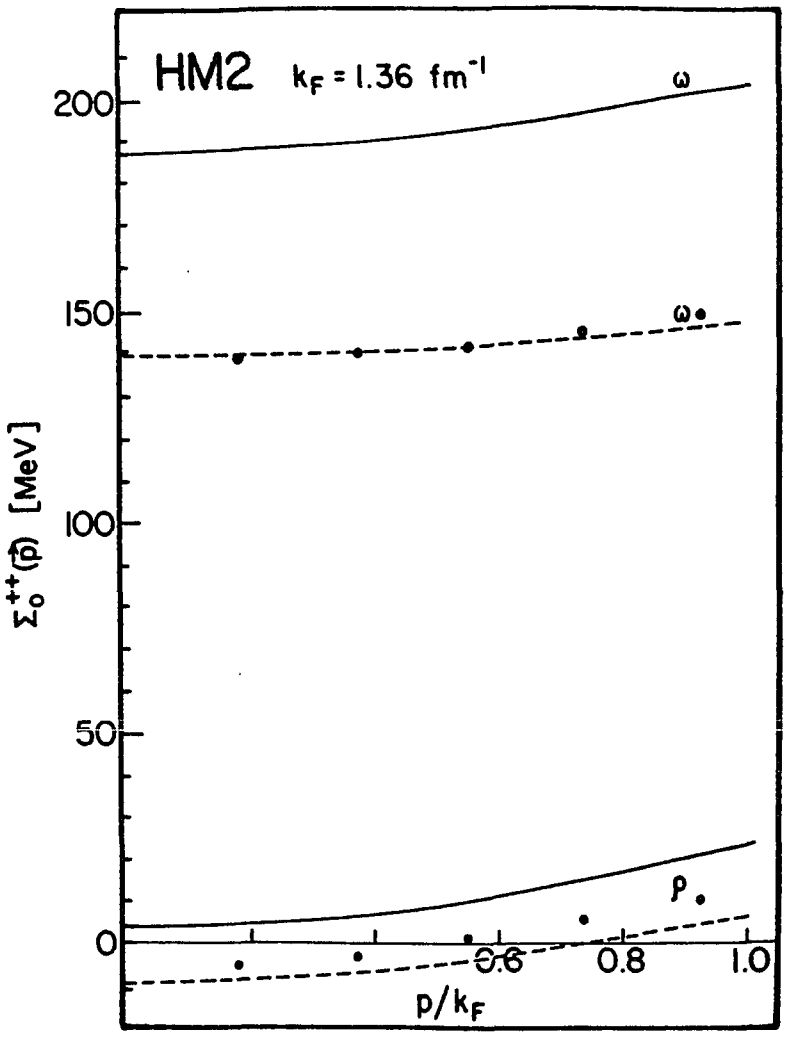

The solid lines exhibit the results as calculated in the Hartree-Fock approximation. The dashed lines show the contribution in the presence of correlations. The upper set of black dots shows the results of ω exchange and a portion of the total pseudo-omega exchange $\{(\delta g^2_\omega/4\pi)_1 = 5.63\}$ calculated in the Hartree-Fock approximation. The lower set of black dots shows the similar results for ρ exchange and a portion of pseudo-omega exchange $\{(\delta g^2_\omega/4\pi)_2 = 0.89\}$ - see Table 4.2. [Note that the <u>total</u> pseudo-omega exchange is calculated with $(\delta g^2_\omega/4\pi) = 5.63 + 0.89 = 6.52$].

Figure 11

Contribution of σ, π exchange to the self-energy $\Sigma_0^{++}(\vec{p})$ for the potential HM2.

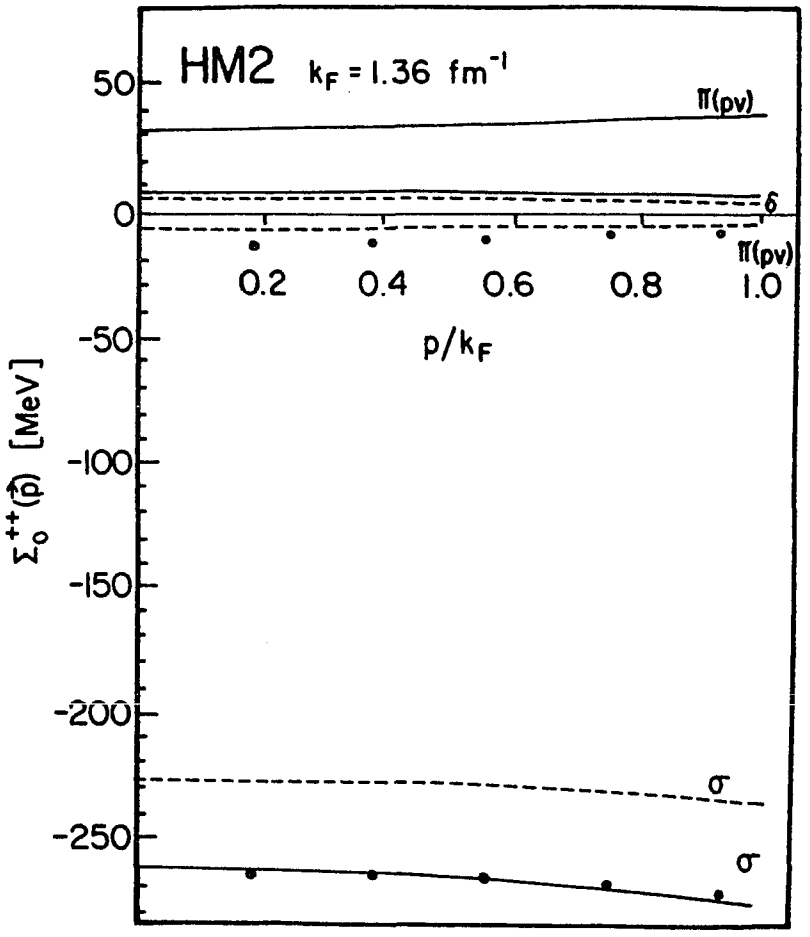

The solid lines exhibit the results as calculated in the Hartree-Fock approximation. The dashed lines are the results in the presence of correlations. The black dots represent sigma and pseudo-sigma exchange [$(\delta g^2_\delta/4\pi)_1$= 4.34 - see Table 4.2] calculated in the Hartree-Fock approximation. In the case of the pion we add a portion of the pseudo-sigma exchange [$(\delta g^2_\sigma/4\pi)_2$ = -5.49 - see Table 4.2] which is taken to be attractive. The total result for pseudo-gigma exchange [$\delta g^2_\sigma/4\pi$ = -1.15 - see Table 3.2] is seen to be attractive.

Figure 12

Self-energy $\Sigma_0^{-+}(\vec{p})$ vs. $|\vec{p}|/k_F$ for the potential HM2.

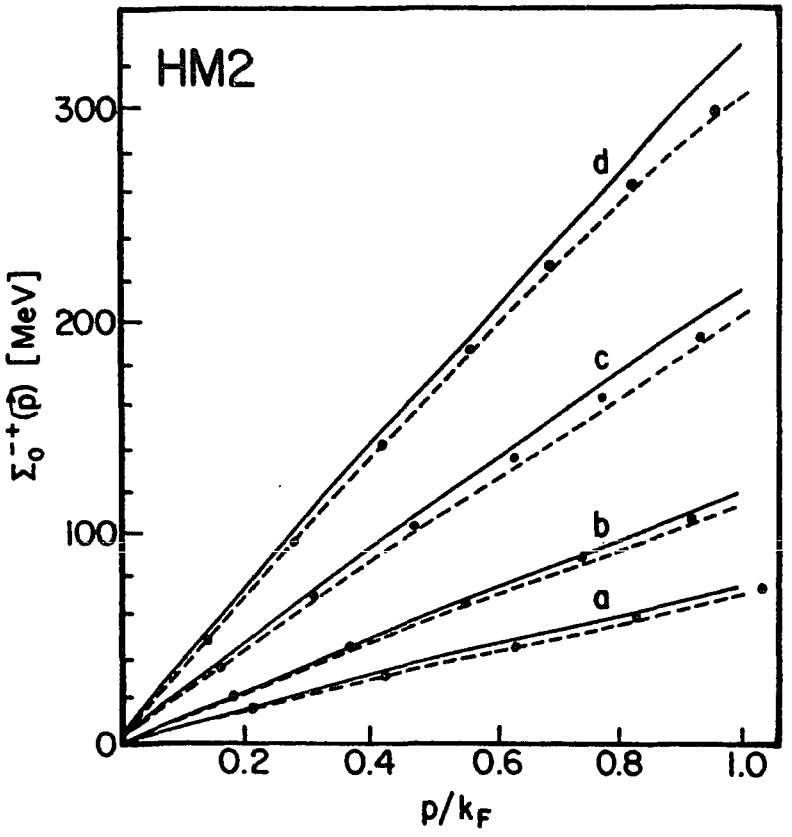

The solid curves are the Hartree-Fock results and the dashed lines include the effects of correlations. [See Ref.7.] The small dots are calculated with V_{eff} of Eqs. (3.1)-(3.3),(3.16-3.17).

(a) $k_F = 1.2$ fm^{-1}, (b) $k_F = 1.36$ fm^{-1}, (c)$k_F = 1.5$ fm^{-1}.

Figure 13

Contribution of σ and ω exchange to the self-energy $\Sigma_0^{-+}(\vec{p})$ for the potential HM2.

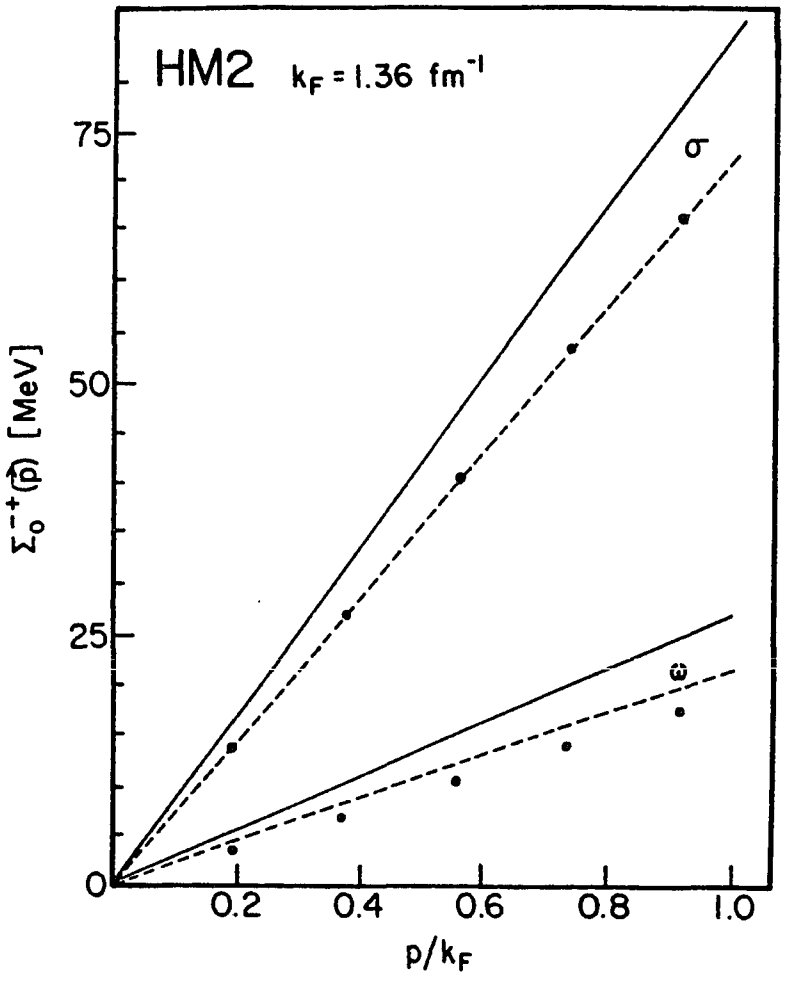

The solid lines denote the Hartree-Fock results and the dashed lines denote the results of RBHF theory. The dots result from adding pseudo-particle exchange to the Hartree-Fock results. [Here $(\delta g^2_\omega/4\pi)_1 = 5.63$ and $(\delta g^2_\sigma/4\pi)_1 = 4.34$ - see Table 3.2.]

Figure 14

Contribution of π and ρ exchange to the self-energy $\Sigma_0^{-+}(\vec{p})$ for the potential HM2.

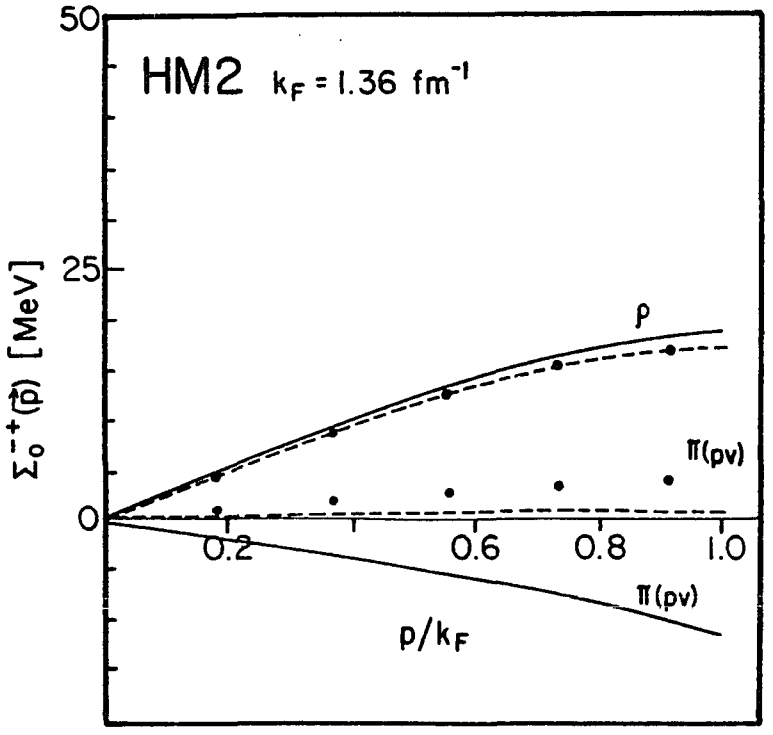

The solid lines exhibit the results as calculated in the Hartree-Fock approximation. The dashed lines exhibit the results as calculated in RBHF theory. Pseudo-vector coupling is used. The upper set of block dots shows the results of ρ exchange and a portion of the total pseudo-omega exchange [$(\delta g^2_\omega/4\pi)_2 = 0.89$] calculated in the Hartree-Fock approximation. The lower set of black dots shows the results for π exchange and a portion of pseud0-sigma exchange with $(\delta g^2_\sigma/4\pi)_2 = -5.49$. See Table 4.2. [Here the negative sign for $(\delta g^2_\sigma/4\pi)$ means that the contribution of the pseudo-sigma particle has the same sign as that obtained for sigma exchange.]

Figure 15

Self-energy $\Sigma_0^{--}(\vec{p})$ vs. $|\vec{p}|/k_F$ for the potential HM2.

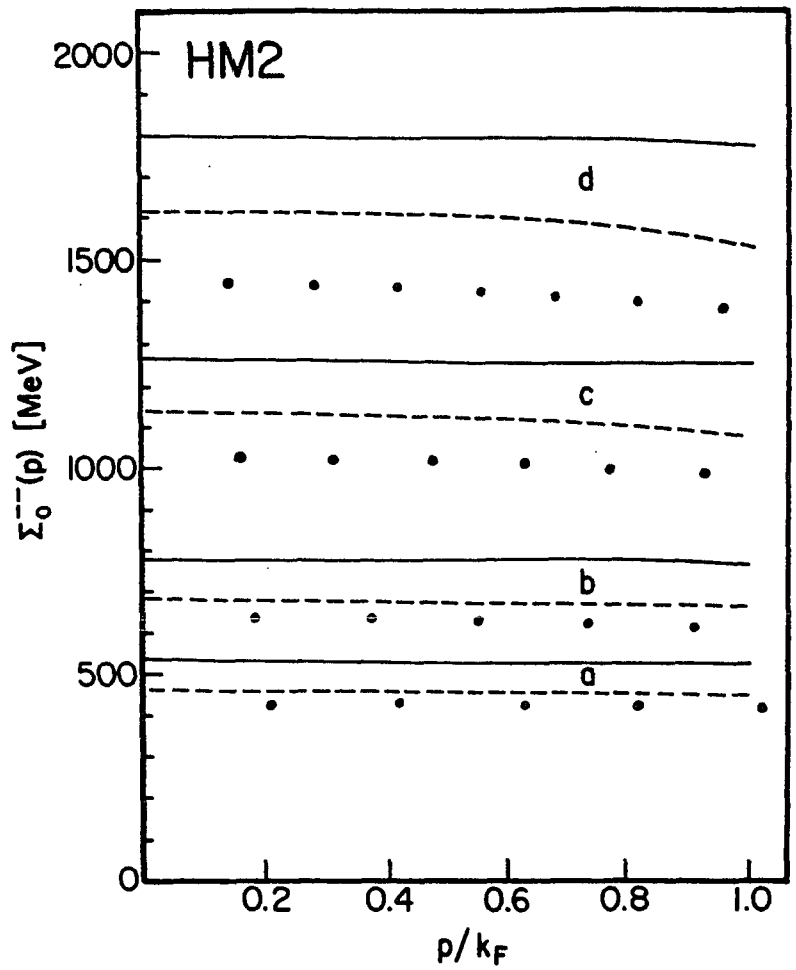

The curves have the same meaning as that described in the caption of Fig.9. Results calculated with V_{eff} are represented by the dots.

Figure 16

Contribution of ω, σ and ρ exchange to the self-energy $\Sigma_0^{--}(\vec{p})$ for the potential HM2.

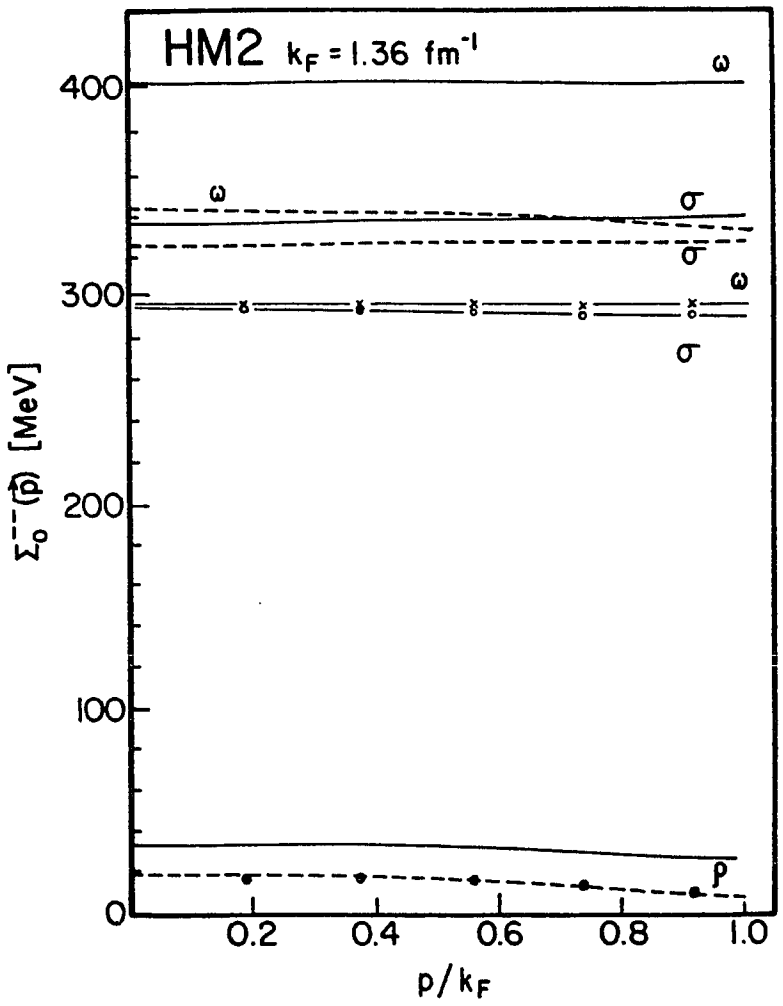

The unbroken solid lines are the Hartree-Fock results and the dashed lines include the effects of correlations[6]. The results of calculations of meson plus pseudo-meson exchange are shown as circles (sigma), crosses (omega), dots (rho).

Figure 17

Self-energy $\Sigma_0^{++}(\vec{p})$ vs. $|\vec{p}|/k_F$ for an alternative approximation for the potential HEA.

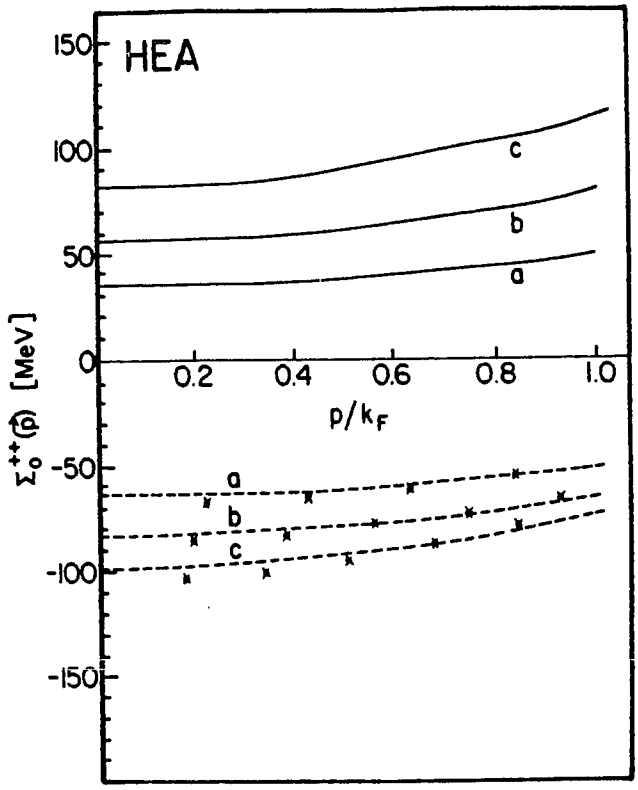

The curves have the same meaning as that described in caption of Fig.1. The results of calculations of meson plus pseudo-meson exchange are shown as dots and crosses. The black dots are obtained by using the pseudoparticle coupling constants $\delta g^2_\sigma/(4\pi) = 5.0, \delta g^2_\omega/(4\pi) = 20.2, \delta g^2_\delta/(4\pi) = -6.54$, for $k_F = k_F^{NM} = 1.36$ fm^{-1} while crosses are obtained by using the pseudoparticle coupling constants $\delta g^2_\sigma/(4\pi) = 1.18$, $\delta g^2_\omega/(4\pi) = 26.8$, $\delta g^2_\delta/(4\pi) = -4.49$, for $k_F = k_F^{NM} = 1.36$ fm^{-1} The mass parameters in both case are $M_\sigma = M_\omega = M_\delta = 1.5$ GeV. (See Section 3.4 and Eqs. 3.18-3.19.)

Figure 18

Self-energy $\Sigma_0^{++}(\vec{p})$ vs. $|\vec{p}|/k_F$ for an alternative approximation for the potential HEA.

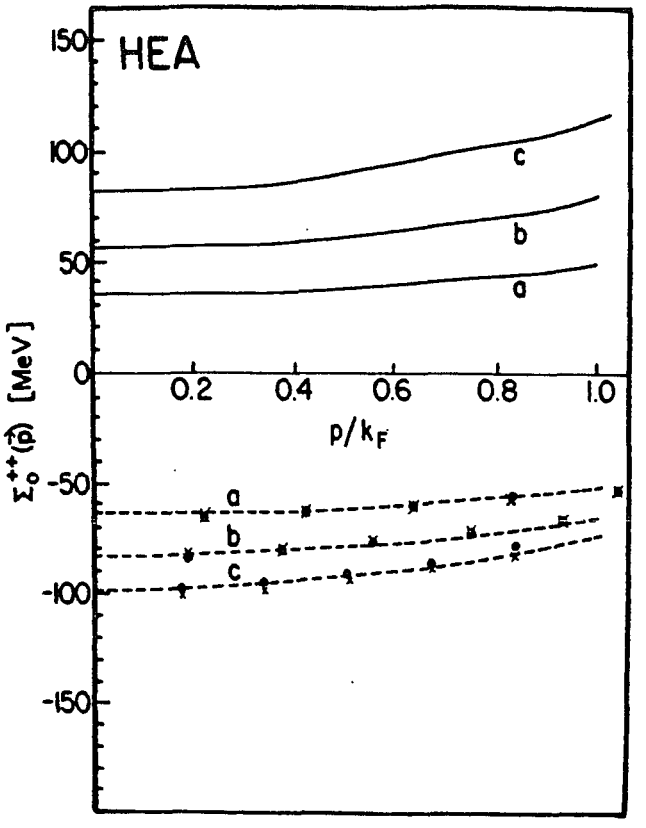

The curves and the dots have the same meaning as that described in caption of Fig.1. The results of calculations of meson plus pseudo-meson exchange are shown as crosses. Here we use the pseudoparticle coupling constants (Approx.3 in Table 3.3) $\delta g^2_\sigma/(4\pi) = -3.50, \delta g^2_\omega/(4\pi) = 16.6, \delta g^2_\delta/(4\pi) = 2.54$, for $k_F = k_F^{NM} = 1.36$ fm^{-1} ($M_\sigma = M_\omega = 1$ GeV, $M_\delta = 1.25$ GeV. (See Section 3.4.)

Figure 19

Self-energy $\Sigma_0^{++}(\vec{p})$ vs. $|\vec{p}|/k_F$ for an alternative approximation for the potential HEA.

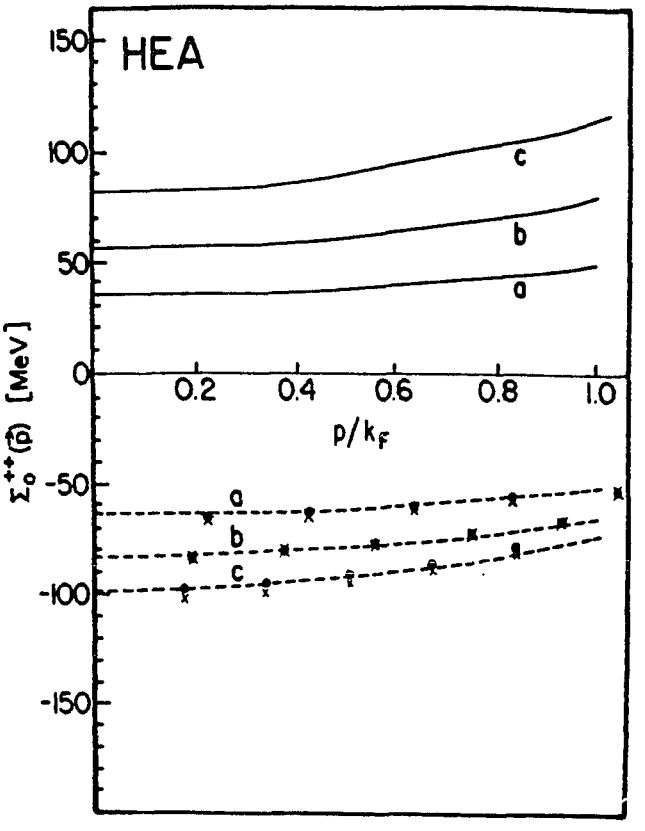

The curves and the dots have the same meaning as that described in caption of Fig.1. The results of calculations of meson plus pseudo-meson exchange are shown as crosses. Here we use the pseudoparticle coupling constants (Approx.6 in Table 3.3) $\delta g^2_\sigma/(4\pi) = -1.81, \delta g^2_\omega/(4\pi) = 16.2, \delta g^2_\delta/(4\pi) = 5.81$, for $k_F = k_F^{NM} = 1.36$ fm^{-1} ($M_\sigma = M_\omega = 1$ GeV, $M_\delta = 1.25$ GeV. (See Section 3.4.)

Figure 20

Self-energy $\Sigma_0^{++}(\vec{p})$ vs. $|\vec{p}|/k_F$ for an alternative approximation for the potential HEA.

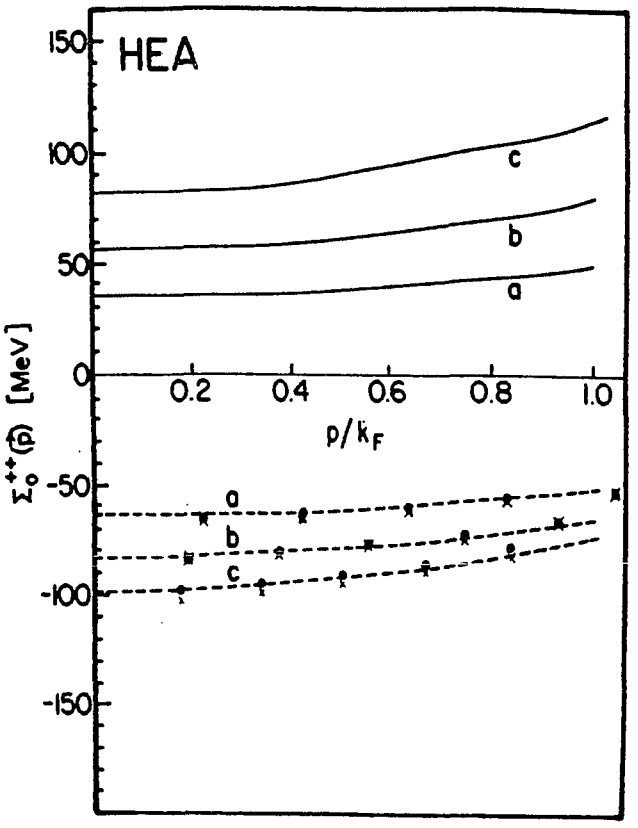

The curves and the dots have the same meaning as that described in caption of Fig.1. The results of calculations of meson plus pseudo-meson exchange are shown as crosses Here we use the pseudoparticle coupling constants (Approx.7 in Table 3.3) $\delta g^2_\sigma/(4\pi)$ =-4.30, $\delta g^2_\omega/(4\pi)$ = 13.2, $\delta g^2_\delta/(4\pi)$ = 3.54, for $k_F = k_F^{NM}$ = 1.36 fm^{-1} ($M_\sigma = M_\omega$ = 1 GeV, M_δ = 1.25 GeV. (See Section 3.4.)

Figure 21

$U_{eff}(\vec{p})$ vs. $|\vec{p}|$ for the potential HEA. (Here $\rho = \rho_{NM}$.)

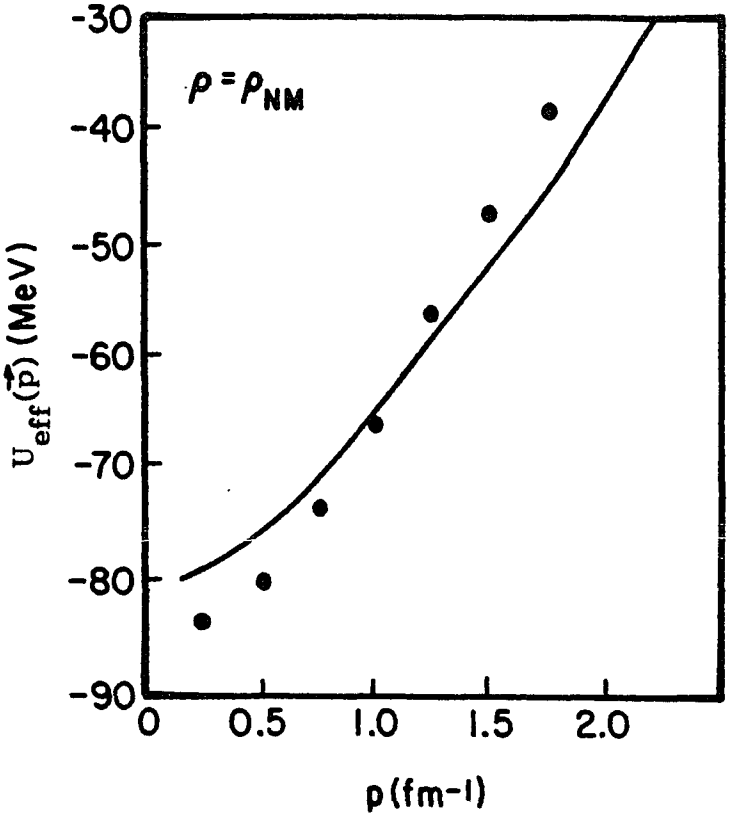

The effective potential, $U_{eff}(\vec{p})$, calculated using the relativistic BHF theory (solid line) and the values of $U_{eff}(\vec{p})$ calculated using V_{eff} of Eqs. (3.1)-(3.3), (3.12)-(3.15).

Figure 22

$U_{eff}(\vec{p})$ vs. $|\vec{p}|$ for the potential HEA. (Here $\rho = 5/4\ \rho_{NM}$.)

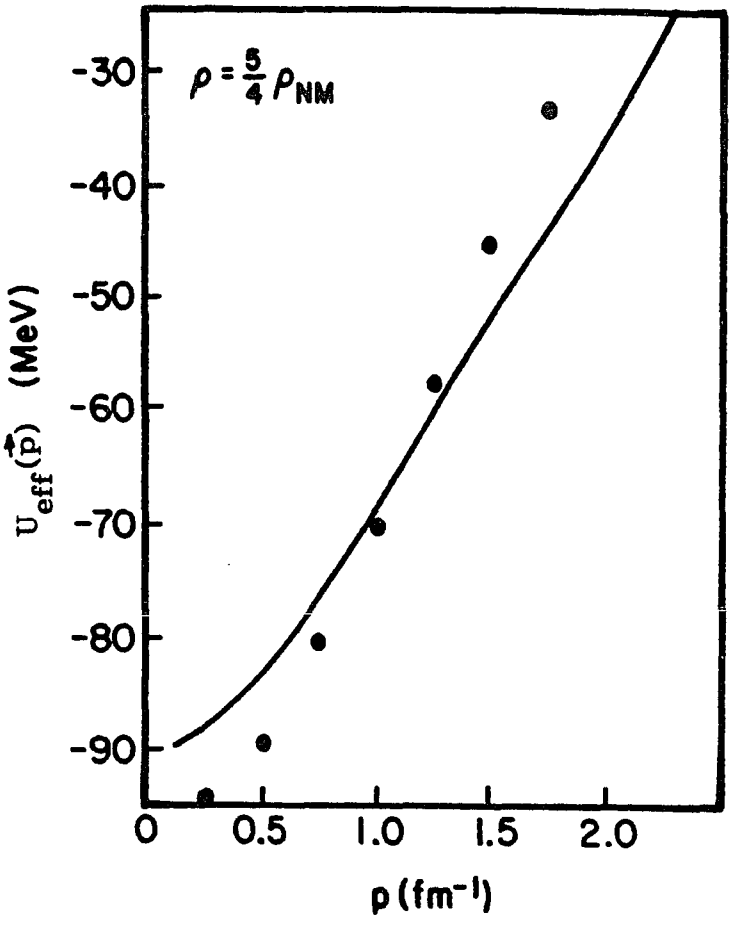

The effective potential, $U_{eff}(\vec{p})$, calculated using the relativistic BHF theory (solid line) and the values of $U_{eff}(\vec{p})$ calculated using V_{eff} of Eqs. (3.1)-(3.3), (3.12)-(3.15).

Figure 23

$U_{eff}(\vec{p})$ vs. $|\vec{p}|$ for the potential HEA. (Here $\rho = 3/4\ \rho_{NM}$.)

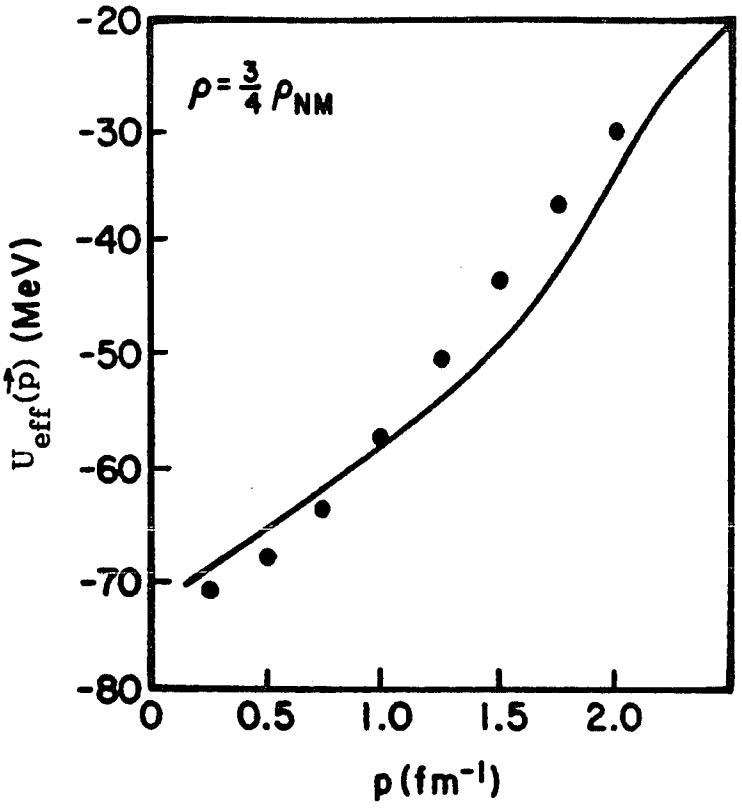

The effective potential, $U_{eff}(\vec{p})$, calculated using the relativistic BHF theory (solid line) and the values of $U_{eff}(\vec{p})$ calculated using V_{eff} of Eqs. (3.1)-(3.3), (3.12)-(3.15).

Figure 24

$U_{eff}(\vec{p})$ vs. $|\vec{p}|$ for the potential HEA. (Here $\rho = 1/2\ \rho_{NM}$.)

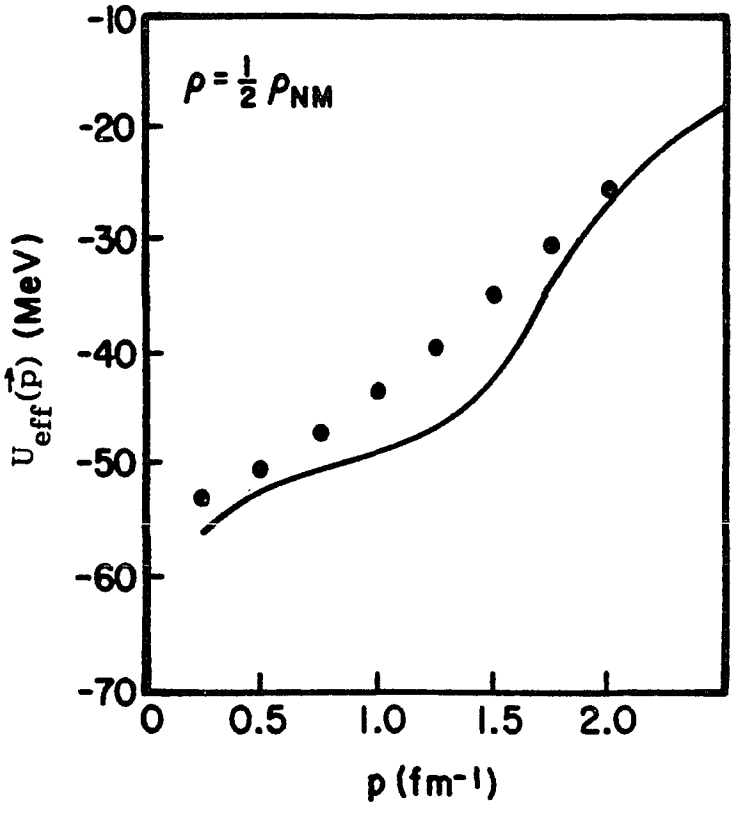

The effective potential, $U_{eff}(\vec{p})$, calculated using the relativistic BHF theory (solid line) and the values of $U_{eff}(\vec{p})$ calculated using V_{eff} of Eqs. (3.1)-(3.3), (3.12)-(3.15).

Figure 25

$U_{eff}(\vec{p})$ vs. $|\vec{p}|$ for the potential HEA. (Here $\rho = 1/4\ \rho_{NM}$.)

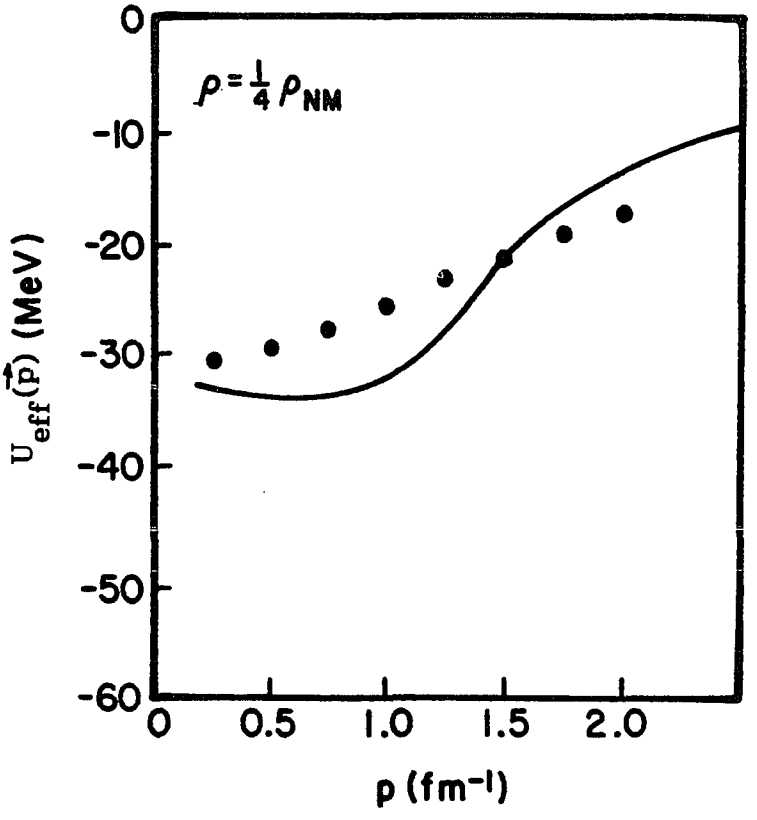

The effective potential, $U_{eff}(\vec{p})$, calculated using the relativistic BHF theory (solid line) and the values of $U_{eff}(\vec{p})$ calculated using V_{eff} of Eqs. (3.1)-(3.3), (3.12)-(3.15).

Figure 26

Binding energy per nucleon, E_B/A vs. k_F for the potential HEA (density-dependent case).

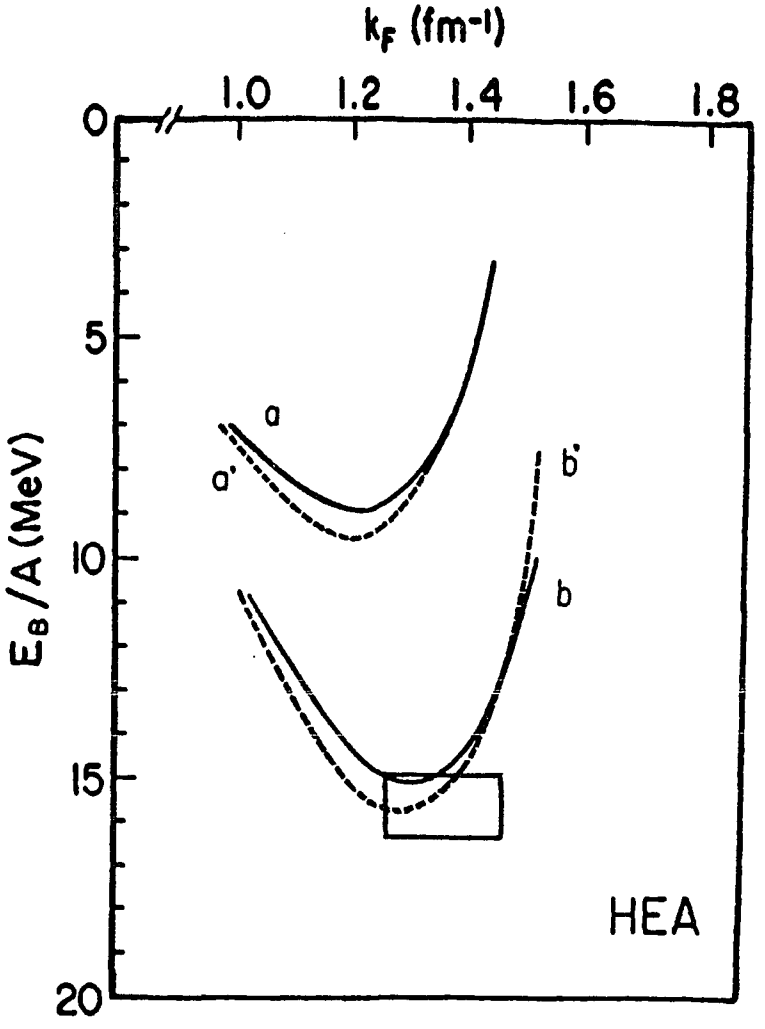

The curves labelled a' and a denote the Hartree-Fock results for the potential $V_{eff} = U + \delta U$ introduced in Section 3.3. Here curve a' denotes the non-self-consistent result and a denotes the self-consistent result. The curves b' and b are obtained by modifying the coupling constant of the pseudo-omega particle. Here curve b' denotes the non-self-consistent result and curve b denotes the self-consistent result. (See Section 5.2, Section 6.4 and Table 5.1.) The empirical values for the density and binding energy lie within the rectangle.

Figure 27

Binding energy per nucleon, E_B/A, vs. k_F for the potential HEA (density-independent case).

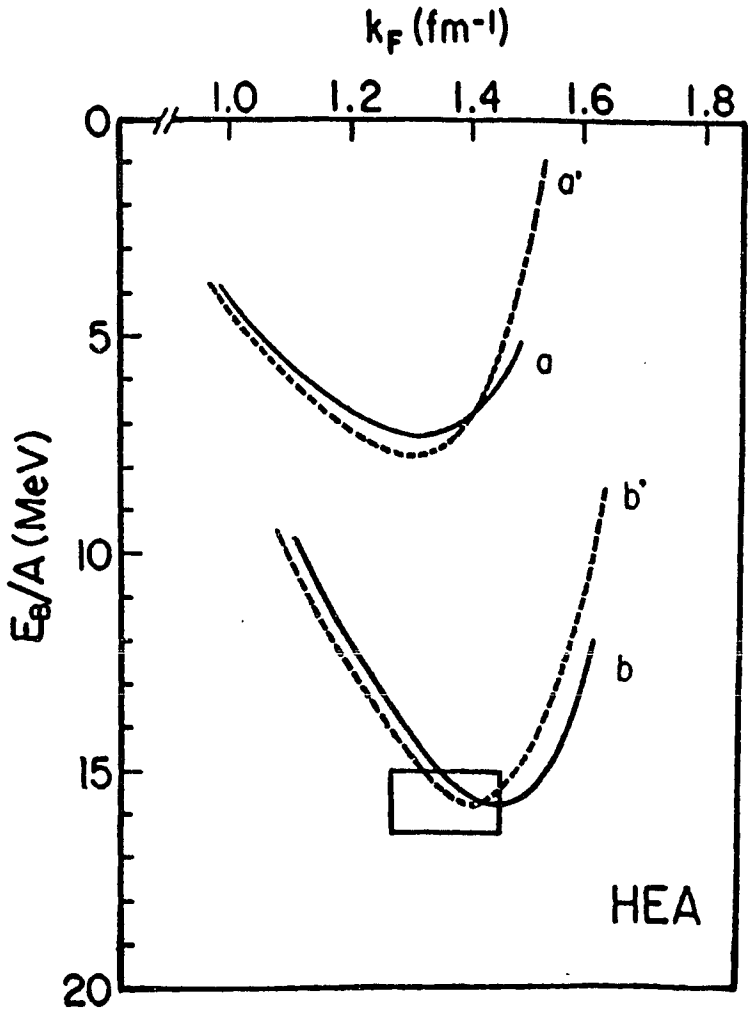

The same caption as Fig.26 except that the density dependence of the coupling constants of the pseudoparticles determined in Section 3.3 [Eqs.(3.12)-(3.15)] is neglected.

Figure 28

Binding energy per nucleon for different approximations: E_B/A vs. k_F for the potential HEA.

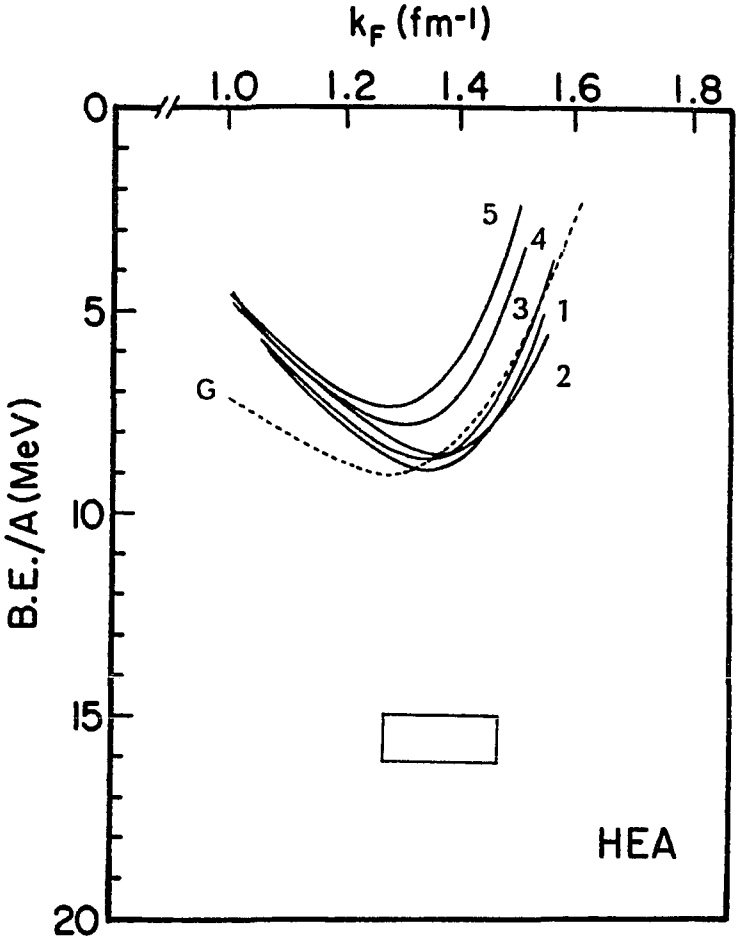

The same caption as curve a' in Fig.26 except that the coefficients a_1, a_2, a_3 in Eq.3.14 for different Approximations are listed in Table 3.3. The curves labelled 1, 2, 3, 4, and 5 denote the results correspoding the Approximations 1, 2, 3, 4, 5, presented in Table 3.3. THe dashed line labelled G denotes the saturation curve calculated by using RBHF theory. (See Fig.2.24(a) in Ref.7.)

Figure 29

Binding energy per nucleon, E_B/A, vs. k_F for the potential HM2 (density-dependent case).

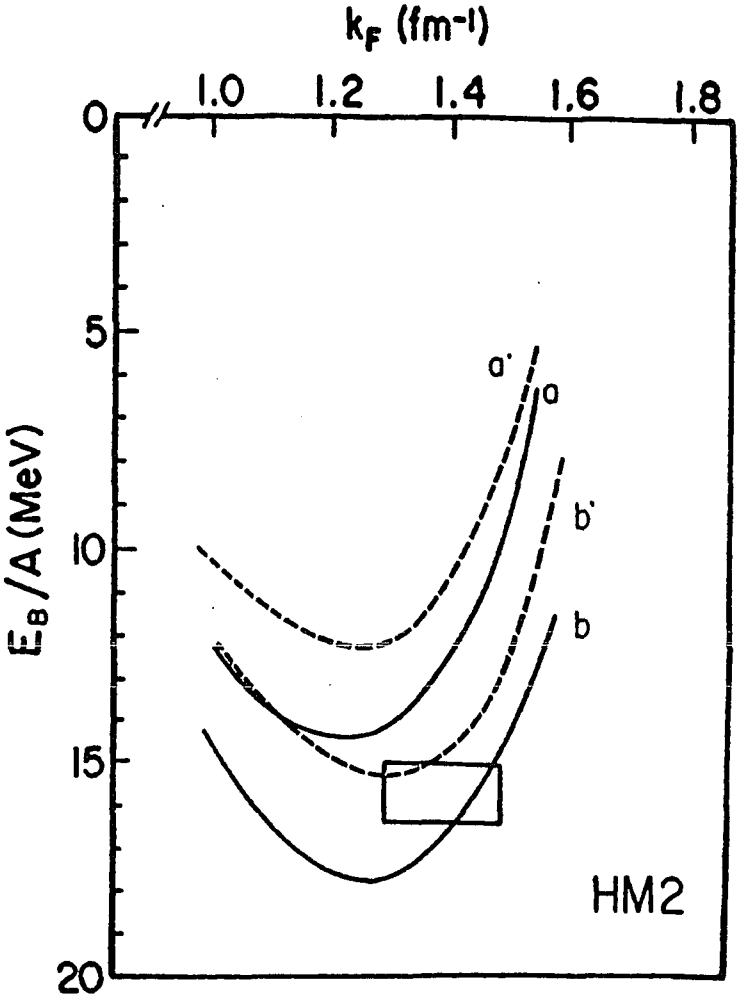

The same caption as Fig.26, except that the potential is HM2 and the density dependence of the coupling constants of the pseudoparticls was determined by Eqs. (3.16)-(3.17). The curves b' and b again correspond to a modification of the pseudo-omega coupling constant. (See Section 5.3, Section 6.4 and Table 5.1.)

Figure 30

Binding energy per nucleon, E_B/A, vs. k_F for the potential HM2 (density-independent case).

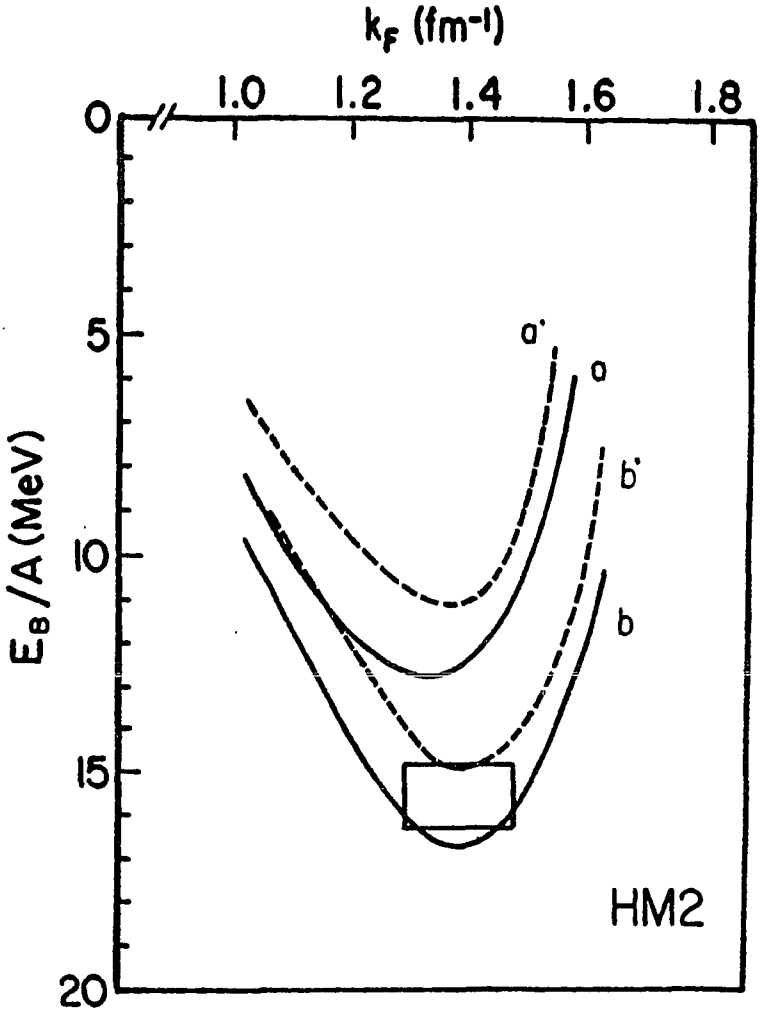

The same caption as Fig.29, except that we omit the density dependence of the pseudoparticle coupling constants which was determined in Eqs.(3.16)-(3.17).

Figure 31

Binding energy per nucleon for different approximations: E_B/A vs. k_F for the potential BMR2.

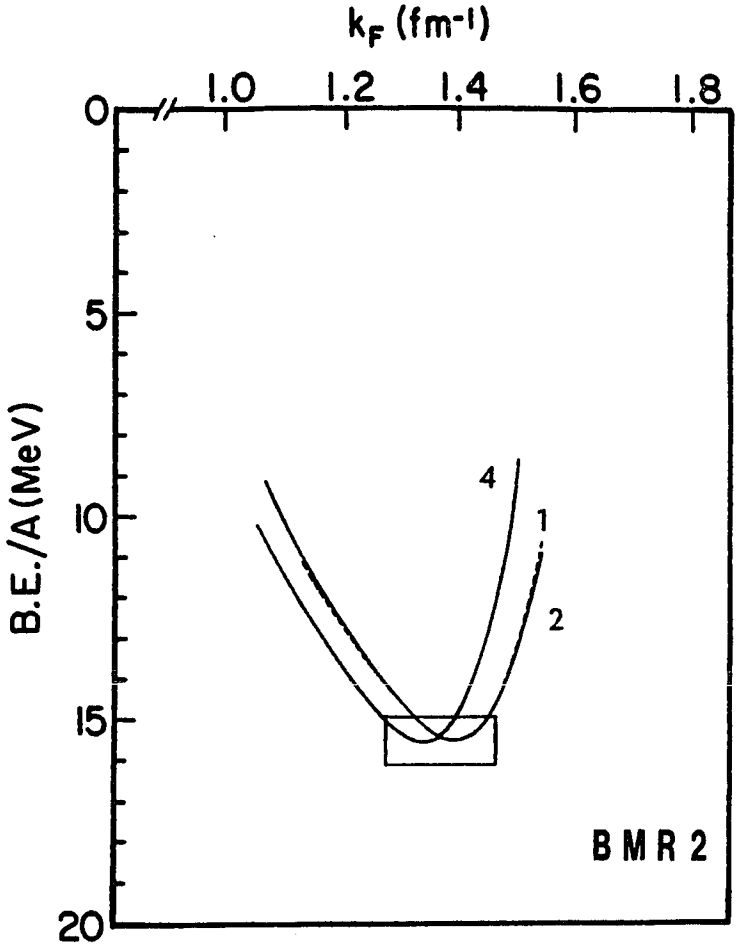

The same caption as curve a' in Fig.26 except that the potential is BRM2. The curves labelled 1, 2, and 4 denote the results correspoding the Approximations 1, 2, 4, presented in Table 5.2. We take iteration accuracy 0.001 in the calculation. (See Section 6.3.)

Figure 32

Binding energy per nucleon, E_B/A, vs. k_F for the potential HM2.

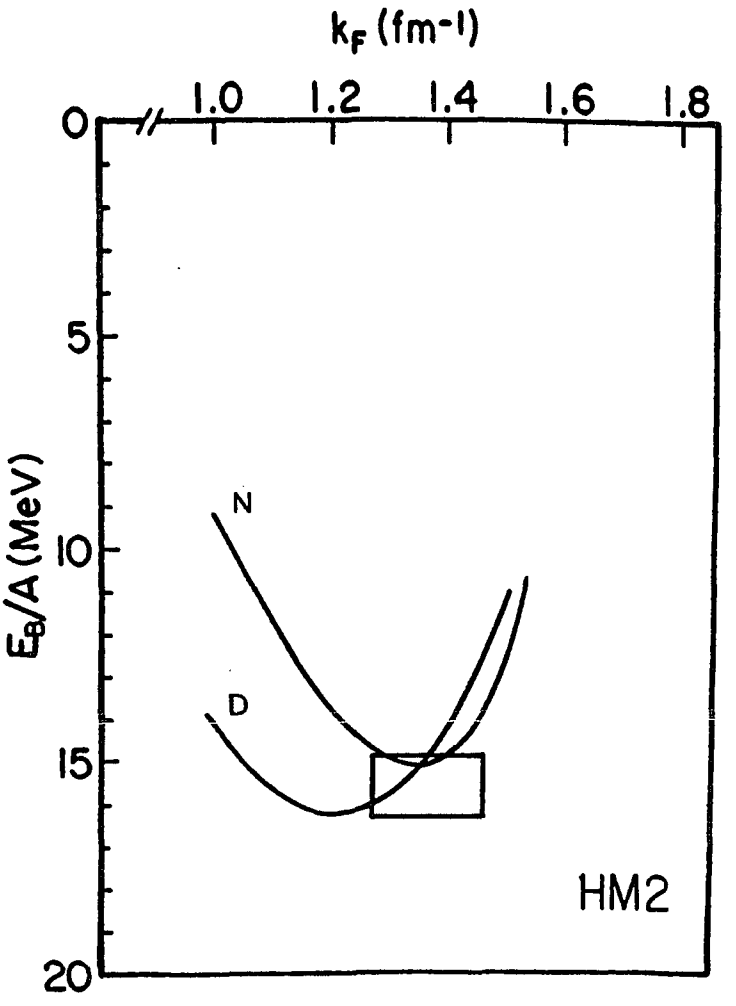

The curves labelled D and N denote the self-consistant results for the potential, $V_{eff} = U + \delta U$, introduced in Section 3.3. Here we use the modified pseudoparticle coupling constants $\delta g^2_\sigma/4\pi = -1.15$, , $\delta g^2_\omega/4\pi = 6.98$, for $k_F = k_F^{NM} = 1.36$ fm^{-1} ($M_\sigma = 1$ GeV, $M_\omega = 1$ GeV). Curve N denotes the results for density-independent pseudoparticle coupling constants while curve D denotes the results for density-dependent pseudoparticle coupling constants. (See Eqs.3.16-3.17.)

Figure 33

Binding energy per nucleon for different iteration accuracy: E_B/A vs. k_F for the potential HEA.

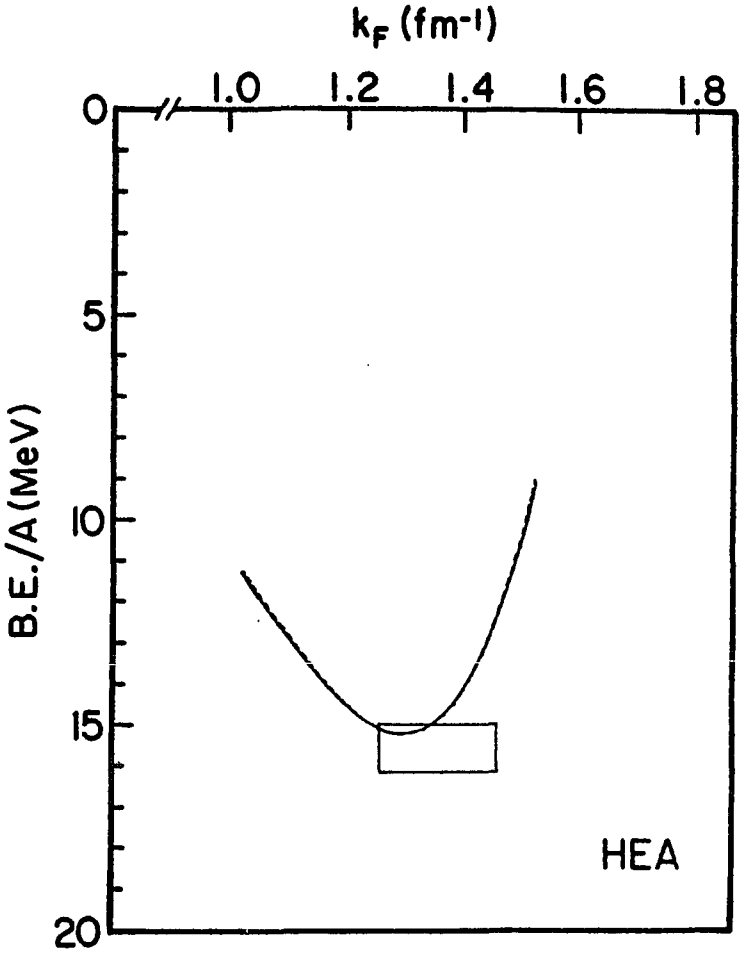

The same caption as curve b in Fig.26, except that the solid line was obtained by using an iteration accuracy of 0.0001, while the dashed line was obtained by using an iteration accuracy of 0.01. (See Sections 6.3-6.4.) The curves are almost identical.

Figure 34

Binding energy per nucleon for different iteration accuracy: E_B/A vs. k_F for the potential HM2.

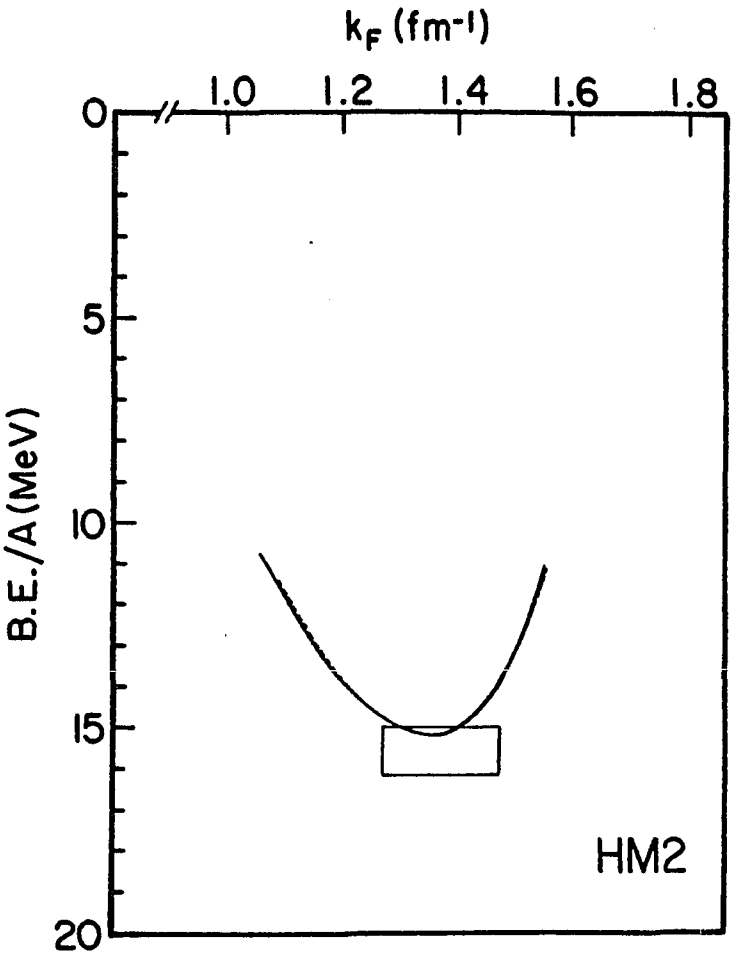

The same caption as curve N in Fig.32, except that the solid line was obtained by using an iteration accuracy of 0.0001, while the dashed line was obtained by using an iteration accuracy of 0.01. (See Sections 6.3-6.4.) The curves are almost identical.

Figure 35

Binding energy per nucleon of different iteration accuracy: E_B/A vs. k_F for the potential BMR2.

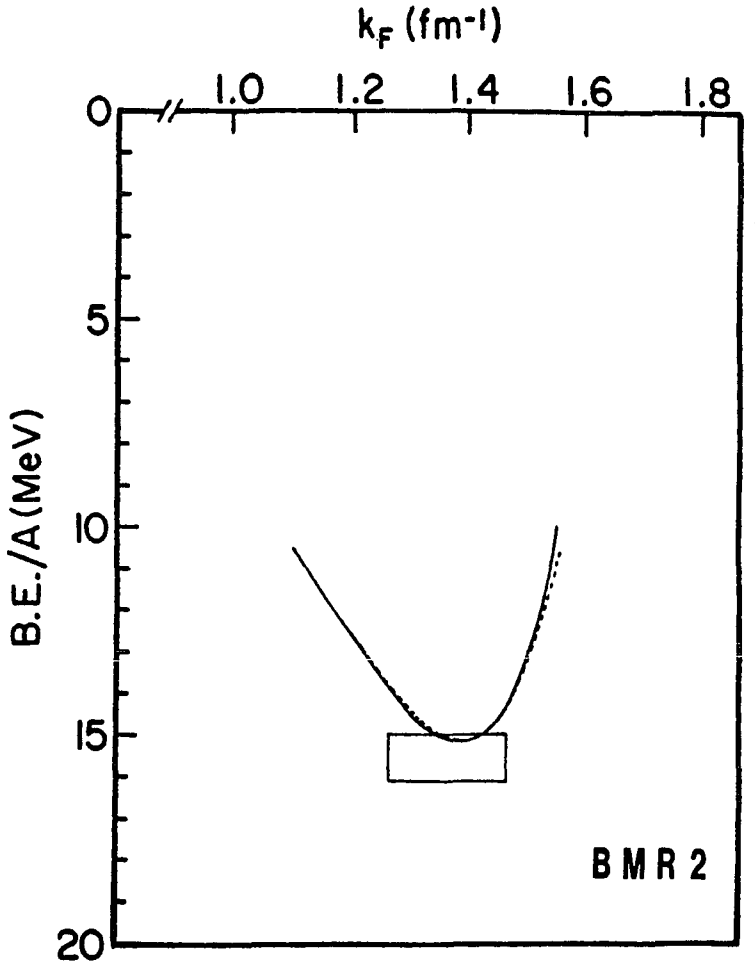

The same caption as in Fig.31, except that here we use $\delta g^2_\omega/4\pi = 14.20$. The solid line was obtained by using an iteration accuracy of 0.0001, while the dashed line was obtained by using an iteration accuracy of 0.01. (See Sections 6.3-6.4.) The curves are almost identical.

Appendix A

Eikonal Form Factor[19]

In this Appendix we show how we to use the eikonal form factor in self-consistent calculations.

For the potential HM2, we use the eikonal form factor $F_i(t,u|q_0^2)$, where i = σ,ω,ρ,π....mesons. We have

$$F_i(t,u|q_0^2)=\exp[2i\{[\chi(t)-\chi(m_i^2)]+[\chi(u)-\chi(4m_N^2-s-m_i^2)\}] \quad , \tag{A.1}$$

where

$$t = (E_q,- E_q)^2 - (\vec{q}'- \vec{q})^2 \quad , \tag{A.2}$$

$$u = (E_q,- E_q)^2 - (\vec{q}'+ \vec{q})^2 \quad , \tag{A.3}$$

$$E_q^2 = \vec{q}^2 + m_N^2 \quad . \tag{A.4}$$

The starting energy[19] s is

$$s = (E_q,+ E_q)^2 - (\vec{q}' + \vec{q})^2 \quad , \tag{A.5}$$

and

$$i\chi(y)=\begin{cases} -2\gamma \dfrac{2m_N^2 - y}{\sqrt{y\,(4m_N^2 - y)}} \arctan\sqrt{\dfrac{y}{4m_N^2 - y}} \\ \qquad (\ 0 < y < 4m_N^2 \ ) \\ -2\gamma \dfrac{2m_N^2 - y}{\sqrt{-\,y(4m_N^2 - y)}} \ln\left[\sqrt{\dfrac{-\,y}{4m_N^2}} + \sqrt{1 - \dfrac{y}{4m_N^2}}\,\right] \\ \qquad (\ y < 0 \ ) \end{cases} \tag{A.6}$$

In the self-consistent calculation the quantity m_N in in the expressions for t, u, s is changed to the self-consistent mass $\tilde{m}$ determined by the iteration process, so that

t changes to $\tilde{t}$,

u changes to $\tilde{u}$,

s changes to $\tilde{s}$.

We do not modify ix(y). This procedure yields the results reported in the text.

Appendix B

Alternative Normalization

In this Appendix we present another definition of the relativistic nucleon wave function in nuclear matter and discuss the corresponding normalization.

Recall Eq.(2.8):

$$[\gamma\cdot p - m_N - \Sigma(\{f(\vec{p},s)\},p)]f(\vec{p},s)=0 \quad . \tag{2.8}$$

Upon inserting Eq.(2.27), we obtain

$$[\ \vec{\gamma}\cdot\vec{p} + \tilde{m}\ ]f(\vec{p},s) = \gamma^0\tilde{E}f(\vec{p},s) \quad , \tag{B.1}$$

where

$$\tilde{m}= \frac{m_N + A(p)}{1 + \dfrac{C(p)}{m_N}} \quad , \quad \tilde{E} = \sqrt{\vec{p}^{\,2} + \tilde{m}^2} = \frac{p^0 - B(p)}{1 + \dfrac{C(p)}{m_N}} \quad . \tag{B.2}$$

Keeping in mind the form of the free Dirac spinor, we can write a spinor $f(\vec{p},s)$ as follows:

$$f(\vec{p},s) = \sqrt{\frac{\tilde{E}(\vec{p})+ \tilde{m}}{2\ \tilde{m}}} \begin{pmatrix} \chi_s \\ \dfrac{\vec{\sigma}\cdot\vec{p}}{\tilde{\epsilon}(\vec{p})}\ \chi_s \end{pmatrix} \quad , \tag{B.3}$$

where

$$\tilde{\epsilon} = \tilde{E}(p) + \tilde{m} \quad . \tag{B.4}$$

We choose the normalization

$$f^{+}(\vec{p},s')f(\vec{p},s) = \delta_{ss'} \ , \tag{B.5}$$

for the spinor $f(\vec{p},s)$. Therefore, we can write the relativistic nucleon wave function in nuclear matter as

$$\Psi^{rel}_{s,\tau}(\vec{p}) = \sqrt{\frac{\tilde{m}}{\tilde{E}(\vec{p})}}\ f(\vec{p},s)\frac{e^{i\vec{p}\cdot\vec{x}}}{(2\pi)^{3/2}}\chi_{\tau} \ . \tag{B.6}$$

We also have

$$\phi^{+}_{s}(\vec{p})\phi_{s}(\vec{p}) = 1 \ . \tag{B.7}$$

Note that if $\tilde{m} \rightarrow m_N$ we have $f(\vec{p},s) \rightarrow u(\vec{p},s)$, which is the standard, positive-energy solution of the free Dirac equation. It is very convenient to use this normalization in Appendix D. When we calculate the fully on-shell amplitude, for all those results obtained by using the spinor $u(\vec{p},s)$, one only needs to make the change $m_N \rightarrow \tilde{m}$ and $E_N(\vec{p},m_N) \rightarrow \tilde{E}(\vec{p},\tilde{m})$ to obtain the results of the fully on-shell amplitude corresponding to the spinor $f(\vec{p},s)$.

Appendix C

Fierz Transformation

For nucleon-nucleon scattering, which arises from the exchange of mesonic fields, we have direct and exchange terms. We can rearrange the indices of the exchange term by using the Fierz transformation. Then, for each value of the isospin we can express the on-shell nucleon-nucleon scattering amplitude in terms of five independent amplitudes:

$$
\begin{aligned}
(p_1', p_2' |\ M^{on}_{\alpha'\beta'\alpha\ \beta}\ | p_1, p_2) = {} & M_S(s,t)\left(\mathbb{I}(1)\right)_{\alpha'\alpha}\left(\mathbb{I}(2)\right)_{\beta'\beta} \\
& + M_V(s,t)\left(\gamma^{\mu}(1)\right)_{\alpha'\alpha}\left(\gamma_{\mu}(2)\right)_{\beta'\beta} \\
& + M_T(s,t)\left(\sigma^{\mu\nu}(1)\right)_{\alpha'\alpha}\left(\sigma_{\mu\nu}(2)\right)_{\beta'\beta} \\
& + M_A(s,t)\left(\gamma^5(1)\gamma^{\mu}(1)\right)_{\alpha'\alpha}\left(\gamma_5(2)\gamma_{\mu}(2)\right)_{\beta'\beta} \\
& + M_P(s,t)\left(\gamma^5(1)\right)_{\alpha'\alpha}\left(\gamma_5(2)\right)_{\beta'\beta} \ .
\end{aligned}
\tag{4.27}
$$

The various exchange terms will contribute to the full range of amplitudes, i.e. we can rearrange the indices of the exchange term so that the labelling corresponds to that used in Eq.(4.27). In this Appendix we provide various relations needed in performing the Fierz transformation and show how these relations may be derived.

As an illustrative example, let us put

$$\begin{aligned}\left(\gamma^{\mu}(1)\right)_{\beta',\alpha}\left(\gamma_{\mu}(2)\right)_{\alpha',\beta} &= a_S\left(\mathbb{I}(1)\right)_{\alpha',\alpha}\left(\mathbb{I}(2)\right)_{\beta',\beta} \\ &+ a_V\left(\gamma^{\mu}(1)\right)_{\alpha',\alpha}\left(\gamma_{\mu}(2)\right)_{\beta',\beta} \\ &+ a_T\left(\sigma^{\mu\nu}(1)\right)_{\alpha',\alpha}\left(\sigma_{\mu\nu}(2)\right)_{\beta',\beta} \\ &+ a_A\left(\gamma^5(1)\gamma^{\mu}(1)\right)_{\alpha',\alpha}\left(\gamma_5(2)\gamma_{\mu}(2)\right)_{\beta',\beta} \\ &+ a_P\left(\gamma^5(1)\right)_{\alpha',\alpha}\left(\gamma_5(2)\right)_{\beta',\beta} \quad .\end{aligned} \tag{C.1}$$

1). We begin by mutiplying the both sides of Eq.(C.1) by $[\mathrm{II}(1)]_{\alpha\alpha'}[\mathrm{II}(2)]_{\beta\beta'}$, and then sum on α', α, β', β to determine a_s. We use the notation in Section 2.1 and the trace theorems and identities for the γ matrices:

$$\sum_{\alpha'\beta'} A_{\beta',\alpha'}B_{\alpha',\beta'} = \mathrm{Tr}(AB) \ , \tag{C.2}$$

$$\mathrm{Tr}\mathbb{I} = 4 \ , \tag{C.3}$$

$$\mathrm{Tr}\ \gamma^{\mu} = 0 \ , \tag{C.4}$$

$$\mathrm{Tr}\ \gamma^5 = 0 \ , \tag{C.5}$$

$$\mathrm{Tr}(\gamma^5\gamma^{\mu}) = 0 \ , \tag{C.6}$$

$$\mathrm{Tr}(\gamma^{\mu}\gamma^{\nu}) = 4g^{\mu\nu} \ , \tag{C.7}$$

$$\mathrm{Tr}(\sigma^{\mu\nu}) = 0 \ , \tag{C.8}$$

$$\{\gamma^{\mu},\ \gamma^{\nu}\} = 2g^{\mu\nu}\mathbb{I} \ , \tag{C.9}$$

$$\{\gamma^{\mu},\ \gamma^{5}\} = 0 \quad . \tag{C.10}$$

Then

$$\text{Left side} = \sum_{\substack{\alpha\ \beta \\ \alpha'\beta'}} \left(\gamma^{\mu}(1)\right)_{\beta',\alpha}\left(\mathbb{I}(1)\right)_{\alpha\alpha'}\left(\gamma_{\mu}(2)\right)_{\alpha',\beta}\left(\mathbb{I}(2)\right)_{\beta\beta'}$$

$$= \sum_{\alpha'\beta'} \left(\gamma^{\mu}(1)\right)_{\beta'\alpha'}\left(\gamma_{\mu}(2)\right)_{\alpha'\beta'}$$

$$= \mathrm{Tr}\left(\gamma^{\mu}\gamma_{\mu}\right) = 4\mathrm{Tr}\mathbb{I} = 16 \ ,$$

$$\text{Right side} = a_S\ \mathrm{Tr}[\mathbb{I}(1)]\mathrm{Tr}[\mathbb{I}(2)] = 16\ a_S \quad .$$

We see that

$$a_S = 1 \ .$$

2). We mutiplying both sides of Eq.(C.1) by $[\gamma^1(1)]_{\alpha'\alpha}[\gamma_1(2)]_{\beta'\beta}$, and then sum on α', α, β', β , to find

$$\text{Left side} = \mathrm{Tr}[\gamma^0\gamma_0\gamma^1\gamma_1] - \mathrm{Tr}[\gamma^1\gamma_1\gamma^1\gamma_1] - \mathrm{Tr}[\gamma^2\gamma_2\gamma^1\gamma_1] - \mathrm{Tr}[\gamma^3\gamma_3\gamma^1\gamma_1]$$

$$= -2\ \mathrm{Tr}\mathbb{I} = -8 \ ,$$

$$\text{Right side} = a_V\mathrm{Tr}[\gamma^1(1)\gamma^1(1))\mathrm{Tr}[\gamma_1(2)\gamma_1(2)]$$

$$= a_V\mathrm{Tr}[-\mathbb{I}]\mathrm{Tr}[-\mathbb{I}]$$

$$= 16\ a_V \ .$$

We see that

$$a_V = -(1/2) .$$

In a similar fashion we find that $a_T=0$, $a_A=-1/2$, $a_P=-1$. We summarize the Fierz transformation as follows:

let $\Gamma_S=II$, $\Gamma_V=\gamma_\mu$, $\Gamma_T=\sigma_{\mu\nu}$, $\Gamma_A=\gamma_\mu\gamma_5$, $\Gamma_P=\gamma_5$.

Then

$$\sum_i g_i(\Gamma_i)_{\alpha'\alpha}(\Gamma_i)_{\beta'\beta} = \sum_j \hat{g}_j(\Gamma_j)_{\alpha'\beta}(\Gamma_j)_{\beta'\alpha} \quad , \tag{C.11}$$

where the indices i, j run over the set S, V, T, A and P. The g_i's are related to $\hat{g}_j$'s by the following matrix

$$\begin{pmatrix} \hat{g}_S \\ \hat{g}_V \\ \hat{g}_T \\ \hat{g}_A \\ \hat{g}_P \end{pmatrix} = \frac{1}{4} \begin{pmatrix} 1 & 1 & \frac{1}{2} & -1 & 1 \\ 4 & -2 & 0 & -2 & -4 \\ 12 & 0 & -2 & 0 & 12 \\ 4 & -2 & 0 & -2 & 4 \\ 1 & -1 & \frac{1}{2} & 1 & 1 \end{pmatrix} \begin{pmatrix} g_S \\ g_V \\ g_T \\ g_A \\ g_P \end{pmatrix} . \tag{C.12}$$

For isospin indices we perform trace operations to find

$$\delta_{\alpha_T'\beta_T}\delta_{\beta_T'\alpha_T} = n_0\delta_{\alpha_T'\alpha_T}\delta_{\beta_T'\beta_T} + n_1\left(\vec{\tau}(1)\right)_{\alpha_T'\alpha_T}\left(\vec{\tau}(2)\right)_{\beta_T'\beta_T} , \tag{C.13}$$

$$\left(\vec{\tau}(1)\right)_{\alpha_T'\beta_T}\left(\vec{\tau}(2)\right)_{\beta_T'\alpha_T} = n_2\delta_{\alpha_T'\alpha_T}\delta_{\beta_T'\beta_T} + n_3\left(\vec{\tau}(1)\right)_{\alpha_T'\alpha_T}\left(\vec{\tau}(2)\right)_{\beta_T'\beta_T} , \tag{C.14}$$

with $n_0 = 1/2$, $n_1 = 1/2$, $n_2 = 3/2$ and $n_4 = -1/2$.

Appendix D

Calculation of the Fully-On-Shell Amplitude

Recall the fully on-shell amplitudes:

$$\bar{u}_\alpha(\vec{p}_1's_1')\bar{u}_\beta(\vec{p}_2's_2')(\vec{p}_1',\vec{p}_2'|M^{on}_{\alpha\beta\alpha'\beta'}|\vec{p}_1,\vec{p}_2)u_{\alpha'}(\vec{p}_1,s_1)u_{\beta'}(\vec{p}_2,s_2). \tag{4.28}$$

In Appendix C, we have already shown how to use the Fierz transformation to express the on-shell nucleon-nucleon scattering amplitude in terms of five independent amplitudes. In this appendix we will show how to calculate the five quantities needed to obtain the functions $f(\vec{p}_1,\vec{p}_2)$, $f'(\vec{p}_1,\vec{p}_2)$, $g(\vec{p}_1,\vec{p}_2)$, $g'(\vec{p}_1,\vec{p}_2)$, $h(\vec{p}_1,\vec{p}_2)$ and $h'(\vec{p}_1,\vec{p}_2)$ in $\mathcal{F}^{NR}(\vec{p}_1,\vec{p}_2)$ and $\mathcal{F}(\vec{p}_1,\vec{p}_2)$ (see Eqs. 4.5-4.6):

I:

$$\bar{u}_{\alpha'}(\vec{k}_1,s_1')[\mathbb{I}(1)]_{\alpha',\alpha}u_\alpha(\vec{k}_1,s_1)\bar{u}_{\beta'}(\vec{k}_2,s_2')[\mathbb{I}(2)]_{\beta',\beta}u_\beta(\vec{k}_2,s_2), \tag{D.1}$$

II:

$$\bar{u}_{\alpha'}(\vec{k}_1,s_1')[\gamma^\mu(1)]_{\alpha',\alpha}u_\alpha(\vec{k}_1,s_1)\bar{u}_{\beta'}(\vec{k}_2,s_2')[\gamma_\mu(2)]_{\beta',\beta}u_\beta(\vec{k}_2,s_2), \tag{D.2}$$

III:

$$\bar{u}_{\alpha'}(\vec{k}_1,s_1')[\sigma^{\mu\nu}(1)]_{\alpha',\alpha}u_\alpha(\vec{k}_1,s_1)\bar{u}_{\beta'}(\vec{k}_2,s_2')[\sigma_{\mu\nu}(2)]_{\beta',\beta}u_\beta(\vec{k}_2,s_2), \tag{D.3}$$

IV:

$$\bar{u}_{\alpha'}(\vec{k}_1, s_1')[\gamma^5(1)\gamma^{\mu}(1)]_{\alpha',\alpha} u_{\alpha}(\vec{k}_1, s_1) \times \bar{u}_{\beta'}(\vec{k}_2, s_2')[\gamma_5(2)\gamma_{\mu}(2)]_{\beta',\beta} u_{\beta}(\vec{k}_2, s_2) \ , \tag{D.4}$$

V:

$$\bar{u}_{\alpha'}(\vec{k}_1, s_1')[\gamma^5(1)]_{\alpha',\alpha} u_{\alpha}(\vec{k}_1, s_1) \times \bar{u}_{\beta'}(\vec{k}_2, s_2')[\gamma_5(2)]_{\beta',\beta} u(\vec{k}_2, s_2) \ . \tag{D.5}$$

As an illustrative example let us calculate III. Using the propertities of the γ matrices and Pauli spin matices $\vec{\sigma}$, we have the following six relations [$\varepsilon = E + m$, $E = (\vec{p}^2 + m^2)^{1/2}$]:

$$1). \ \sum_{il} \epsilon_{il k}[\ \sigma_k(1) + \sigma_k(2)\ ] = 0 \ . \tag{D.6}$$

$$2) \quad \left(\frac{\vec{\sigma}_1 \cdot \vec{k}_1}{\epsilon}\right)\vec{\sigma}_1 \cdot \left(\frac{\vec{\sigma}_2 \cdot \vec{k}_2}{\epsilon}\right)\vec{\sigma}_2$$

$$= \Sigma\, k_i(1)k_l(2)[\delta_{ij} + i\epsilon_{ijk}\sigma_k(1)][\delta_{jl} + i\epsilon_{jl\eta}\sigma_\eta(2)]$$

$$= \Sigma\, k_i(1)k_l(2)[\delta_{ij}\delta_{jl} + i\delta_{jl}\epsilon_{ijk}\sigma_k(1) + i\delta_{ij}\epsilon_{jl\eta}\sigma_\eta(2)$$

$$- \epsilon_{ijk}\epsilon_{il\eta}\sigma_k(1)\sigma_\eta(2)]$$

$$= \vec{k}_1 \cdot \vec{k}_2 + (\vec{\sigma}_1 \cdot \vec{\sigma}_2)(\vec{k} \cdot_1 \vec{k}_2) - (\vec{\sigma}_1 \cdot \vec{k}_2)(\vec{\sigma}_2 \cdot \vec{k}_1). \tag{D.7}$$

3). $$\left(-\frac{\vec{\sigma}_1\cdot\vec{k}_1}{\epsilon}\vec{\sigma}_1+\vec{\sigma}_1\frac{\vec{\sigma}_1\cdot\vec{k}_1}{\epsilon}\right)\left(-\frac{\sigma_2\cdot k_2}{\epsilon}\sigma_2+\sigma_2\frac{\sigma_2\cdot k_2}{\epsilon}\right)$$

$$=\frac{4}{\epsilon^2}\left((\vec{\sigma}_1\cdot\vec{k}_2)(\vec{\sigma}_2\cdot\vec{k}_1)-(\vec{\sigma}_1\cdot\vec{\sigma}_2)(\vec{\kappa}_1\cdot\vec{k}_2)\right). \qquad (D.8)$$

4). $$\frac{\vec{\sigma}_1\cdot\vec{k}_1}{\epsilon}\vec{\sigma}_1\frac{\vec{\sigma}_1\cdot\vec{k}_1}{\epsilon}=2(\vec{\sigma}_1\cdot\vec{k}_1)\vec{k}-(\vec{k}_1\cdot\vec{k}_1)\vec{\sigma}_1 \ . \qquad (D.9)$$

5). $$\left(\vec{\sigma}_1-\frac{\vec{\sigma}_1\cdot\vec{k}_1}{\epsilon}\vec{\sigma}_1\frac{\vec{\sigma}_1\cdot\vec{k}_1}{\epsilon}\right)\left(\vec{\sigma}_2-\frac{\vec{\sigma}_2\cdot\vec{k}_2}{\epsilon}\vec{\sigma}_2\frac{\vec{\sigma}_2\cdot\vec{k}_2}{\epsilon}\right)$$

$$=\left(\frac{2E}{\epsilon}\vec{\sigma}_1-\frac{2}{\epsilon^2}(\vec{\sigma}_1\cdot\vec{k}_1)\vec{k}_1\right)\left(\frac{2E}{\epsilon}\vec{\sigma}_2-\frac{2}{\epsilon^2}(\vec{\sigma}_2\cdot\vec{k}_2)\vec{k}_2\right)$$

$$=\frac{4E^2}{\epsilon^2}\vec{\sigma}_1\cdot\vec{\sigma}_2-\frac{4E}{\epsilon^3}(\vec{\sigma}_1\cdot\vec{k}_1)(\vec{\sigma}_2\cdot\vec{k}_1)-\frac{4E}{\epsilon^3}(\vec{\sigma}_1\cdot\vec{k}_1)(\vec{\sigma}_2\cdot\vec{k}_1)$$

$$+\frac{4}{\epsilon^4}(\vec{\sigma}_1\cdot\vec{k}_1)(\vec{\sigma}_2\cdot\vec{k}_2)(\vec{k}_1\cdot\vec{k}_2) \ . \qquad (D.10)$$

6). $$\sigma^{\mu\nu}(1)\sigma_{\mu\nu}(2)=2\begin{pmatrix}\vec{\sigma}_1 & 0\\ 0 & \vec{\sigma}_1\end{pmatrix}\begin{pmatrix}\vec{\sigma}_2 & 0\\ 0 & \vec{\sigma}_2\end{pmatrix}+2\begin{pmatrix}0 & \vec{\sigma}_1\\ \vec{\sigma}_1 & 0\end{pmatrix}\begin{pmatrix}0 & \vec{\sigma}_2\\ \vec{\sigma}_2 & 0\end{pmatrix}. \qquad (D.11)$$

Then, we have

$$\mathrm{III}=\left\{\frac{2\epsilon^2}{4m^2}\left(-\frac{\vec{\sigma}_1\cdot\vec{k}_1}{\epsilon}\vec{\sigma}_1+\vec{\sigma}_1\frac{\vec{\sigma}_1\cdot\vec{k}_1}{\epsilon}\right)\left(-\frac{\vec{\sigma}_2\cdot\vec{k}_2}{\epsilon}\vec{\sigma}_2+\vec{\sigma}_2\frac{\vec{\sigma}_2\cdot\vec{k}_2}{\epsilon}\right)\right.$$

$$+\frac{2\epsilon^2}{4m^2}\left(\vec{\sigma}_1-\frac{\vec{\sigma}_1\cdot\vec{k}_1}{\epsilon}\vec{\sigma}_1\frac{\vec{\sigma}_1\cdot\vec{k}_1}{\epsilon}\right)\left(\vec{\sigma}_2-\frac{\vec{\sigma}_2\cdot\vec{k}_2}{\epsilon}\vec{\sigma}_2\frac{\vec{\sigma}_2\cdot\vec{k}_2}{\epsilon}\right)\Bigg\}$$

$$\times\delta_{\alpha'\alpha}\delta_{\beta'\beta}\delta_{s_1's_1}\delta_{s_2's_2} \qquad (D.12)$$

$$=\Bigg\{\frac{2}{m^2}\left(-(\vec{\sigma}_1\cdot\vec{\sigma}_2)(\vec{k}_1\cdot\vec{k}_2)+(\vec{\sigma}_1\cdot\vec{k}_2)(\vec{\sigma}_2\cdot\vec{k}_1)\right)$$

$$+\frac{2E}{m^2}\left(E\,\vec{\sigma}_1\cdot\vec{\sigma}_2-\frac{1}{\epsilon}(\vec{\sigma}_1\cdot\vec{k}_2)(\vec{\sigma}_2\cdot\vec{k}_2)-\frac{1}{\epsilon}(\vec{\sigma}_2\cdot\vec{k}_1)(\vec{\sigma}_1\cdot\vec{k}_1)\right.$$

$$\left.+\frac{2}{\epsilon^2}(\vec{\sigma}_1\cdot\vec{k}_1)(\vec{\sigma}_2\cdot\vec{k}_2)(\vec{k}_1\cdot\vec{k}_2)\right)\Bigg\}\delta_{\alpha'\alpha}\delta_{\beta'\beta}\delta_{s_1's_1}\delta_{s_2's_2}.$$

We consider the center of momentum system, with $\vec{P}_{center} = 0$. The relative momentum is $\vec{p} = (\vec{k}_1-\vec{k}_2)/2$ for two quasi-particles at the Fermi surface. Here $|\vec{k}_1| = |\vec{k}_2| = k_F$. Let θ be the angle between $\vec{k}_1$ and $\vec{k}_2$, and put $x = \cos\theta$. We have

$$III = \Bigg\{\frac{2}{m^2}\left(E^2-\frac{2E\vec{p}^2}{3\epsilon}-k_F^2x-\frac{\vec{p}^2}{3}-\frac{k_F^2x\vec{p}^2}{3\epsilon^2}\right)\vec{\sigma}_1\cdot\vec{\sigma}_2$$

$$+\frac{2}{m^2}\left(-\frac{\vec{p}^2}{3}-\frac{2E\vec{p}^2}{3\epsilon}-\frac{k_F^2x\vec{p}^2}{3\epsilon^2}\right)S_{12}(\vec{p})\Bigg\}\delta_{\alpha'\alpha}\delta_{\beta'\beta}\delta_{s_1's_1}\delta_{s_2's_2}. \qquad (D.13)$$

where $S_{12}(\vec{p})$ is the tensor operator:

$$S_{12}(\vec{p}) = \frac{3(\vec{\sigma}_1\cdot\vec{p})(\vec{\sigma}_2\cdot\vec{p})}{\vec{p}^2}-\vec{\sigma}_1\cdot\vec{\sigma}_2 \quad . \qquad (D.14)$$

Neglecting higher order terms, we find

$$III = \left\{ \frac{2}{m^2}\left(E^2 - \frac{2E\vec{p}^2}{3\epsilon} - k_F^2 x - \frac{\vec{p}^2}{3}\right)\vec{\sigma}_1 \cdot \vec{\sigma}_2 + \frac{2}{m^2}\left(-\frac{\vec{p}^2}{3} - \frac{2E\vec{p}^2}{3\epsilon}\right) S_{12}(\vec{p}) \right\}$$

$$= \left\{ \left(2 + \frac{2k_F^2(1-x)}{m^2}\left[1 - \frac{1}{6}\left(1 + \frac{2E}{\epsilon}\right)\right]\right)\vec{\sigma}_1 \cdot \vec{\sigma}_2 - \frac{1}{3m^2}\left(1 + \frac{2E}{\epsilon}\right)k_F^2(1-x)S_{12}(\vec{p}) \right\} \delta_{\alpha'\alpha}\delta_{\beta'\beta}\delta_{s_1's_1}\delta_{s_2's_2} \quad . \tag{D.15}$$

We make the approximation $E \simeq m$, $\epsilon \simeq 2m$, so that

$$III = \left\{ \left(2 + \frac{4k_F^2}{3m^2}(1-x)\right)\vec{\sigma}_1 \cdot \vec{\sigma}_2 - \frac{2k_F^2}{3m^2}(1-x)S_{12}(\vec{p}) \right\} \delta_{\alpha'\alpha}\delta_{\beta'\beta}\delta_{s_1's_1}\delta_{s_2's_2} . \tag{D.16}$$

In a similar fashion we can show that

$$I = \delta_{\alpha'\alpha}\delta_{\beta'\beta}\delta_{s_1's_1}\delta_{s_2's_2} \quad . \tag{D.17}$$

$$II = \left\{ \frac{E^2}{m^2} - \frac{k_F^2 x}{m^2} \right\} \delta_{\alpha'\alpha}\delta_{\beta'\beta}\delta_{s_1's_1}\delta_{s_2's_2} \ . \tag{D.18}$$

$$IV = \left\{ -\left(1+\frac{k_F^2(1-x)}{3\,m^2}\right)\vec{\sigma}_1\cdot\vec{\sigma}_2 - \frac{k_F^2(1-x)}{3\,m^2} S_{12}(\vec{p}) \right\} \delta_{\alpha'\alpha}\delta_{\beta'\beta}\delta_{s_1's_1}\delta_{s_2's_2} . \tag{D.19}$$

$$V = 0 \ . \tag{D.20}$$

For the spinor $f(\vec{p},s)$, which is the solution of Eq.(2.8), we can derive following five relations:

$$\bar{f}_{\alpha'}(\vec{k}_1,s_1')[I\!I(1)]_{\alpha'\alpha} f_{\alpha}(\vec{k}_1,s_1)\bar{f}_{\beta'}(\vec{k}_2,s_2')[I\!I(2)]_{\beta'\beta} f_{\beta}(\vec{k}_2,s_2)$$

$$= \delta_{\alpha'\alpha}\delta_{\beta'\beta}\delta_{s_1's_1}\delta_{s_2's_2} \ . \tag{D.21}$$

$$\bar{f}_{\alpha'}(\vec{k}_1,s_1')[\gamma^{\mu}(1)]_{\alpha'\alpha} f_{\alpha}(\vec{k}_1,s_1)\bar{f}_{\beta'}(\vec{k}_2,s_2')[\gamma_{\mu}(2)]_{\beta'\beta} f_{\beta}(\vec{k}_2,s_2)$$

$$= \left(\frac{\tilde{E}^2}{\tilde{m}^2} - \frac{k_F^2 x}{\tilde{m}^2} \right) \delta_{\alpha'\alpha}\delta_{\beta'\beta}\delta_{s_1's_1}\delta_{s_2's_2} . \tag{D.22}$$

$$\bar{f}_{\alpha'}(\vec{k}_1,s_1')[\sigma^{\mu\nu}(1)]_{\alpha'\alpha} f_{\alpha}(\vec{k}_1,s_1)\bar{f}_{\beta'}(\vec{k}_2,s_2')[\sigma_{\mu\nu}(2)]_{\beta'\beta} f_{\beta}(\vec{k}_2,s_2)$$

$$= \left\{ \left(2 + \frac{2k_F(1-x)}{\tilde{m}^2}\left[1 - \frac{1}{6}\left(1+\frac{2\tilde{E}}{\tilde{\epsilon}}\right)\right)\vec{\sigma}_1\cdot\vec{\sigma}_2 \right.$$

$$\left. - \frac{1}{3\tilde{m}^2}\left(1+\frac{2\tilde{E}}{\tilde{\epsilon}}\right)k_F^2(1-x)S_{12}(\vec{p}) \right\} \delta_{\alpha'\alpha}\delta_{\beta'\beta}\delta_{s_1's_1}\delta_{s_2's_2} \ . \tag{D.23}$$

$$\bar{f}_{\alpha'}(\vec{k}_1, s_1')[\gamma^5(1)\gamma^\mu(1)]_{\alpha',\alpha} f_\alpha(\vec{k}_1, s_1)\bar{f}_{\beta'}(\vec{k}_2, s_2')[\gamma_5(2)\gamma_\mu(2)]_{\beta',\beta} f_\beta(\vec{k}_2, s_2)$$

$$= \left\{ -\left(1 + \frac{k_F^2(1-x)}{3\,\tilde{m}^2}\right)\vec{\sigma}_1\cdot\vec{\sigma}_2 - \frac{k_F^2(1-x)}{3\,\tilde{m}^2}\, S_{12}(\vec{p}) \right\} \delta_{\alpha',\alpha}\delta_{\beta',\beta}\delta_{s_1' s_1}\delta_{s_2' s_2} \quad . \tag{D.24}$$

$$\bar{f}_{\alpha'}(\vec{k}_1, s_1')[\gamma^5(1)]_{\alpha',\alpha} f_\alpha(\vec{k}_1, s_1)\bar{f}_{\beta'}(\vec{k}_2, s_2')[\gamma_5(2)]_{\beta',\beta} f_\beta(\vec{k}_2, s_2)$$

$$= 0 \quad . \tag{D.25}$$

Appendix E

Gordon Decomposition

When we study the interaction arising from the exchange of a ρ meson, the following Gordon Decomposition formulas are useful. Here the u(q,s) and f(q,s) are initial-state spinors, while the u(p,s) and f(p,s) are final-state spinors. We have

$$\bar{u}(p,s)\gamma^{\mu}u(q,s)= \frac{1}{2\ m}\ \bar{u}(p,s)\Big((p+q)^{\mu}+i\sigma^{\mu\nu}(p-q)_{\nu}\Big)u(q,s).$$

(E.1)

$$\bar{u}(p,s)\gamma^{\mu}\gamma^{5}u(q,s)= \frac{1}{2\ m}\ \bar{u}(p,s)\Big((p-q)^{\mu}\gamma^{5}+i\sigma^{\mu\nu}(p+q)_{\nu}\gamma_{5}\Big)u(q,s).$$

(E.2)

$$\bar{f}(p,s)\gamma^{\mu}f(q,s)= \frac{1}{2\ \tilde{m}}\ \bar{f}(p,s)\Big((p+q)^{\mu}+i\sigma^{\mu\nu}(p-q)_{\nu}\Big)f(q,s)\ .$$

(E.3)

$$\bar{f}(p,s)\gamma^{\mu}\gamma^{5}f(q,s)\ = \frac{1}{2\ \tilde{m}}\ \bar{f}(p,s)\Big((p-q)^{\mu}\gamma^{5}+i\sigma^{\mu\nu}(p+q)_{\nu}\gamma_{5}\Big)f(q,s).$$

(E.4)

REFERENCES

1. K.A. Brueckner and J.L. Gammel, Phys. Rev. 109, 1023 (1958).

2. For a review and references to early work, see B.D. Day, Rev. Mod. Phys. 39, 719 (1967); 50, 495 (1978).

3. K. Erkelenz, Phys. Reports 13C, 191 (1974).

4. K. Holinde and R. Machleidt, Nucl. Phys. A247, 495 (1975).

5. D. Schutte, Nucl. Phys. A221, 450 (1974).

6. M.R. Anastasio, L.S. Celenza, W.S. Pong and C.M. Shakin, Phys.Rep. 100, 327 (1983).

7. L.S. Celenza and C.M. Shakin, Relativistic Nuclear Physics: Theories of Structure and Scattering (World Scientific, Singapore, 1986).

8. B.D Serot and J.D. Walecka, in Advances in Nuclear Physics, edited by J. Negele and E. Vogt (Plenum, New York,1985), Vol. 16.

9. K. Kotthoff, K. Holinde, R. Machleidt and D. Schutte, Nucl. Phys. A242, 429 (1975).

10. K. Kotthoff, R. Machleidt and D. Schutte, Nucl. Phys. A264, 484 (1976).

11. T.S.H. Lee and F. Tabakin, Nucl. Phys. A191, 332 (1972).

12. K. Nakayama, S. Krewald and J. Speth, Phys. Lett. 145B, 310 (1984).

13. K. Nakayama, S. Drozdz, S. Krewald and J. Speth, Nucl. Phys. A470, 573 (1987).

14. K. Nakayama, S.Krewald and J. Speth, Phys. Lett. 148B, 399 (1984).

15. C.J. Horowitz and B.D. Serot, Nucl. Phys. A368, 503 (1981).

16. A. Bouyssy, J.F. Mathiot, Nguyen Van Giai and S. Marcos, Report No.IPNO/TH 86-27, 1986.

17. J.D. Bjorken and S.D. Drell, Relativistic Quantum Mechanics (McGraw Hill, New York, 1964).

18. K. Holinde, K. Erkelenz and R. Alzetta, Nucl. Phys. A198, 598 (1972).

19. K. Holinde and R. Machleidt, Nucl. Phys. A256, 479 (1976).

20. R. Machleidt and R. Brockman, in Proceedings of the LAMPF Workshop on Dirac Approches to Nuclear Physics, Edited by J.R. Shepard, C.Y. Cheung and R.L. Boudrie, Los Alamos Report La-10438C (1985).

21. L.S. Celenza and C.M. Shakin, Phys. Rev. C28, 1256 (1983).

22. A. Scotti and D.Y. Wong, Phys. Rev. 138, B145 (1965).

23. E.E. Salpeter and H.A. Bethe, Phys. Rev. 84, 1232 (1951).

24. K. Holinde, Phys. Reports 68, 121 (1981).

25. L.S. Celenza and W.S. Pong and C.M. Shakin, Phys. Rev. C25, 3115 (1982).

26. G.E. Brown, in Proc. Fifth Int. Conf. on High-Energy Physics and Nuclear Structure, Uppsala (1973), ed. by G. Tibell (North Holland, Amsterdam, 1974).

27. A.M. Green and P. Haapakoski, Nucl. Phys. A221, 429 (1974).

28. K. Erkelenz, K.Holinde and K. Bleuler, Nucl. Phys. A161, 155 (1971).

29. B.C. Clark, S. Hama, R.L. Mercer, L. Ray and B.D. Serot, Phys. Rev. Lett. 50, 1644 (1983).

30. J.R. Shepard, J.A. McNeil and S.J. Wallace, Phys. Rev. Lett. 50, 1443 (1983).

31. J.A. McNeil, J.R. Shepard and S.J. Wallace, Phys. Rev. Lett. 50, 1439 (1983).

32. V.M. Bannur, L.S. Celenza and C.M. Shakin, Brooklyn College Report: BCCNT 87/071/168 (1987) -submitted for publication.

33. V.M. Bannur, L.S. Celenza and C.M. Shakin, Brooklyn College Report: BCCNT 87/091/169 (1987) -submitted for publication.